



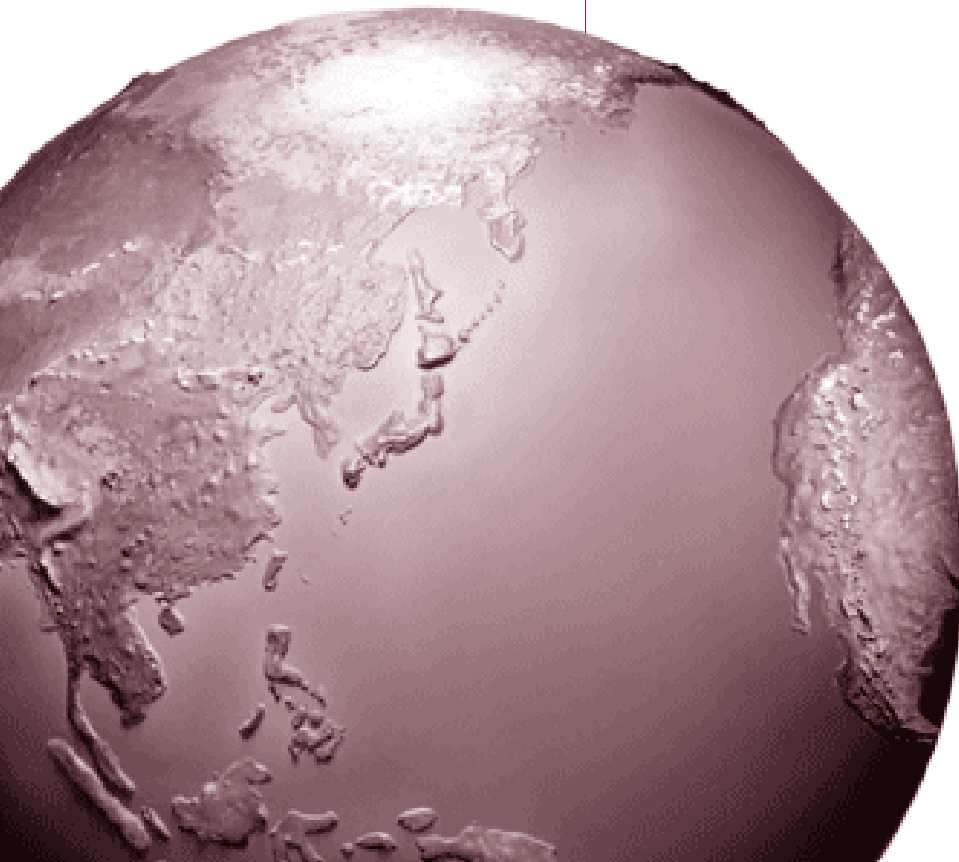
RESEARCH REPORT

HEALTH
EFFECTS
INSTITUTE

Number 194
February 2018

A Dynamic Three-Dimensional Air Pollution Exposure Model for Hong Kong

Benjamin Barratt, Martha Lee, Paulina Wong, Robert Tang,
Tsz Him Tsui, Wei Cheng, Yang Yang, Poh-Chin Lai, Linwei Tian,
Thuan-Quoc Thach, Ryan Allen, and Michael Brauer



A Dynamic Three-Dimensional Air Pollution Exposure Model for Hong Kong

Benjamin Barratt, Martha Lee, Paulina Wong, Robert Tang, Tsz Him Tsui, Wei Cheng,
Yang Yang, Poh-Chin Lai, Linwei Tian, Thuan-Quoc Thach, Ryan Allen, and Michael Brauer

with a Critique by the HEI Review Committee

Research Report 194
Health Effects Institute
Boston, Massachusetts

Trusted Science • Cleaner Air • Better Health

Publishing history: This document was posted at www.healtheffects.org February 2018.

Citation for document:

Barratt B, Lee M, Wong P, Tang R, Tsui TH, Cheng W, et al. 2018. A Dynamic Three-Dimensional Air Pollution Exposure Model for Hong Kong. Research Report 194. Boston, MA: Health Effects Institute.

© 2018 Health Effects Institute, Boston, Mass., U.S.A. Cameographics, Union, Me., Compositor. Printed by Recycled Paper Printing, Boston, Mass. Library of Congress Catalog Number for the HEI Report Series: WA 754 R432.

♻️ Cover paper: made with at least 55% recycled content, of which at least 30% is post-consumer waste; free of acid and elemental chlorine. Text paper: made with 100% post-consumer waste recycled content; acid free; no chlorine used in processing. The book is of permanent archival quality.

CONTENTS

About HEI	vii
About This Report	ix
Preface	xi
HEI STATEMENT	1
INVESTIGATORS' REPORT <i>by Barratt et al.</i>	5
ABSTRACT	5
Introduction	5
Methods	5
Results	6
Conclusions	6
INTRODUCTION	6
SPECIFIC AIMS	8
METHODS AND STUDY DESIGN	8
Protection of Human Subjects	8
Study Design	8
WP1: 2D LUR Model Development	8
WP2: 3D LUR Model Development	8
WP3: D3D LUR Model Development	8
WP4: Model Evaluation and Translation	9
WP1: Development of a 2D Land-Use Regression Model for Hong Kong	9
Field Sampling	9
Pollutant Concentrations	9
Predictors	10
Model Building	10
Evaluation	11
WP2: Vertical Monitoring Field Campaign and Development of a 3D LUR Model	11
Selection of Sampling Sites	11
Recruitment Process	11
Vertical Sampling Campaign	12
Data Quality Control	13
Calculation of Decay Rates	13
Calculation of Infiltration Efficiencies	13
WP3: Integration of Population Movements to Create a Dynamic 3D LUR Model	14
Population Mobility Data	14
Deriving Population Movement Patterns	14
Subjects with Missing Trip Information	15
Time-Weighted Air Pollution Exposure	15
Exposure in Different Microenvironments	15
Air Pollution Data	15
Data Analysis	17

Report 194

WP4: Model Evaluation and Translation for Application in Other Megacities	17
Cohort Data	17
Health Outcomes	18
Exposure Data	18
Visualization of 3D Dispersion Patterns for Public Engagement	19
STATISTICAL METHODS AND DATA ANALYSIS	20
Cox Proportional Hazard Models (WP4)	20
Covariates	20
Comparison Between Pollutants	20
Comparison with Satellite-Derived Exposure Estimates	20
Sensitivity Analyses	20
RESULTS	20
WP1: Development of a 2D Land-Use Regression Model for Hong Kong	20
Measurements	20
Model Results and Evaluation	21
WP2: Vertical Monitoring Field Campaign and Development of a 3D LUR Model	21
Sampling Site Characteristics	21
Equipment Performance	21
Vertical Decay Rates	26
Alternative Decay Exposure Profile	31
Infiltration Efficiencies	32
WP3: Integration of Population Movements to Create a Dynamic 3D LUR Model	32
Exposure and Time Spent in Different Microenvironments	32
Time-Weighted Exposure by Model Stage	33
Stratified Analysis for Different Population Subgroups	34
WP4: Model Evaluation and Translation for Application in Other Megacities	36
Cohort Data	36
Exposure Data	36
Associations Between Long-Term Air Pollution Exposure and Mortality	36
Sensitivity Analyses	39
Application of Alternative Decay Profile	39
Visualization of 3D Dispersion Patterns	40
DISCUSSION AND CONCLUSIONS	40
Implications for Future Use of Low-Cost Air Quality Sensors	40
Development of a 2D Land-Use Regression Model for Hong Kong	41
Vertical Decay of TRAP and Derivation of a Canyon Typology	41
Building Infiltration Efficiencies	42
Dynamic Exposure Modeling	42

Report 194

Staged Epidemiological Analysis of Mortality Rates in an Elderly Cohort	43
Impact of Model Assumptions	44
Application of TRAP Exposure Methodology in Other High-Rise Asian Cities	44
IMPLICATIONS OF FINDINGS	45
ACKNOWLEDGMENTS	46
REFERENCES	46
MATERIALS AVAILABLE ON THE HEI WEBSITE	50
ABOUT THE AUTHORS	50
OTHER PUBLICATIONS RESULTING FROM THIS RESEARCH	52
CRITIQUE <i>by the Review Committee</i>	53
INTRODUCTION	53
APPROACH	54
Aims	54
Methods	54
Two-Dimensional LUR models (Work Package 1)	54
Three-Dimensional LUR Models (Work Package 2)	54
Dynamic Three-Dimensional LUR models (Work Package 3)	55
Application to the Cohort (Work Package 4)	56
SUMMARY OF RESULTS	56
Exposure Models with Increasing Complexity	56
Application of the Exposure Models to the Cohort	56
REVIEW COMMITTEE EVALUATION	57
Strengths of the Study	57
Data Challenges	57
Adding a Vertical Component to the Exposure Model	60
Adding a Dynamic Component to the Exposure Model	61
Development of the Two-Dimensional Exposure Models	61
Overarching Final Considerations	61
SUMMARY AND CONCLUSIONS	62
ACKNOWLEDGMENTS	62
REFERENCES	63
Abbreviations and Other Terms	65
Related HEI Publications	67
HEI Board, Committees, and Staff	69

ABOUT HEI

The Health Effects Institute is a nonprofit corporation chartered in 1980 as an independent research organization to provide high-quality, impartial, and relevant science on the effects of air pollution on health. To accomplish its mission, the institute

- Identifies the highest-priority areas for health effects research;
- Competitively funds and oversees research projects;
- Provides intensive independent review of HEI-supported studies and related research;
- Integrates HEI's research results with those of other institutions into broader evaluations; and
- Communicates the results of HEI's research and analyses to public and private decision makers.

HEI typically receives balanced funding from the U.S. Environmental Protection Agency and the worldwide motor vehicle industry. Frequently, other public and private organizations in the United States and around the world also support major projects or research programs. HEI has funded more than 330 research projects in North America, Europe, Asia, and Latin America, the results of which have informed decisions regarding carbon monoxide, air toxics, nitrogen oxides, diesel exhaust, ozone, particulate matter, and other pollutants. These results have appeared in more than 260 comprehensive reports published by HEI, as well as in more than 1,000 articles in the peer-reviewed literature.

HEI's independent Board of Directors consists of leaders in science and policy who are committed to fostering the public–private partnership that is central to the organization. The Research Committee solicits input from HEI sponsors and other stakeholders and works with scientific staff to develop a Five-Year Strategic Plan, select research projects for funding, and oversee their conduct. The Review Committee, which has no role in selecting or overseeing studies, works with staff to evaluate and interpret the results of funded studies and related research.

All project results and accompanying comments by the Review Committee are widely disseminated through HEI's website (www.healtheffects.org), printed reports, newsletters and other publications, annual conferences, and presentations to legislative bodies and public agencies.

ABOUT THIS REPORT

Research Report 194, *A Dynamic Three-Dimensional Air Pollution Exposure Model for Hong Kong*, presents a research project funded by the Health Effects Institute and conducted by Dr. Benjamin Barratt of King's College London, United Kingdom, and his colleagues. The report contains three main sections.

The HEI Statement, prepared by staff at HEI, is a brief, nontechnical summary of the study and its findings; it also briefly describes the Review Committee's comments on the study.

The Investigators' Report, prepared by Barratt and colleagues, describes the scientific background, aims, methods, results, and conclusions of the study.

The Critique, prepared by members of the Review Committee with the assistance of HEI staff, places the study in a broader scientific context, points out its strengths and limitations, and discusses remaining uncertainties and implications of the study's findings for public health and future research.

This report has gone through HEI's rigorous review process. When an HEI-funded study is completed, the investigators submit a draft final report presenting the background and results of the study. This draft report is first examined by outside technical reviewers and a biostatistician. The report and the reviewers' comments are then evaluated by members of the Review Committee, an independent panel of distinguished scientists who have no involvement in selecting or overseeing HEI studies. During the review process, the investigators have an opportunity to exchange comments with the Review Committee and, as necessary, to revise their report. The Critique reflects the information provided in the final version of the report.

PREFACE

HEI's Research Program to Improve Assessment of Exposure to Traffic-Related Air Pollution

INTRODUCTION

Traffic emissions are an important source of urban air pollution. Emissions from motor vehicles and ambient concentrations of most monitored traffic-related pollutants have decreased steadily over the last several decades in most high-income countries as a result of air quality regulations and improvements in vehicular emission control technologies, and this trend is likely to continue. However, these positive developments have not been able to fully compensate for the rapid growth of the motor vehicle fleet due to growth in population and economic activity, increasing vehicular congestion, as well as the presence of older or malfunctioning vehicles on the roads.

In 2010, HEI published Special Report Number 17, *Traffic-Related Air Pollution: A Critical Review of the Literature on Emissions, Exposure, and Health Effects*. This report, developed by the HEI Panel on the Health Effects of Traffic-Related Air Pollution ("Panel"), summarized and synthesized research related to the health effects from exposure to traffic emissions. The Panel in its conclusions "identified an exposure zone within a range of up to 300 to 500 m from a major road as the area most highly affected by traffic emissions (the range reflects the variable influence of background pollution concentrations, meteorologic conditions, and season)." The Panel estimated that 30% to 45% of people living in large North American cities reside within these zones. Based on a review of health studies, the Panel concluded that exposure to traffic-related air pollution was causally linked to worsening asthma symptoms. It also found "suggestive evidence of a causal relationship with onset of childhood asthma, nonasthma respiratory symptoms, impaired lung function, total and cardiovascular mortality, and cardiovascular morbidity" (HEI

Panel on the Health Effects of Traffic-Related Air Pollution 2010).

The report also noted that exposure assessment of traffic-related air pollution is challenging; it is a complex mixture of particulate and many gaseous pollutants, many of which are also emitted by other sources, and is characterized by high spatial and temporal variability with the highest traffic-related air pollution concentrations occurring at or close to major roads. Therefore, identifying an appropriate exposure metric that uniquely indicates traffic-related air pollution and modeling the distribution of exposure at a sufficiently high degree of spatial and temporal resolution have been difficult.

The most commonly used exposure metrics are measured or modeled concentrations of individual pollutants considered to be indicators of traffic-related air pollution (such as nitrogen dioxide [NO₂] or black carbon [BC]) and simple indicators of traffic (such as distance of the residence from busy roads or traffic density near the residence).

A range of models, such as dispersion, land-use regression, and hybrid models, have been developed to estimate exposure. Some attempts to account for indoor infiltration and time-activity patterns have been made to refine such estimates. Although many improvements in these exposure models have occurred over time (especially the use of geographic information system approaches and the application of more sophisticated statistical methods), their usefulness still depends on the model assumptions and data quality. Few studies have compared the performance of different models and evaluated exposure measurement error and possible bias in health estimations.

To start addressing these concerns, HEI issued a Request for Applications in 2013. In order to inform the development of the RFA, the HEI Research Committee

Preface

held a workshop in April 2012 with experts in the areas of atmospheric chemistry, pollutant measurements, exposure models, epidemiology, and health assessment to discuss and identify the highest priority research questions.

OBJECTIVES OF RFA 13-1

RFA 13-1, *Improving Assessment of Near-Road Exposure to Traffic Related Pollution*, aimed to solicit studies to improve exposure assessment for use in future work on the health effects of traffic-related air pollution. The RFA had three major objectives:

- Demonstrate novel surrogates of near-road traffic-related pollution, taking advantage of new sensors and/or existing monitoring data.
- Determine the most important variables that explain spatial and temporal variance of near-road traffic-related pollutant concentrations at the personal, residential, and/or community levels, and explain the implications of these for future monitoring, modeling, exposure, and health effects studies.
- Improve inputs for exposure models for traffic-related health studies; evaluate and compare the performance of alternative models to existing models and actual measurements to quantify exposure measurement error.

DESCRIPTION OF THE PROGRAM

Five studies were funded under RFA 13-1 to represent a variety of geographical locations and cover the various RFA objectives. The study by Barratt and colleagues described in this report (Research Report 194) is the first to be published. All five studies are summarized below.

“The Hong Kong D3D Study: A Dynamic Three-Dimensional Exposure Model for Hong Kong,” Benjamin Barratt, King’s College London, United Kingdom (Principal Investigator) In the study presented in this report, Barratt and colleagues estimated exposure to traffic-related air pollution using a dynamic three-dimensional land-use regression model for Hong Kong, which has many high-rise buildings, resulting in street canyons.

Different exposure models were developed with increasing complexity (e.g., incorporating infiltration indoors, vertical gradients, and time–activity patterns) and applied in an epidemiological study to evaluate the potential impact of exposure measurement error in mortality estimates.

Enhancing Models and Measurements of Traffic-Related Air Pollutants for Health Studies Using Bayesian Melding,” Stuart Batterman, University of Michigan, Ann Arbor, Michigan (Principal Investigator) Batterman and colleagues estimated exposure of traffic-related air pollution using a variety of methods and models, including air pollution dispersion models and novel data fusion methods that would be able to propagate uncertainty more fully into the exposure estimates. The study made extensive use of data collected in the Near-road EXposures and effects of Urban air pollutants Study (NEXUS), a cohort study designed to examine the relationship between near-roadway pollutant exposures and respiratory outcomes in children with asthma who live close to major roadways in Detroit. The study has been completed and is currently in review.

“Characterizing the Determinants of Vehicle Traffic Emissions Exposure: Measurement and Modeling of Land-Use, Traffic, Transformation, and Transport,” Christopher Frey, North Carolina State University, Raleigh, North Carolina (Principal Investigator) Frey and colleagues investigated key factors that influence exposure to traffic-related air pollution: traffic and its composition; built environment including road characteristics and land use; and dispersion, transport, and transformation processes. The study collected extensive measurements of fine particulate matter (PM_{2.5}), ultrafine particles (UFPs), oxides of nitrogen (NO_x), and semi-volatile organic compounds (SVOCs) in various near-road locations in the Raleigh–Durham area. This study was completed at the end of 2017.

“Developing Multipollutant Exposure Indicators of Traffic Pollution: The Dorm Room Inhalation to Vehicle Emissions (DRIVE) Study,” Jeremy Sarnat, Emory University, Atlanta, Georgia (Principal Investigator) Sarnat and colleagues evaluated novel multipollutant traffic surrogates by collecting measurements in and around two student dormitories in Atlanta and explored the use of

Preface

metabolomics to identify possible exposure-related metabolites. The DRIVE study made use of a unique emission-exposure setting in Atlanta, on the Georgia Institute of Technology campus, with one dorm immediately adjacent to the busiest and most congested highway artery in the city (with more than 300,000 vehicles per day), and another dorm located farther away. This study has been completed and is currently in review.

“Evaluation of Alternative Sensor-Based Exposure Assessment Methods,” Edmund Seto, University of Washington, Seattle, Washington (Principal Investigator) Seto and colleagues performed an evaluation of novel low-cost air pollution sensors to characterize traffic-related air pollution in the San Francisco Bay area. They have deployed various low-cost air pollution sensors — including Shinyei particulate matter sensors and Alphasense electrochemical sensors — for an extended period of time. Sensors were colocated with reference monitors to evaluate sensor performance. This study has been completed and is currently in review.

NEXT STEPS

As these studies near completion, valuable lessons learned may be integrated into new research. Continuing its commitment to research on traffic-related air pollution, in January 2017 HEI issued RFA 17-1, *Assessing Adverse Health Effects of Exposure to Traffic-Related Air Pollution, Noise, and Their Interactions with Socioeconomic Status*, seeking studies to assess adverse health effects of short- and/or long-term exposure to traffic-related air pollution. The applicants were asked to consider spatially correlated factors that may either confound or modify the health effects of traffic-related air pollution, most notably, traffic noise, socioeconomic

status, and factors related to the built environment, such as presence of green space.

At the time of publication of this report, three studies have been selected for funding and are expected to start in 2018. Payam Dadvand and Jordi Sunyer from the Barcelona Institute for Global Health will set up a new cohort of healthy pregnant women in Barcelona to examine the effects of traffic-related pollution and other factors on birth weight, fetal growth, and placental function. Ole Raaschou-Nielsen from the Danish Cancer Society Research Center, Copenhagen, Denmark, will make use of very large administrative databases to evaluate effects of traffic-related air pollution and other factors on myocardial infarction, stroke, and diabetes in Denmark. Meredith Franklin from the University of Southern California, Los Angeles, will build on the Children’s Health Study in Southern California to evaluate the adverse effects of non-tailpipe emissions and of noise on children’s respiratory health.

In addition, since the release of HEI’s critical review of the traffic literature in 2010, many additional studies about traffic-related air pollution have been published, and regulations and vehicular technology have advanced significantly. Therefore, HEI is currently in the process of conducting a new literature review of the health effects of traffic-related air pollution. Further information on these activities can be obtained at the HEI website, www.healtheffects.org/air-pollution/traffic-related-air-pollution.

REFERENCES

HEI Panel on the Health Effects of Traffic-Related Air Pollution. 2010. *Traffic-Related Air Pollution: A Critical Review of the Literature on Emissions, Exposure, and Health Effects*. HEI Special Report 17. Boston, MA: Health Effects Institute.

HEI STATEMENT

Synopsis of Research Report 194

A Dynamic Three-Dimensional Exposure Model for Hong Kong

INTRODUCTION

Exposure to traffic-related air pollution has been associated with various adverse health effects. However, exposure assessment is challenging because traffic-related air pollution is a complex mixture of many particulate and gaseous pollutants and is characterized by high spatial and temporal variability. A range of models, such as dispersion, land-use regression, and hybrid models, have been developed to estimate exposure to traffic-related air pollution, and these have been largely two-dimensional so far. Dr. Benjamin Barratt from King's College London and his team proposed to estimate exposure to traffic-related air pollution using a dynamic three-dimensional land-use regression (LUR) model for Hong Kong. Such a model would potentially have a wide application given that high-density, high-rise megacities have become more prominent globally. High-rise buildings, which can house hundreds or even a few thousand people, are therefore of great interest and have risen rapidly in most megacities; such buildings can also create urban street canyons, which are the focus of the current study.

APPROACH

The investigators conducted street-level outdoor monitoring campaigns to measure particulate matter $\leq 2.5 \mu\text{m}$ in aerodynamic diameter ($\text{PM}_{2.5}$), black carbon (BC), nitrogen monoxide (NO), and nitrogen dioxide (NO_2) concentrations at about 100 locations during two weeks in the warm season and two weeks in the cold season of 2014. The investigators then constructed exposure models of increasing complexity. First, the measurements were used to develop two-dimensional land-use regression models to estimate long-term exposure for Hong Kong. Among the many predictor variables considered in the models

were *conventional* variables, such as traffic intensity, land-use variables, and distance to sources (e.g., ports or airports), as well as some more complex urban development predictors, such as aspect ratio (the ratio of building height to street width) to capture street canyons.

What This Study Adds

- High-density high-rise megacities have become more prominent globally. This is one of the first studies to integrate vertical gradients and time-activity patterns into an air pollution exposure model.
- Strong aspects of the study include the extensive air quality measurements, the development of exposure models using state-of-the-art approaches, and the application of those models to an existing Hong Kong elderly cohort for epidemiological analyses.
- Associations were fairly similar when comparing results from the complex models to the two-dimensional models for $\text{PM}_{2.5}$, BC, NO, and NO_2 . Neither the incorporation of vertical gradients nor that of dynamic components, including indoor pollutant infiltration, into the exposure estimates resulted in meaningful or consistent changes in the associations with all-natural-cause, cardiovascular, and respiratory mortality in the cohort.
- Based on this and other work, it appears that the addition of a vertical gradient improves exposure model performance, although the added value may be modest, depending on pollutant and study area.

Additionally, the investigators carried out vertical outdoor and indoor air pollution monitoring of PM_{2.5} and BC at four heights at both sides of six streets — four canyon streets and two open streets. The mean sampling heights of the lowest sampling points across the streets was 10 meters above street level (1st residential floor). The maximum sampling height was 60 meters (21st residential floor). Subsequently, outdoor PM_{2.5} and BC data were used to develop three-dimensional land-use regression models. Indoor sampling was included to assess infiltration rates, which were integrated into the dynamic land-use regression model described later.

Next, the investigators developed what they termed *dynamic* models to incorporate time-activity patterns into the land-use regression exposure models, using aggregated data from a large travel behavior survey of Hong Kong residents. This information was combined with results from previous monitoring studies in different modes of transport in Hong Kong to predict exposure in different transport microenvironments.

Finally, Barratt and colleagues applied the exposure models with increasing complexity in an epidemiological study using an existing elderly cohort of 66,000 Hong Kong residents to evaluate the potential impact of exposure measurement error in mortality estimates. The cohort was recruited in 1998–2001, and mortality data were collected until the end of 2011. The average residential height above street level was 39 meters (~11th floor). Exposure was estimated at the recruitment residential address using the 2014 exposure estimates, and back-extrapolated to the recruitment period using data from regulatory monitoring sites. The investigators ran standard Cox proportional hazard models that were adjusted for important individual-level confounder variables, such as age, sex, body mass index, physical activity, smoking, and socioeconomic status.

MAIN RESULTS AND INTERPRETATION

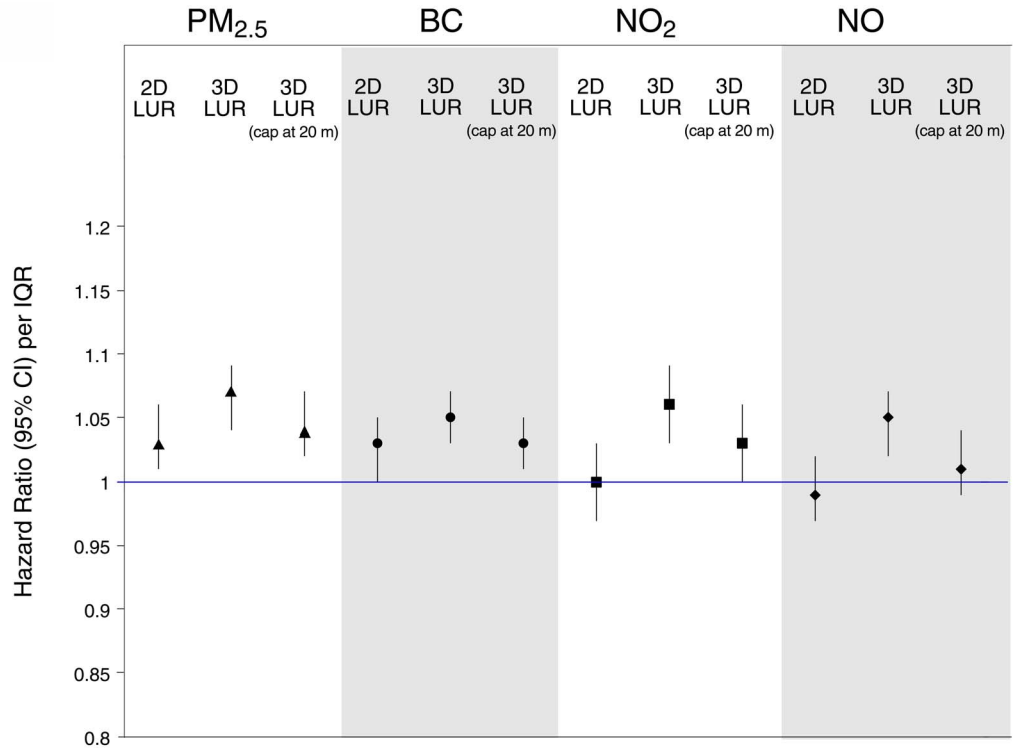
In its independent review of the study, the HEI Review Committee concluded that Barratt and colleagues conducted a novel study — one of the first to integrate vertical gradients and time-activity patterns into an air pollution exposure model. Strong aspects of the study include the extensive air quality measurements, the development of exposure models using state-of-the-art approaches, and the application of those models to an existing Hong Kong elderly cohort for epidemiological analyses.

The Committee concluded that Barratt and colleagues have found fairly similar associations when comparing results from the complex models to the two-dimensional models for PM_{2.5}, BC, NO, and NO₂. Neither the incorporation of vertical gradients nor that of dynamic components, including indoor pollutant infiltration, into the exposure estimates resulted in meaningful or consistent changes in the associations with all-natural-cause (see Statement Figure), cardiovascular, and respiratory mortality in the Hong Kong elderly cohort.

The Committee noted that the investigators encountered many challenges in the study and had developed approaches to compensate for those challenges in a variety of ways, but thought that the impacts of the various workarounds on the results had not been fully explored. For example, in the three-dimensional NO₂ and NO models, the investigators used the decay rate of BC to fill the gap in vertical measurements, but the impact was not further explored. Additionally, the Committee thought that the prediction accuracy of the two-dimensional LUR models was rather modest, which may suggest that alternative modeling strategies and decisions may be necessary for further improvements.

The investigators' further exploration of the vertical gradient component of the model at the Committee's request was revealing because it showed that results were sensitive to the choice of the model. Sensitivity analyses revealed the influence of substituting the modeled two-dimensional LUR estimates for missing measurements at lower floors and assuming that the air was well mixed at heights above 20 meters. The Committee thought more insights were gained from the vertical gradient model than from the dynamic component of the model because the latter was based on aggregated survey data, which makes interpretation difficult.

Based on the current study as well as findings from earlier studies, the addition of a vertical gradient — or more generally street configuration and building height to capture exposure on canyon streets — appears to improve exposure model performance, although the added value may be modest, depending on pollutant and study area. It should be realized that relationships between floor of residence in high-rise buildings and health are complex and highly contextual, and that floor of residence may also act as a confounding factor in air pollution health studies. Although appropriate steps were taken throughout the study to increase generalizability of results, it



Statement Figure. Association between air pollution and all-natural-cause mortality using different exposure models (two-dimensional versus three-dimensional models; dynamic model not shown).

remains unclear to what extent the vertical gradient model is applicable to the entire city of Hong Kong and to other Asian megacities with large populations living in high-rise buildings. Finally, the use of a vertical gradient component in exposure models for

future epidemiological studies that make use of administrative databases is likely to be limited, partly because administrative data do not typically contain residential floor information.

A Dynamic Three-Dimensional Air Pollution Exposure Model for Hong Kong

Benjamin Barratt¹, Martha Lee⁴, Paulina Wong², Robert Tang², Tsz Him Tsui², Wei Cheng², Yang Yang², Poh-Chin Lai², Linwei Tian², Thuan-Quoc Thach², Ryan Allen³, and Michael Brauer⁴

¹King's College London, UK; ²The University of Hong Kong, Hong Kong SAR; ³Simon Fraser University, Canada;

⁴University of British Columbia, Canada

ABSTRACT

INTRODUCTION

High-density high-rise cities have become a more prominent feature globally. Air quality is a significant public health risk in many of these cities. There is a need to better understand the extent to which vertical variation in air pollution and population mobility in such cities affect exposure and exposure–response relationships in epidemiological studies.

METHODS

We used a novel strategy to execute a staged model development that incorporated horizontal and vertical pollutant dispersion, building infiltration, and population mobility patterns in estimating traffic-related air pollution (TRAP*) exposures in the Hong Kong Special Administrative Region (HK SAR).

Two street-level spatial monitoring campaigns were undertaken to facilitate the creation of a two-dimensional

land-use regression (LUR) model. A network of approximately 100 passive nitric oxide–nitrogen dioxide (NO–NO₂) monitors was deployed for two-week periods during the cool and warm seasons. Sampling locations were selected based on population and road network density with a range of physical and geographical characteristics represented. Eight sets of portable monitors for black carbon (BC) and particulate matter $\leq 2.5 \mu\text{m}$ in aerodynamic diameter (PM_{2.5}) were rotated so as to be deployed at 80 locations for a 24-hour period. Land-use, geographical, and emissions layers were combined with the spatial monitoring campaign results to create spatiotemporal exposure models.

Vertical air pollution monitoring was carried out at six strategic locations for two weeks in the warm season and two weeks in the cool season. Continuous measurements were carried out at four different heights of a residential building and on both sides of a street canyon. The heights ranged from as close to street level as practically possible up to a maximum of 50 meters (i.e., below the 20th floor). Paired indoor monitoring was included to allow the calculation of infiltration coefficients to feed into the dynamic component of the exposure model.

The final phase of model development addressed population mobility. A population-representative travel behavior survey ($n = 89,358$) was used to produce the dynamic component of the model, with time-weighted exposure estimates split between home and work or school. Transport microenvironment exposures were taken from published literature. Time–activity exposure estimates were split by age, sex, and employment status.

Development of the exposure model in distinct packages allowed the application of a staged approach to an existing cohort data set. Mortality risk estimates for an elderly cohort of 66,000 Hong Kong residents were calculated using increasing exposure model complexity.

This Investigators' Report is one part of Health Effects Institute Research Report 194, which also includes a Critique by the Review Committee and an HEI Statement about the research project. Correspondence concerning the Investigators' Report may be addressed to Dr. Benjamin Barratt, MRC-PHE Centre for Environment and Health & NIHR GSTFT/KCL Biomedical Research Centre, Analytical and Environmental Sciences Division, Faculty of Life Sciences & Medicine, King's College London, 150 Stamford Street, London, UK SE1 9NH; e-mail: benjamin.barratt@kcl.ac.uk.

Although this document was produced with partial funding by the United States Environmental Protection Agency under Assistance Award CR-83467701 to the Health Effects Institute, it has not been subjected to the Agency's peer and administrative review and therefore may not necessarily reflect the views of the Agency, and no official endorsement by it should be inferred. The contents of this document also have not been reviewed by private party institutions, including those that support the Health Effects Institute; therefore, it may not reflect the views or policies of these parties, and no endorsement by them should be inferred.

* A list of abbreviations and other terms appears at the end of this volume.

RESULTS

The street-level (2-dimensional [2D]) LUR modeling captured important spatial parameters and represented spatial patterns of air quality in Hong Kong that were consistent with the literature. Higher concentrations of gaseous pollutants were centered in Kowloon and the northern region of Hong Kong Island. $PM_{2.5}$ and BC predictions exhibited a north–south/west–east gradient, with higher concentrations in the north-west due to regional transport of particulate pollutants from Mainland China. While the degree of explained variance of the models was in line with other LUR modeling efforts in Asia, R^2 values ranged from 0.46 (NO_2) to 0.59 ($PM_{2.5}$).

Exponential decay rates (k) were calculated at each monitoring location. While it was clear that k values were higher during the warm season than the cool season, no robust patterns were identified relating to the canyon physical parameters. Therefore, a single decay rate was used for each pollutant across the whole region for derivation of the 3-dimensional (3D) exposure layer ($k = 0.004$ and 0.012 for $PM_{2.5}$ and BC, respectively). An alternative decay profile that capped decay at 20 meters above street level was proposed and evaluated. The electrochemical sensors deployed during the canyon campaigns did not exhibit the degree of interunit precision necessary to detect vertical variations in gaseous pollutants, and these results were excluded from the study.

We found that values of the median infiltration efficiencies (F_{inf}) for both BC and $PM_{2.5}$ were especially high during the cool season (91%). F_{inf} values were somewhat lower during the warm season (81% and 88% for $PM_{2.5}$ and BC, respectively), and we found a significant negative correlation between air conditioning use and F_{inf} . The F_{inf} for a mechanically ventilated office building was 45% and 40% during the cool and warm seasons, respectively.

Dynamic exposure estimates were compared against home outdoor estimates. As expected, the addition of an indoor component decreased time-weighted exposure estimates, which were balanced out to some extent by the inclusion of transport microenvironments. Overall, mean time-weighted exposures for the full dynamic model were around 20% lower than home outdoor estimates.

Higher levels of exposures were found with working adults and students than for those neither in work nor study. This was due to the increased mobility of people going to work or school. The exposures to $PM_{2.5}$, BC, and NO_2 were, respectively, 13%, 39%, and 14% higher for people who were under age 18, compared with people who were 65 or older. Exposure estimates for the female population were approximately 4% lower.

The availability of an existing cohort data set of elderly Hong Kong residents ($n = 66,820$) facilitated the calculation and comparison of mortality risk estimates for the different exposure models.

Overall, results indicated that the application of exposure estimates that incorporated infiltration, vertical, and to a lesser extent, dynamic components resulted in higher hazard ratios (HRs) than the standard street-level model and increased the number of significant associations with all-natural-cause, cardiovascular, and respiratory mortality outcomes.

CONCLUSIONS

The results from the study provided the first evidence that considering air pollution exposure in a dynamic 3D landscape would benefit epidemiological studies. Higher HRs and a greater number of significant associations were found between mortality and pollutant exposures that would not have been found had standard 2D exposure models been used. Dynamic models can also identify differential exposures between population subtypes (e.g., students and working adults; those neither in work nor study).

Improved urban building design appears to be stimulating the dispersion of local TRAP in street canyons. Conversely, F_{inf} values found in naturally ventilated buildings were high, and residences provided little protection from ambient air pollution.

We have demonstrated that the creation of effective advanced exposure models is possible in Asian cities without an undue burden on resources. We recommend that vertical exposure patterns be incorporated in future epidemiological studies in high-rise cities where the floor of residence is recorded in health record data.

INTRODUCTION

An increasing proportion of the world's population lives in densely populated urban landscapes. Further, cities in developing countries are projected to absorb nearly all of the future global population growth (United Nations 2015). Many of the world's megacities identified as having the most severe air pollution problems are characterized as high-rise cities with large numbers of people living in tall, densely clustered buildings. Despite this, current TRAP exposure estimates are strictly two-dimensional; neither LUR nor dispersion modeling methods are currently able to account for vertical profiles in air pollution and pollutant behavior. Given this limitation, epidemiological studies of TRAP suffer from exposure misclassification,

and there is a lack of information on exposures to inform risk assessment for land-use and transportation planning.

Most epidemiological studies of the health effects of TRAP estimate exposure based on 2D residential location and do not consider population mobility or time–activity patterns during the day (Smith et al. 2016). In fact, the very actions that lead to TRAP require population mobility and suggest interactions between movement patterns and air pollution levels (Khreis and Nieuwenhuijsen 2017; Spalt et al. 2016). Recent advances in the use of travel smart cards and data mining approaches have facilitated detailed spatiotemporal analysis of individual travel behaviors, providing a much richer and more precise level of detail than is typically available from routine travel surveys (Jensen et al. 2010). For example, a recent analysis of London mobility patterns, based on the aggregation of individual-level Oyster travel smart card data, indicates dramatic population movement into the city core during morning rush hour; lesser, but highly complex movement within the core during the normal workday; and movement back to the periphery at the end of the workday (Gordon 2012). Similar patterns occur in most large cities and can lead to exposure misclassification if not considered (Nyhan et al. 2016; Smith et al. 2016). Simulations based on a travel survey and a regional air quality model (which would not incorporate TRAP exposure gradients) suggest that the incorporation of mobility can affect exposure estimates by as much as 30% (Marshall et al. 2006). Further simulations, including those applied to epidemiological effect estimates derived from LUR models that incorporate mobility, indicate a bias of effect estimates toward the null when mobility is not considered (Setton et al. 2008).

Thus, the development of exposure models that include 3D variability in TRAP and that incorporate population mobility could dramatically reduce exposure misclassification. Further, such models would allow for scenario analysis to assess the impact of changes in transportation patterns and land use on exposure.

A number of published studies have investigated pollutant behavior within street canyons in Asian cities. Chan and Kwok (2000) investigated vertical dispersion of particulate matter in an open street and a street canyon in Hong Kong. An exponential decay function was used to describe vertical dispersion in PM. Vardoulakis and colleagues (2002) also proposed an exponential decay to describe variation in gaseous pollutants within a street canyon in Paris. Li and colleagues (2007) carried out monitoring at four heights within a canyon in Shanghai, China, to study particle size distributions, which they found varied significantly with height. The investigators in these studies were primarily interested in pollutant behavior and did not attempt to apply

their results to health studies or population exposure estimates. Wu and colleagues (2014) investigated the impact of residential height above street level on population exposure in Boston, Massachusetts, U.S.A., downwind of a highway using a mobile monitoring platform and hoist. They found very little variation in $PM_{2.5}$ concentration with height.

As high-density, high-rise cities become increasingly common in Asia, it is important to understand how modeling spatial variation and exposure may differ from European and North American cities where most LUR modeling has been focused (Hoek et al. 2008). European and North American cities have lower pollution and building densities and are likely to have fewer small-scale dispersed pollution sources than the high-density, high-rise cities (Cohen 2004).

Hong Kong, a coastal city in southern China, is one of the most advanced examples of a high-density, high-rise city with significant air quality issues. Being one of the most densely populated regions in the world, Hong Kong has an average population density of 6,690 people/km² with a total population of 7,240,000 as of mid-2014 (Government of Hong Kong Information Services Department 2015). Because of the clustering of developments and mountainous terrain, less than 25% of the total territory of 1,104 km² is developed, leading to extremely high population densities in some areas (Government of Hong Kong 2015; Government of Hong Kong Information Services Department 2015). The clustering effect is further enhanced by the prevalence of high-rise buildings in Hong Kong.

Because of a well-developed network of vehicle flow and pollution monitoring sites, an established public transport system used by 98% of the population, and a current government administration keen on supporting research into their air quality issues, Hong Kong represents an ideal development site for TRAP modeling in high-density, high-rise Asian cities. Such methodology can then be used to inform future modeling in other Asian cities whose information networks are not as well developed.

The study benefitted from an existing cohort of 66,000 elderly residents, with residential floor number recorded as part of the address and a detailed health record database (Schooling et al. 2016). This cohort allowed the study methodology to be evaluated.

The study was a multidisciplinary collaboration between research groups in Hong Kong, the United Kingdom, and Canada with international reputations for air pollution exposure and health assessment research. The team had demonstrable knowledge and experience in each of the study's main themes — LUR modeling, TRAP monitoring and characterization, population mobility, statistical evaluation for population studies, and high-density urban landscapes.

SPECIFIC AIMS

The present study had the overarching aim of creating a dynamic 3D (D3D) TRAP exposure model for Hong Kong, with a fully evaluated methodology that could be applied to other large cities, especially Asian megacities. We hypothesized that the inclusion of dynamic and vertical components in TRAP exposure models applied to Asian cities would lead to increased confidence in associated health outcomes.

The study had three main objectives:

1. to investigate the behavior and distribution of air pollution in a 3D urban landscape with high residential and traffic density;
2. to develop, evaluate, and demonstrate a detailed air pollution exposure model for Hong Kong that would incorporate population mobility and vertical gradients; and
3. to create an incremental exposure assessment methodology that balanced exposure error with input data availability that would be applicable to other megacities across Asia and the developing world.

METHODS AND STUDY DESIGN

PROTECTION OF HUMAN SUBJECTS

The study was approved in the United Kingdom by King's College London College Research Ethics Committee on November 29, 2013, reference BDM/13/14-35. The use of the Hong Kong Elderly Cohort in Work Package 4 (WP4) was approved by the Institutional Review Board of the University of Hong Kong as an amendment to a linked approval, reference UW 11-239. The approved recruitment flyer, information sheet, consent form, and questionnaire documents are included in Additional Materials 1, available on the HEI website. All cohort participants provided informed consent, with ethics approval obtained from the Ethics Committee of the Faculty of Medicine, The University of Hong Kong.

STUDY DESIGN

The study incorporated four work packages (WP1–4):

1. 2D LUR Model Development
2. 3D LUR Model Development
3. D3D LUR Model Development
4. Model Evaluation and Translation

WP1: 2D LUR Model Development

Two street-level spatial monitoring campaigns were undertaken to facilitate the creation of a two-dimensional LUR model following sampling methodologies demonstrated to be effective in state-of-the-art exposure studies such as the Multi-Ethnic Study of Atherosclerosis and Air Pollution (MESA–Air) (Kaufman et al. 2012) and the European Study of Cohorts for Air Pollution Effects (ESCAPE) (Wang et al. 2013). BC, PM_{2.5}, NO, and NO₂ concentrations were measured at approximately 100 locations using a mix of active and passive methods. Land-use, geographical, and emissions layers were combined with the spatial monitoring campaign results to create spatiotemporal models using an approach based on Szpiro and colleagues (2010). Univariate correlations were calculated between pollutant concentrations and each geographical predictor variable. Model performance was evaluated by a leave-one-out cross validation (LOOCV) (Kohavi 1995).

WP2: 3D LUR Model Development

Creation of a LUR capable of assessing exposure in high-rise buildings required an estimation of street-level emission vertical decay rates in a mix of high-density street configurations and meteorological conditions. A comprehensive monitoring campaign was designed to provide the measurements for derivation of a street canyon typology. These decay rates could then be extrapolated across the city and coupled with the 2D LUR model to form a 3D LUR model. Paired indoor monitoring was included to allow the calculation of infiltration coefficients to feed into the dynamic component of the exposure model. The study had pragmatic issues of budget constraints and the number of measuring instruments, which restricted the number of survey sites. Vertical air pollution monitoring was carried out at six strategic locations for two weeks in the warm season and two weeks in the cool season. Continuous measurements were carried out at four different heights of a residential building and on both sides of a street canyon. The heights ranged from as close to street level as practically possible up to a maximum of 50 meters (i.e., below the 20th floor).

WP3: D3D LUR Model Development

The final phase of model development addressed population mobility. Travel behavior questionnaires carried out by the Hong Kong Government were used to produce the dynamic component of the model, with time-weighted exposure estimates split between two locations. Transport microenvironment exposures were taken from published literature. Time–activity exposure estimates were split by age, sex, and employment status.

WP4: Model Evaluation and Translation

Development of the Hong Kong D3D LUR exposure model in distinct packages allowed the application of a staged approach to derive epidemiological effect estimates as applied to an existing cohort data set. Risk estimates for an elderly cohort of 66,000 Hong Kong residents were calculated using the different exposure models with increasing complexity. This modular structure enabled a quantitative and qualitative evaluation of TRAP exposure model design for translation to other developing megacities where data sets may be more limited.

WP1: DEVELOPMENT OF A 2D LAND-USE REGRESSION MODEL FOR HONG KONG

The aim of WP1 was to create a 2D LUR model for Hong Kong as a foundation for future work packages and to allow estimates of exposure in comparison with more detailed LUR models.

Field Sampling

Two sampling campaigns (henceforth referred to as HK2D SC1 and SC2), corresponding to the warm and cool seasons, were conducted in Hong Kong to measure roadside NO₂, NO, PM_{2.5}, and BC concentrations. Sampling of multiple pollutants over different seasons provided a more complete understanding of long-term air quality patterns. NO₂ and NO were collected together using Ogawa badges (Ogawa U. S.A., Pompano Beach, Florida, U.S.A.), while PM_{2.5} and BC were sampled using TSI SidePak AM510 Personal Aerosol Monitors (TSI Inc., Shoreview, MN, U.S.A.), and microAeth AE51 (AethLabs, San Francisco, CA, U.S.A.) monitors, respectively, with both deployed in the same monitoring housing. HK2D sampling was coordinated with an NO₂ sampling campaign conducted by the Environmental Protection Department (EPD) of Hong Kong using Gradko (Gradko International Limited, Winchester, England) diffusion tube samplers. HK2D and EPD sampling occurred during the same periods at many of the same locations. EPD NO₂ data were used to supplement the HK2D NO₂ data.

The first sampling campaign (SC1) ran from April 24, 2014, to May 30, 2014 (37 days), with EPD sampling also conducted within this period. The second campaign (SC2) was split into two periods. PM_{2.5} and BC sampling ran from November 18, 2014 to January 6, 2015 (50 days). Because of civil protests in Hong Kong at the end of 2014, which affected traffic patterns, the EPD delayed their sampling from November 2014 to January 2015 (January 3, 2015, to January 26, 2015, 24 days); the HK2D NO₂ and NO sampling was similarly delayed.

Ninety of the 100 HK2D sites were selected from the 173 EPD campaign sites. The remaining 73 EPD sites were excluded because of proximity to overpasses. The sites were selected to capture maximum variation in concentrations within districts and were all roadside sites, mainly in developed areas. Ten additional sites were identified to expand spatial coverage and capture variation in land use where perceived gaps occurred in the EPD's site distribution. Because of logistics limitations, not all pollutants were sampled at all 100 sites; NO₂ diffusion tube samplers were deployed at 97 sites, Ogawa NO/NO₂ badges were deployed at 43 and 63 sites (SC1 and SC2, respectively), PM_{2.5} and BC samplers were deployed at 84 sites. Subset site selection was based on geographic location, annual average daily traffic (AADT), land use, and population density — aiming to capture a full range of values for these factors. Also, because of logistics and equipment limitations, not all sites were simultaneously sampled.

Sampling campaign study sites are detailed in Appendix A, Table A.1 and Figures A.1 and A.2, available on the HEI website.

Samplers were preferentially deployed on lampposts, approximately 2.5 meters off the ground. Traffic signs, trees, and portable posts were used in a limited number of cases when a lamppost was not available. Diffusion samplers (Ogawa badges and diffusion tubes) were deployed for durations of 15 to 21 days. Ogawa badges were outfitted with two filters (one to capture NO₂ and one to capture oxides of nitrogen [NO_x] with the difference used to calculate NO concentrations) and hung within a white shelter to protect them from sunlight and rain. The EPD deployed three diffusion tubes per site during each campaign. SidePak and microAeth sensors were deployed for 24 hours, except for four two-week sampling sites, which were used for quality control and to develop temporal correction factors. Each pair of PM_{2.5} and BC sensors was housed in a waterproof box with sampling lines run through a downward facing hole; it was protected from rain ingress by a funnel.

Ogawa badges and HK2D diffusion tubes were colocated at ten of the rooftop air quality monitoring stations (AQMS). A SidePak and microAeth were deployed at one of these sites in SC2 for two weeks. Ogawa badges, diffusion tubes, SidePaks, and microAeths were also colocated at each of the three roadside AQMS sites. Duplicate Ogawa badges were used in each campaign along with field and lab blanks.

Pollutant Concentrations

Ogawa badges with NO₂ and NO were analyzed using ion chromatography in the Occupational and Environmental Hygiene Laboratory of the University of British Columbia. Diffusion tubes were analyzed by Gradko Environmental using UV spectrophotometry (Gradko 2012).

A blank correction factor, the average of the appropriate diffusion samplers' field blanks deployed during the sampling campaign, was subtracted from the raw NO₂ and NO concentrations. The diffusion tubes were then adjusted toward the Ogawa badges to normalize NO₂ and NO concentrations for modeling. This correction factor was calculated by linear regression with a zero intercept (no data provided).

The first and last five minutes of each continuous monitoring period (PM_{2.5} and BC) were removed to account for setup and collection of samplers. The data were also cleaned to remove periods of negative values: after filter changes, when sensors were dislodged, or during periods of significant signal noise. PM_{2.5} data were scaled to the reference filter dynamic measurement system (FDMS) monitors housed in the AQMS using a correction factor derived from linear regression based on the two-week collocation runs. This bias correction factor was individually scaled to account for between-SidePak monitor differences using pre- and post-campaign collocation precision tests. BC was not bias adjusted, as the reference monitors were not operating during the collocation period, and therefore no comparison data were available. Filter loading of the microAeths, which causes under-sampling of the BC level as BC mass builds up on the filter, was corrected for using the Virkkula method (Virkkula et al. 2007), where corrected BC = (1 + β × attenuation) × uncorrected BC. The seasonal mean attenuation factor β was derived by comparing changes in readings immediately before and after the microAeth's filter change during the collocation periods at the AQMS sites. After adjustments, samples with less than 18 hours of PM_{2.5} and BC data were removed, as capture rates of less than 75% were deemed inadequate to represent the 24-hour concentration. Sites with 36 hours or more of capture (such as the two-week sites) were split evenly into subsets (18 to 35 hours), and one subset was randomly chosen to represent the site.

A temporal adjustment was then applied to all concentration data to remove the effects of temporal variation on captured concentrations, due to fluctuations in the baseline concentrations when the exposure periods varied between sampling sites. This adjustment was created by calculating the baseline concentrations for the sampling period using the average daily concentrations from all urban rooftop AQMS and then dividing by the baseline concentration for the whole sampling period:

$$CF_T = \frac{\sum_{u=1}^{11} Mean_{SP,u}}{\frac{11}{\sum_{u=1}^{11} Mean_{R,u}}}, \quad (1)$$

where u is the AQMS; $Mean_{SP,u}$ is the average concentration for the full sampling period for each AQMS; $Mean_{R,u}$ is the average concentration for the sampler's exposure period for each AQMS; and CF_T is the temporal correction factor.

Uncorrected PM_{2.5} and BC data and more details regarding the temporal correction factors for each location and pollutant are provided in Additional Materials 1 (available on the HEI website).

Predictors

Candidate spatial metrics were selected based on those used in other LUR models (Allen et al. 2013; Brauer et al. 2006; Chen et al. 2010; Saraswat et al. 2013; Tang et al. 2013; Wang et al. 2013); Hong Kong's public policies on growth, development, and public health; and regulations on air quality. Potential predictor variables (spatial metrics) were divided into two groups: (1) variables representing a point value; and (2) variables representing the cumulative values of an area (buffer variables). Buffered variables were either represented as a density value (standardized by buffer area) or a total value, based on usage in the literature. ArcGIS (ESRI, Redlands, CA, v10.1 and 10.2) and R (R Foundation for Statistical Computing, Vienna, Austria, v3.3.2) were used to evaluate, modify, extract, and aggregate potential predictor variables. In total, 373 spatial predictor variables were calculated — 364 from spatial data layers and 9 (predicted NO₂) from the NO₂ LUR models, which were used solely for NO modeling. All possible predictor variables are listed in Appendix Table A.2 (available on the HEI website).

Model Building

For each pollutant, a model was built using SC1 data, SC2 data, and the average of SC1 and SC2 data (combined) for sites that were sampled in both campaigns. Three additional models were built for each of the three traffic predictor types (road length, AADT, and traffic loading) for a total of 36 models (4 pollutants × 3 SC data sets × 3 traffic predictors).

To be offered to models, each variable had to have at least two nonzero values. Within each of the buffered variable groups (e.g., industrial land use), buffer radii were ranked by Pearson correlation. The pollutant with the top-ranked buffer radius was selected, and any variables in that group that were highly correlated with the selected variable were dropped ($r > 0.6$). Next, the second- and third-ranked of the remaining buffer radii were also offered to models. For distance variables, either the Euclidean or natural log variable was selected based on correlation with the pollutant. All selected variables were

then offered to an exhaustive automated selection process (*regsubset* function in the *leaps* package in R [Lumley 2009]) with maximum adjusted R^2 used for selection. The maximum number of predictors selected was set to one for every ten observations. Predictors were removed if their sign was inconsistent with a priori hypotheses or if not statistically significant ($P \geq 0.10$), and the automated selection process was then repeated until no more variables were dropped. If any model included variables with two buffer radii within 1,500 meters and coefficients with opposite signs, the variable with the lower P value was dropped, and the variable selection process was rerun.

Evaluation

Models were evaluated using LOOCV, and for NO_2 models where more sampling sites were available, 20 sites were selected randomly for hold-out evaluation (HEV) prior to modeling (Hoek et al. 2008).

Model assumptions were tested using diagnostic plots, variance inflation factor (VIF, a measure of multicollinearity), and the Moran I (a measure of spatial autocorrection). VIF cutoff was set at three, based on the available literature (Aguilera et al. 2008; Amini et al. 2014; Clougherty et al. 2013; Gulliver et al. 2013; O'Brien 2007).

WP2: VERTICAL MONITORING FIELD CAMPAIGN AND DEVELOPMENT OF A 3D LUR MODEL

The aim of WP2 was to augment the 2D LUR created in WP1 with a vertical and horizontal TRAP rate of decay layer to create a citywide 3D LUR model. This was achieved through seasonal vertical monitoring campaigns in six selected sites across the region.

Selection of Sampling Sites

Because of practical and budgetary limitations, vertical sampling was initially restricted to four canyon locations and two open locations. Sampling sites were selected in a range of locations representative of population exposure. A series of classification screening tests was first carried out to identify candidate locations, followed by field visits to establish suitability from a practical perspective.

First, paper land-use maps were obtained from the Hong Kong Government Planning Department. These maps were converted into digital format and updated using digital orthophotos from the Hong Kong Government Lands Department. This allowed neighborhoods to be classified into three categories:

- Class 1 — Tall high-rise buildings in residential areas; mostly recently built, with large empty spaces with green areas between buildings. Represented by

communities in the New Territories, parts of Kowloon, and North Point on the Hong Kong Island.

- Class 2 — A mix of recent and old high-rise buildings with a high floor occupation. Represented by densely populated parts of the Hong Kong Island, such as Central and Wan Chai districts.
- Class 3 — Chinese style buildings; thin buildings of three to six stories. Represented by old settlement areas of Hong Kong.

Second, candidate sampling locations within selected neighborhoods were identified by considering population density, traffic flows, canyon aspect ratio, canyon length, and prevailing winds. A more detailed description of the selection process is contained in Appendix Table A.4 (available on the HEI website).

Third, a field visit was conducted to inspect the physical layout and alignment of candidate sites, discuss access with building managers, and identify strong confounding local non-TRAP sources, such as building works. During this process, it became clear that, while Class 3 buildings often represented the worst case scenario of very narrow canyons coupled with high local traffic flows, access to these buildings was very complex and of unacceptably high risk to researchers. However, this class of residential building is becoming increasingly rare as government clearance and reconstruction initiatives replace them with newer Class 1 or Class 2 buildings.

Recruitment Process

As the study design required access to multiple residential homes, significant effort was required to recruit households to the study. Initial contact was by mail. At each potential sampling location, recruitment letters were sent to all flats and apartments below the 20th floor that had openable windows facing the target street side. Recruitment of a total of 40 homes was required in the study design (approximately 1% recruitment rate); however, these homes had to be distributed on or close to specified floors. A total of 3,500 recruitment letters were mailed across eight potential sampling locations, with an overall response rate of 4%. Recruitment at lower floors was particularly challenging, resulting in the rejection of some potential sampling sites. Telephone interviews followed by flat visits were conducted with all respondents to assess compliance with recruitment criteria: (1) residents must be nonsmokers, (2) suitable space must be available facing the street for placement of monitoring equipment, and (3) at least one household member must be available during the daytime over the two-week period in both the summer and winter campaigns to allow researcher access into the flat to

replace filters and check equipment. One resident of each participating home unit was also asked to maintain a record of their daily activities inside the premises. The participating resident of a home unit fully engaged in both campaigns was compensated an amount of 800 HKD (~100 USD).

All recruitment information and questionnaire templates are available in Additional Materials 1.

Vertical Sampling Campaign

TRAP monitoring equipment had to be portable enough for installation inside a residential flat and be sufficiently quiet to be situated in a living area without inconveniencing the residents. PM_{2.5} and BC were sampled at a one-minute time resolution using TSI SidePak AM510 (TSI Inc., Shoreview, MN, U.S.A.) and microAeth AE51 (AethLabs, San Francisco, CA, U.S.A.) monitors, housed in a soundproof box. AQMesh (Environmental Instruments Ltd, Stratford-upon-Avon, UK) electrochemical monitoring pods were used to record carbon monoxide (CO), NO, NO₂, ozone, temperature, and humidity at a 15-minute time resolution.

The ideal distribution of monitoring units is shown in Figure 1. However, the screening process revealed that very few candidate sites had residences at the ground floor. The typical layout of high-rise buildings in Hong Kong is to have commercial, retail, or restaurant concerns on the lower two or three floors. Consequently, the mean height above street level of the lowest monitoring point was 10.2 meters across the six canyons.

Once suitable flats had been identified and recruited to the study, eight sets of monitoring units were installed outdoors, up both sides of the canyons (positions A and B in Figure 1). After seven days of continuous monitoring, the monitors on the windward side of the canyon were moved indoors to the same location as the leeward side monitors to monitor indoor concentrations (position C in Figure 1) for a further seven days. After prior arrangement with the resident, the equipment was connected to a power supply and set near a window facing the street away from the kitchen. Where residences had suitable balconies, the outdoor unit was placed outside. Otherwise, sample lines were passed out of windows, which were then taped shut unless the resident routinely left that window open. A fanned manifold system was used for the passive electrochemical AQMesh unit. MicroAeth filters were changed by a researcher every two to three days.

After two weeks of continuous sampling, all equipment was removed and installed at the next sampling site.

In collaboration with the Hong Kong EPD, additional canyon monitoring was carried out during the warm season of 2015 to extend the range of canyon sampling sites. The surrounding building topography at each AQMS monitoring site was inspected, and five of these were found to be suitable for canyon monitoring. Sampling units were placed alongside AQMS equipment and at street level (for rooftop sites) or rooftop level (for roadside sites) for seven days. Measurements taken at the five paired roadside-rooftop locations were used as independent data sets to evaluate the application of calculated decay rates.

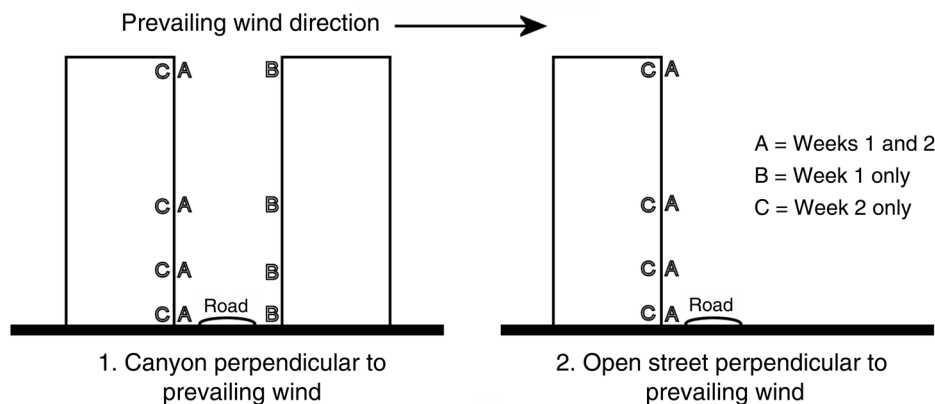


Figure 1. Spatial distribution of monitoring devices: (1) a street canyon and (2) an open street. A = leeward side (outdoor); B = windward side (outdoor); C = leeward side (indoor).

The warm season vertical monitoring campaign ran from August 7, 2014, to September 25, 2014 (first four sites), and from May 5, 2015, to June 23, 2015 (remaining sites). The cool season vertical monitoring campaign ran from October 31, 2014, to March 26, 2015 (all sites).

Data Quality Control

Interunit precision was particularly important to this study because of the potentially small vertical gradients in pollutants. Before and after each seasonal campaign, all monitoring units were operated for a period of at least 48 hours in the same location to test precision. Throughout the measurement period of each monitoring campaign, one set of monitoring equipment was colocated at the nearest AQMS reference monitoring site to allow reference scaling and subsequent temporal correction. However, no reference BC monitors were available for scaling of the micro-Aeth units. Reference correction of Sidepak and AQMesh monitors was calculated separately for each campaign to allow for variable atmospheric conditions. Sidepak units were flow checked and zero calibrated with HEPA filters prior to each canyon deployment.

Previous studies have shown that the default aethalometer algorithm underestimates BC concentration as the BC mass on the filter increases (Kirchstetter and Novakov 2007; Park et al. 2010). A number of different methods were tested to correct this effect, resulting in a method that followed Virkkula and colleagues (2007), with attenuation correction factors (β) derived for each canyon and season.

After precision and reference scaling, data were cleaned to remove outliers, defined as concentrations lying outside of three standard deviations (SDs) from the mean of the combined concurrent canyon measurements. These outliers represented either short-lived local sources that were not relevant for decay-rate calculation or instrument noise or malfunction. Measurements taken during the first and last five minutes of each deployment were excluded to allow for instrument stabilization, set up, and take down.

Calculation of Decay Rates

Only data where valid measurements were available from all outdoor vertical sampling points on side A were used for decay rate calculation. Data sets from individual outdoor monitors returning less than 50% valid capture for the two-week deployment were removed. The threshold was initially set at 75%, but this resulted in too few sampling heights becoming available for decay rate calculation, an indication of the impact of the harsh operating environments causing frequent equipment faults.

The exponential relationship between pollutant concentration and height is expressed as:

$$C_h = C_0 e^{-kh}, \quad (2)$$

where C_h is the concentration at height h , C_0 is the concentration at the ground level, h is the height in meters from the emission source (street level), and k is the decay rate constant (Capannelli et al. 1977; Chan and Kwok 2000).

Decay rate constants were calculated for each canyon and each season by averaging all log-transformed outdoor measurements at each height, and then deriving loglinear gradients. Data were further split by hour of day to investigate diurnal variations in decay rate constants.

This process revealed a shortcoming in the field campaign design caused by practical constraints of instrument siting. As described above, the mean lowest sampling point across the canyons was 10.2 meters, leaving an important gap in the decay rate curve from street level to this first sampling point. Evidence from the supplementary monitoring carried out at street and rooftop level alongside AQMS sites indicated that the majority of the dispersion of local TRAP emissions occurred over this initial distance. To fill this gap, we extracted the modeled concentrations from the 2D LUR relating to the latitude and longitude of each canyon campaign site. This approach was based on the ultimate goal of merging the 2D model with the vertical decay measurements to create the 3D model. We then applied temporal correction using measurements from the nearest roadside AQMS to create warm and cool season means matched to each campaign's sampling dates. These points were added to each decay rate calculation at a height of 2 meters (the height at which street-level roadside sampling was carried out). As BC monitoring was not routinely carried out at the AQMS sites, temporal correction factors for BC were derived from NO_x concentrations; therefore, there is a greater uncertainty in street-level BC estimates in the canyon decay calculations.

Calculation of Infiltration Efficiencies

The infiltration efficiency (given by F_{inf}) for each residence where paired in-out sampling was undertaken was derived for $\text{PM}_{2.5}$ and BC using procedures described by Allen and colleagues (2012). F_{inf} is a unitless quantity defined as the equilibrium concentration of outdoor pollution that penetrates indoors and remains suspended. The derivation model states that the average indoor concentration during time period t (C_{in}^t) is equal to the sum of a fraction of the average outdoor concentration during the same time period (C_{out}^t), a fraction of the average indoor concentration from

the previous time period (C_{t-1}^{in}), and the contribution from indoor sources (S_t^{in}):

$$C_t^{in} = a_1(C_t^{out}) + a_2(C_{t-1}^{in}) + S_t^{in}. \quad (3)$$

Parameter a_1 describes the fate of ambient particles once they penetrate indoors; a_2 describes the decay of indoor particles. We applied a censoring algorithm to identify periods impacted by indoor sources. Typically, only the rising edge (and not the decay) of the indoor peak was censored because at the time (t) when an indoor source is shut off and the indoor concentration begins to decay, the S_t^{in} term in Equation 3 becomes zero, and the particles generated by the indoor source become part of the C_{t-1}^{in} term (i. e., part of the indoor concentration during the previous time step). Retaining the decay of indoor peaks provides information from which to estimate the total particle loss rate, which is a key component of a building's infiltration efficiency.

The censoring method does not identify constant indoor sources. Unidentified (constant) indoor sources would be incorrectly considered to be outdoor particles that have infiltrated, thus causing an overestimation of F_{inf} . This is unlikely to cause a major bias in the estimates of infiltration efficiency because pollution resulting from indoor sources generally occurs as spikes relating to resident activities, displaying a rapid increase and subsequent decay (Abt et al. 2000). Thus, constant indoor sources may account for a very small percentage of the total indoor contribution in most residences.

After censoring, F_{inf} was estimated using a linear regression (forcing the intercept to zero) of Equation 4 to solve for a_1 and a_2 . F_{inf} was then calculated from

$$F_{inf} = \frac{a_1}{1 - a_2}. \quad (4)$$

Basic diary cards (English version) were kept by residents during the campaigns, an example of which is shown in Additional Materials 1 (available on the HEI website). Information on cooking, window opening, and air conditioning use during the warm and cool seasons was used to investigate variations in F_{inf} and incidences of indoor spikes for censoring. Participants were not allowed to smoke inside.

Additional monitoring was carried out inside and outside of an administrative building within the University of Hong Kong, Pok Fu Lam district, for seven days in the warm season using the same methodology to establish infiltration efficiencies for mechanical ventilation and air conditioning (MVAC) system buildings for use in the dynamic model (WP3).

WP3: INTEGRATION OF POPULATION MOVEMENTS TO CREATE A DYNAMIC 3D LUR MODEL

The aim of WP3 was to assimilate, characterize, and integrate population movement to create a dynamic LUR model layer for the population of Hong Kong, utilizing the 2D LUR created in WP1 and the Hong Kong Government's Travel Characteristics Survey.

Population Mobility Data

For this project, we used a large population-representative survey to characterize travel behavior and population movement patterns in Hong Kong. The Travel Characteristics Survey 2011, published by the Transport Department of Hong Kong, polled 50,000 randomly chosen households, with each household member providing detailed trip information, including time and duration of journey to place of work or study (Transport Department 2014). The number of subjects totaled 101,385, with self-reported mode, route, and frequency of travel recorded during the sample day. The survey did not capture weekend travel patterns. Individual data on age, sex, and occupation were available for each subject, but no information on residential or work/school addresses. The survey allowed generalized patterns in territory-wide weekday travel movement to be derived. In addition, we also used the Hong Kong 2011 Census to validate results (Census and Statistics Department 2011). The use of a smart payment card for travel is widespread in Hong Kong; however, these data were not accessible for this study because of privacy and data protection concerns.

Deriving Population Movement Patterns

From the original number of subjects ($N = 101,385$), we established some assumptions to exclude subjects who may not represent the general population travel pattern, or may not represent the population typically studied in air pollution cohorts. We excluded subjects who (1) were professional drivers; (2) were mobile residents and domestic helpers; and (3) had made cross-boundary trips and trips to airports, as they were assumed to travel outside the study area. After these exclusion criteria were applied, the total number of subjects included in model development was 89,358. The impact of application of exclusion criteria on subject numbers is shown in Appendix Table A.11.

Next, we constructed time-activity patterns for each survey subject, based on information on the travel time, location, and purpose of the trips they made during the survey day. We assembled this information on population mobility from the survey data in detail, including movements between tertiary planning units (TPUs) per hour of the day. TPUs are the smallest spatial administrative units

in Hong Kong ($N = 289$, TPU map shown in Appendix Figure A.21), devised for population census and town planning purposes. Data from the Hong Kong 2011 Census were also available at the TPU level.

Subjects with Missing Trip Information

Because of the questionnaire design of the Travel Characteristics Survey, only trips made on mechanized modes of transport were recorded in detail. There were around 34,071 subjects who had trips with walking as their mode of travel, and therefore had missing time–activity information between trips. To resolve this, we developed a systematic method to replace gaps in trip information. First, we estimated each walking trip to last for 15 minutes, the population average duration as suggested by local walkability studies (Cerin et al. 2011). The subjects were then classified into population subgroups, assuming they commuted to school and work locations on foot in the same TPU. This assumption is consistent with the 2011 Census, which suggested a large proportion of students commute on foot to schools located in the same district. For those who were neither in work nor study, a review of population time–activity patterns (Chau et al. 2002) indicated that these people spend about 86% of the time in a day indoors in Hong Kong. The same assumptions were applied for subjects with a combination of mechanized and walking trips who had missing hours.

Time-Weighted Air Pollution Exposure

Time–activity patterns were derived for each survey subject. We then combined these with predicted air pollution concentrations in outdoor, indoor, and transport microenvironments and accounted for diurnal pollution patterns to calculate the time-weighted air pollution exposure for each survey subject.

The general form of the equation used to calculate time-weighted exposure was

$$E_i = \sum_j^J C_j t_{ij}, \quad (5)$$

where E_i is the time-weighted integrated exposure for each subject i ; C_j is the pollutant concentration in microenvironment j ; t_{ij} is the aggregate time that subject i spends in microenvironment j ; and J is the total number of microenvironments that subject i moves through during the sample day.

Exposure in Different Microenvironments

We defined the microenvironments where subjects were exposed to TRAP as (1) home indoor; (2) commercial indoor; (3) school indoor; (4) other indoor; (5) outdoor; and

(6) in transit. Examples of building types for each classification are described in Appendix Table A.12.

A staged modeling approach was used to assess the impact of dynamic model components on estimated TRAP exposure, starting with static, then moving to more sophisticated dynamic components representing different outdoor, indoor, and transport microenvironments in a series of stages. The modeling stages and associated time-weighted exposure equations were as follows:

1. Static outdoor
2. Static indoor
3. Dynamic indoor
4. Dynamic indoor + in transit
5. Dynamic indoor + in transit + diurnal variation
6. Dynamic outdoor + in transit + diurnal variation

Stage 6 was included as a sensitivity test to separate the impacts of mobility and infiltration efficiencies.

We calculated the time-weighted exposure for each subject for each stage. The total exposure to TRAP in each model component was calculated by multiplying the time each individual spent in each microenvironment by the pollutant concentration at the specific microenvironment, considering the spatial (i.e., movement between TPUs) and, where relevant, the pollutant diurnal profile. Each component estimate was then summed and divided by the total time T . For example, to calculate the time-weighted exposure for a subject at Stage 4, we used

$$TWE_T = \frac{[C_h t_h + C_w t_w + C_s t_s + C_{oi} t_{oi} + C_o t_o + C_t t_t]}{T}, \quad (6)$$

where C_h , C_w , C_s , C_{oi} , C_o , and C_t are the pollutant concentrations at home indoor, commercial indoor, school indoor, other indoor, outdoor, and in transit microenvironments, respectively; t_h , t_w , t_s , t_{oi} , t_o , and t_t are the time spent each in the respective microenvironment; and T is the total duration of time–activity pattern in hours, based on the subject's movement data.

Air Pollution Data

There were four components to the air pollution exposure estimates: (1) mean predicted ambient concentrations for each TPU; (2) indoor microenvironment factors; (3) transport microenvironment exposure concentrations; and (4) diurnal profile factors. Dynamic model estimates were produced for BC, NO₂, and PM_{2.5}.

Outdoor exposure concentrations were extracted from the 2D LUR model and averaged across the TPU boundaries, using the Zonal Statistics function in ArcMap (ESRI; ver 10.2). We could not use 3D exposure estimates in this

component as the floor of residence was not available in the travel survey database.

We estimated pollutant concentrations in indoor microenvironments with the use of infiltration efficiencies derived in WP2 from the canyon monitoring campaign. Indoor–outdoor relationships obtained from local studies were used for NO₂ (Lee and Chang 2000; Lee et al. 2002). Air conditioning systems are used extensively in nonresidential buildings in Hong Kong; therefore different infiltration efficiencies were used for indoor microenvironments with natural ventilation or with the use of MVAC systems (Table 1).

School buildings were assumed to be naturally ventilated, as the use of ceiling fans is common (Lee and Chang 1999). Window-type air conditioners are installed in classrooms; however, infiltration would differ from offices with central MVAC systems, and students do not spend time at schools during summer holidays when air conditioning use is most common.

For transport microenvironments, we reclassified 23 modes of travel used in the survey and matched data with monitored concentrations in transport microenvironments from local studies. For PM_{2.5}, we used the PM₁₀ (PM ≤ 10 μm in aerodynamic diameter) concentrations reported in Chau and colleagues (2002), with guideline PM₁₀/PM_{2.5} conversion factors from the Hong Kong EPD (Environmental Protection Department 2016). As only a few studies have investigated transit levels of BC and NO₂ in the study area, we estimated pollution levels from personal monitoring studies (Chan et al. 1999; Yang et al. 2015) and used PM ratios to predict concentrations in transport modes that were unavailable (Table 1).

Diurnal adjustment factors were derived by calculating the mean ratio of hour-of-day mean concentration by annual mean concentration across the government network monitoring sites between January 1, 2013, and January 1, 2015. Factors ranged from 0.86 to 1.13 for PM_{2.5}, 0.46 to 1.37 for BC, and 0.55 to 1.37 for NO₂. Minima for all three pollutants occurred at 04:00. Maxima occurred at 20:00, 08:00,

Table 1. Infiltration Efficiency of Building Microenvironments and Concentration in Different Transport Microenvironments Used in the Dynamic Model Components

Indoor Microenvironments		Infiltration Efficiency (F_{inf})		
		PM _{2.5}	BC	NO ₂
Home indoor		0.82	0.89	0.79
Commercial indoor		0.40	0.45	0.72
School indoor		0.92	0.88	0.71
Other indoor		0.92 natural 0.40 MVAC	0.88 natural 0.45 MVAC	0.70 natural 0.72 MVAC
Transport Microenvironments ^a		Concentration (μg/m ³)		
		PM _{2.5}	BC	NO ₂
	Number of Trips			
Private/car	10,505	71	21	130
Bus	51,071	103	31	130
Minibus	19,104	103	31	109
Truck/van	212	90	27	130
Mass transit rail (underground)	48,333	69	21	47
Mass transit rail (surface)	1,549	71	21	66
Tram	784	88	26	147
Ferry	244,326	64	19	96
Walking	585	44	13	139
Bicycle	318	44	13	139
Motorcycle	10,505	44	13	139

^a The air pollution values from the transport microenvironments were derived from local studies (Chan et al. 1999, Chau et al. 2002, Yang et al. 2015).

and 18:00 for PM_{2.5}, BC, and NO₂, respectively. Factors are shown in Appendix Table A.13.

Data Analysis

After calculation for staged exposure estimates for all 89,358 subjects, we examined how the time-weighted exposures varied across the population. Stratified analyses on age, sex, and population subgroups were carried out. The survey subjects were categorized into three age groups: <18, 18–65, 65 and older; and into three population subgroups according to their occupations: students, working adults, and those who are neither in work nor study. These age categories were derived based on the range and distribution of the youngest and oldest individuals. All statistical analyses were carried out using R software.

WP4: MODEL EVALUATION AND TRANSLATION FOR APPLICATION IN OTHER MEGACITIES

The aim of WP4 was to contrast epidemiological effect estimates based on an existing cohort of 66,000 Hong Kong residents above the age of 65. Risk estimates and confidence intervals (CIs) were calculated for a range of health outcomes using increasing exposure model complexity: 2D, 3D, and D3D.

Cohort Data

This study utilized data from the Elderly Health Service of the Hong Kong Department of Health, as described in detail by Schooling and colleagues (2016). In brief, the study includes 66,820 participants, 65 years or older, who enrolled in the Elderly Health Centers from July 1998 to December 2001. Elderly Health Centers located in each of the 18 districts in Hong Kong provided health assessments, using standardized and structured interviews and comprehensive clinical examinations. Information on sociodemographic, lifestyle, and disease history was collected by doctors and registered nurses (Lam et al. 2004b). The cohort was set up to promote understanding of aging in this developed non-Western setting where the patterns of common chronic diseases and their determinants may differ from those in the West. Hong Kong is an ideal place to study the association between long-term air pollution exposure and health, because of its low levels of smoking and alcohol use but relatively high levels of air pollution exposure.

All enrollees were recruited on a voluntary basis, accounting for 9% of the 65 or older population at the baseline year (the sampling fractions ranging from 6.6%–17.5% of the population older than 65 years of age in each district; Census and Statistics Department 2002). The participants were self-selected for enrollment and were enrolled at a

preventive service, so they may be more health conscious and less likely to be missing in the follow-up, which may lead to a selection bias. Detailed characteristics of the study cohort are provided in Table 2.

The recruited subjects were followed up for mortality outcomes until the end of 2011. Death records were the primary follow-up source in this study (with an average of 10.3 years and a range of 1–13 years of follow up). Vital status and causes of death were ascertained by record linkage to death registration in Hong Kong using a unique identity card number. Most of the Hong Kong residents died in the hospital, ensuring accurate ascertainment

Table 2. Descriptive Statistics for Health and Covariate Variables in the Analysis

Variable	Percent or Mean ± SD N = 60,548
Individual Level	
Age at entry	70.2 ± 5.5
Sex	
Male (%)	19,739 (32.6)
Female (%)	40,809 (67.4)
BMI quartiles:	
1 st [<21.6] (%)	31,001 (51.2)
2 nd – 3 rd [21.6–26.3] (%)	13,260 (21.9)
4 th [>26.3] (%)	16,227 (26.8)
Smoking status	
Never (%)	44,079 (72.8)
Former (%)	11,020 (18.2)
Current (%)	5,389 (8.9)
Exercise in days per week	
Never [0] (%)	9,082 (15.0)
Medium [1–6](%)	7,811 (12.9)
High [7](%)	43,655 (72.1)
Education	
Below primary (%)	27,792 (45.9)
Primary (%)	22,342 (36.9)
Secondary or above (%)	10,475 (17.3)
Expenses/month in USD	
Low [<128] (%)	10,051 (16.6)
Medium [128–384] (%)	41,536 (68.6)
High [≥385] (%)	8,961 (14.8)
TPU^a Level	
Age ≥65	12.1 ± 4.2
> Secondary education	13.1 ± 8.0
Income ≥ 1,923 USD/month	60.0 ± 11.6
District Level	
Smoking rate	11.0 ± 0.9

^a TPU = tertiary planning unit.

of the cause of death. Those whose vital status could not be determined were assumed to be alive. The exact residential address at baseline and changes of address during follow-up were available for all subjects.

Health Outcomes

The health outcomes were defined on the basis of the underlying cause of death recorded on the death registration. Deaths from all natural causes and from cardiovascular and respiratory diseases were assessed. The cause of death was coded as per the International Classification of Diseases, 10th Revision (ICD-10; World Health Organization 2016b) with the following categories: natural causes (codes A00–R99); cardiovascular diseases (I00–99) with subcategories of ischemic heart disease (IHD; I20–25) and cerebrovascular disease (I60–69); respiratory diseases (J00–47, 80–99) with subcategories of pneumonia (J12–18) and chronic-obstructive pulmonary disease (COPD; J40–44, 47); and external causes (S00–T99). Study participants were excluded from analysis if they died within one year of enrollment or from a cause other than the categories above.

Exposure Data

Exposure to Air Pollutants We used the modeled pollutant concentrations from the cross-validated LUR models created in earlier work packages. Predicted annual concentrations of PM_{2.5}, BC, NO, and NO₂ for 2014 were available as raster layers for the study area. The predicted concentrations were truncated to the measurement range recorded from monitoring campaigns. In addition, for NO the prediction surface was smoothed to 500 meters to improve the distribution of exposure estimates. A geographical layer was constructed to combine the geocoded baseline addresses of participants and the pollution surface. The 2014 exposure estimates of subjects were extracted, and then back-extrapolated to the cohort baseline period (1998–2001). These estimates were adjusted for vertical and dynamic components, based on the floor of the residential address and generalized population exposure characteristics, respectively. Overall air pollution exposure estimates (i.e., 2D, 3D, and D3D) for all pollutants (i.e., PM_{2.5}, BC, NO, and NO₂) were produced and assigned to all participants based on their residential addresses at baseline periods. The distributions of the predicted exposures were evaluated and checked for extreme values.

Back-Extrapolation of Exposure Estimates To estimate historical exposures, we used measurements from the eight rooftop government network stations that had been in operation during the entire study period (1998–2014). The data were used to calculate trends in pollutant concentrations over time and correlations between pollutant

concentrations of different years. These factors were then applied to the LUR modeled concentrations to estimate baseline air pollution exposure. Elemental carbon measurements were used to calculate BC trends, as BC measurements were unavailable for the majority of the study period, under the assumption that the elemental carbon:BC ratio would not have changed significantly during the study period.

We considered two methods to extrapolate pollutant concentrations back in time, as suggested in the ESCAPE manual (ESCAPE 2012): (1) the *absolute difference* method; and (2) the *ratio* method. Regional pollutant concentrations in Hong Kong have followed distinctly different trends from those of local pollutants in recent decades, as most originate from the Pearl River Delta in Mainland China, which has experienced very different economic, industrial, and policy development. Therefore, the ratio method was applied to pollutants dominated by local emissions (NO and NO₂), and the absolute difference method was applied to pollutants dominated by regional emissions (PM_{2.5} and BC). This method assumes that the spatial distribution of pollutant concentration remains constant over the study period, as has been observed by others (Eeftens et al. 2011; Wang et al. 2013). We felt that this was a reasonable assumption as there were no large geographical changes in road network and point emission sources within Hong Kong between 1998 and 2014.

For the absolute difference method, we used the AQMS data to calculate, for each study subject, the absolute difference between the average one year before and one year after the recruitment date and the annual average covering the modeled measurement period. The back-extrapolated concentration was estimated by adding the difference to the modeled annual mean concentration. Whereas for the ratio method, we calculated the back-extrapolated concentrations by multiplying the modeled annual mean concentration with the ratio between the average one year before and one year after the recruitment date and the annual average covering the measurement period for each study subject. The baseline exposure was characterized based on the exact recruitment date and a year before and after to avoid weather influences in back-extrapolation calculations, which may be important as the cohort was recruited over three consecutive years.

Air Pollution Exposure Estimates (2D, 3D, and D3D)

To apply vertical and dynamic components to back-extrapolated results, we first geocoded subjects according to the floor level of their residential addresses. To calculate 3D exposure, we matched the subject's floor level with the pollutant's vertical decay rate derived in WP2. The 3D exposure estimates thus accounted for both spatial and vertical

variation in pollutants across the study area. BC decay rates were used for NO and NO₂, as these pollutants showed higher correlation than PM_{2.5} in AQMS measurements.

The generalized population mobility pattern and the related air pollution levels in microenvironments derived in WP3 were used to adjust for dynamic air pollution exposure. We compared the exposure of different age, sex, and population subgroups relative to the population mean concentrations (Table 3) and applied these ratios to predicted 3D results. These estimates thus accounted for exposure in various indoor, outdoor, and transport microenvironments. For NO, BC factors were used as surrogates as these pollutants showed the highest correlation in AQMS measurements. When applying these factors, we assumed all study subjects to be in the “neither at work nor study” population subgroup, as questions on occupation were not asked in the cohort questionnaires, coupled with the fact that the cohort was beyond the typical Hong Kong retirement age of 65.

Statistical analyses are described in the Statistical Methods and Data Analysis section.

Visualization of 3D Dispersion Patterns for Public Engagement

We hypothesized that 3D visualization methods would provide an engaging and intuitive method of presenting

complex TRAP dispersion information to the public. To visualize air pollutants’ dispersion within whole street canyons, interpolation methods (Kriging) were required to derive continuous concentration fields between monitoring points, both vertically and horizontally. Ambient measurements of PM_{2.5} and BC taken during the canyon campaigns were used to produce visualizations for the JDC1 site canyon using the Environmental Visualization System (EVS-Pro) software (C Tech Development Corporation, Las Vegas, Nevada, U.S.A.) by the following processing stages:

1. Multilevel ambient canyon measurements were aggregated at 30-minute intervals across a mean 24-hour period to produce a diurnal temporal variation.
2. Data were extrapolated vertically using the decay rate calculated in WP2. Data were extrapolated horizontally under the assumption that concentrations at a specific height were constant along the canyon.
3. A 2D floor plan of buildings forming the canyon and its surrounds were extruded upward using building height data to produce a 3D environment for visualization.
4. The data matrix was entered into EVS-Pro software and extended into a cube-shape cloud filling the whole canyon space.
5. EVS-Pro was used to produce a continuous-changing 3D animation over 24 hours at 30-minute intervals.

Table 3. Dynamic Exposure Factors Derived from WP2 and WP3, Where h is the Residential Height Above Street Level

	PM _{2.5}	BC	NO	NO ₂
Vertical Decay				
Height of residence above street level	$e^{-0.004h}$	$e^{-0.012h}$	$e^{-0.012h}$	$e^{-0.012h}$
Age^a				
Below 18	1.09	1.18	1.18	1.04
18–64	0.99	1.00	1.00	1.01
≥ 65	0.96	0.85	0.85	0.91
Sex				
Male	1.01	1.04	1.04	1.02
Female	0.99	0.99	0.99	0.98
Population Subgroup^a				
Working adults	0.98	1.03	1.03	1.06
Students	1.10	1.18	1.18	1.03
Neither in work or study	0.97	0.87	0.87	0.90

^a Grayed out values are only shown for comparison as they were not applicable to the study population.

STATISTICAL METHODS AND DATA ANALYSIS

COX PROPORTIONAL HAZARD MODELS (WP4)

Cox regression models have been applied in studies to elucidate the effects of long-term air pollution exposure on mortality (Dockery et al. 1993; Pope et al. 2002). In standard Cox regression analysis, the hazard function is the probability that an individual will experience an event (i.e., death) within a time interval. The HR and 95% CI for death can be estimated from Cox models for survival, with adjustment for both the individual level confounders and area covariates (e.g., age, sex, education, occupation, and area socioeconomic characteristics). We adopted these models to assess the mortality risks in relation to long-term exposures to TRAP in elderly subjects. Study subjects were assessed from year of recruitment to year of death for the causes being modeled or censored at the year of the follow-up in 2011. Statistical analyses were performed using function *coxph* in the R package *survival* (Therneau 2015).

Covariates

HRs and 95% CIs were calculated using Cox models, adjusted for individual, ecological, and environmental covariates. The independent variable was exposure to pollutant concentrations at baseline. Model covariates included individual-level demographic, socioeconomic, and lifestyle factors obtained from interviews (Lam et al. 2004b, Wong et al. 2015). Individual-level variables in the final model were age (continuous), sex, body mass index (<21.6, 21.6–26.3, >26.3 kg/m²), smoking (never smoker, former smoker, current smoker), physical exercise (days per week), education (<primary, primary, ≥secondary), and monthly expenses (<128, 128–384, >384 USD). For ecological and environmental covariates, we geocoded subjects into TPUs, as well as into the 18 larger administrative districts in Hong Kong. We then derived sociodemographic variables obtained from the 2001 Census (Census and Statistics Department 2002). The final models were adjusted for TPU-level proportion of the population ≥65 years of age, the proportion with more than a secondary education, and the average monthly income in each TPU. Additionally, we adjusted for the proportion of smokers in each district. District-level proportion of smokers (>15 years of age) from 1998 to 2011 was included as a covariate. Covariates are tabulated in Table 2 and in Appendix Table A.19 (available on the HEI website).

Comparison Between Pollutants

For the ease of comparing the health effects between different pollutants, we estimated the HRs and associated 95% CIs scaled to the interquartile range (IQR) based on

average distributions, for each pollutant and mortality outcome combination. Statistical significance was based on a *P* value of <0.05. In addition, we estimated HRs of PM_{2.5} exposure per unit increase (i.e., 10 µg/m³). The IQR-based measure allowed us to compare the size of effects estimates across pollutants (as the ranges of concentrations differed between pollutants), where calculations of HR per unit increment allowed the comparison of epidemiological effects with exposures derived from satellite-based methods (Wong et al. 2015).

Comparison with Satellite-Derived Exposure Estimates

In our earlier study (Wong et al. 2015), a simplistic method was applied to measure exposure estimated from satellite information surface extinction coefficients on a 1 × 1 km horizontal grid. The long-term effects on mortality due to all natural causes, cardiovascular disease, and respiratory disease were assessed. We compared the differences in HRs obtained from satellite-based and D3D LUR exposure estimates when applied to the same cohort. We compared results to examine whether the 3D model provided a wider exposure distribution than the 2D model, and whether such changes improved exposure estimations and hence altered estimated health effects.

Sensitivity Analyses

We performed sensitivity analyses to observe changes to the associations between exposure and mortality. We observed change in HRs when (1) yearly exposure to a pollutant was used; (2) participants who died during the first year after enrollment were included; and (3) participants who died in the first 1–3 years were excluded. In addition, we performed two stratified analyses: (1) subject's age (as defined by two age groups: <71 or ≥71 years old — based on the cohort's median age of 70), and (2) sex of the participants. We also examined the effects of back-extrapolation on exposure distributions and associations between 2D, 3D, and D3D estimates. All statistical analyses were carried out using functions in R software, version 3.3.2.

RESULTS

WP1: DEVELOPMENT OF A 2D LAND-USE REGRESSION MODEL FOR HONG KONG

Measurements

Combined measured concentrations from both campaigns were (a) NO₂ (*Mean* = 106 µg/m³, *Median* = 98 µg/m³, *SD* = 38.5, *N* = 95), (b) NO (*Mean* = 147 µg/m³,

Median = 131 $\mu\text{g}/\text{m}^3$, $SD = 88.9$, $N = 40$), (c) $\text{PM}_{2.5}$ (Mean = 35 $\mu\text{g}/\text{m}^3$, Median = 35 $\mu\text{g}/\text{m}^3$, $SD = 6.3$, $N = 64$), and (d) BC (Mean = 10.6 $\mu\text{g}/\text{m}^3$, Median = 10 $\mu\text{g}/\text{m}^3$, $SD = 5.3$, $N = 76$). Concentration distributions for all of the pollutants were skewed slightly right. Substantial spatial variation in concentration was seen across the territory for all pollutants. NO_2 , NO, and BC concentrations differed by one order of magnitude across the territory. The highest concentrations of gaseous pollutants were found in Kowloon and Hong Kong Island, the central and the traditional developed regions of Hong Kong. This pattern was not reflected for $\text{PM}_{2.5}$ and BC concentrations where higher concentrations were measured in the northern regions of the New Territories, closer to the border with Mainland China. Statistically significant differences in concentrations between sampling campaigns were noted only for $\text{PM}_{2.5}$ concentrations (mean difference = 17.80, $P < 0.001$) where SC2 mean, medium, minimum, and maximum were approximately 20 $\mu\text{g}/\text{m}^3$ greater than in SC1.

Model Results and Evaluation

From the nine models built for each pollutant, the preferred models used the combined SC1 and SC2 road-length models (Table 4). Road-length models overall performed slightly better than those with the other traffic variables, and road length was the most reliable traffic variable, as continuous road-type data were available as inputs, whereas traffic counts had to be interpolated between measurement locations to provide complete spatial coverage. Since the goal of the modeling was to predict long-term exposure, the combined SC1 and SC2 models were preferred. For preferred models, R^2 values ranged from 0.46 (NO_2) to 0.59 ($\text{PM}_{2.5}$). The number of predictor variables in these models ranged from four to eight (depending on sample size), and all models included at least one traffic variable. Land use was also present in all preferred models.

The LOOCV R^2 values for the preferred models were 15% to 44% lower than the models' R^2 values (Table 4). The NO_2 HEV R^2 values for all the NO_2 models were greater than most of the LOOCV R^2 except for two of the traffic-loading models. This was unexpected as it is generally assumed that HEV values should be lower than the LOOCV R^2 (Wang et al. 2012). In the preferred NO_2 model, the HEV R^2 was higher than the model R^2 , which was also unexpected.

Diagnostic plots showed that the models met the conditions of linearity, homoscedasticity, and normality. Moran I values for the residuals for the preferred models ranged from -0.26 to -0.0068 , meaning spatial correlation ranged from slightly dispersive to slightly clustered and that spatial autocorrelation was minimal. This absence of spatial autocorrelation also meant that interpolated residuals could not be used as an additional predictor variable.

Multicollinearity was a concern during the modeling process, and a few of the initial 36 models were rerun because of high VIF values (the VIF cutoff was set at three). A major source of multicollinearity was large buffered predictor variables, particularly 4,000 meters and 5,000 meters, as correlation was high for variables of this buffer size between most spatial metrics.

Prediction surfaces were created for the preferred models (Figure 2). Predictions were truncated to $\pm 20\%$ of the range of the corrected combined SC1 and SC2 measured concentrations entered into the models, with the exception of the NO_2 model since the predicted values were within this range (Amini et al. 2014; Henderson et al. 2007).

Alternative model results are shown in Additional Materials 1 (available on the HEI website).

WP2: VERTICAL MONITORING FIELD CAMPAIGN AND DEVELOPMENT OF A 3D LUR MODEL

Sampling Site Characteristics

After the canyon selection and recruitment protocol described in the Methods section, cool and warm season monitoring was carried out at six street canyon and open-street sites. These sites represented a range of physical canyon types, biased toward locations with high AADT counts (Table 5). All were in areas with high population density. A small number of residents withdrew from the study during or between seasonal campaigns. When this occurred, a replacement residence was recruited on a floor as close as possible.

Table 5 also shows a description of the typical buildings adjacent to the canyons and two open sites. The old slab residential blocks built over the past century are being replaced by individual towers with regular gaps. At the same time, an increasing proportion of the population is living in public or private housing estates, comprising a cluster of tall towers on podiums. The selected sites incorporated a mix of these residential slabs (JDC1, SWO1, CHO1), mixed towers (NPC1), and residential tower estates (HHC1, MKC1). Only JDC1 represented the now uncommon old narrow slab canyon, with no interruptions on either side. However, this canyon had a low AADT count, as is typical for such types of canyon. Photographs of each canyon location are shown in Figure 3.

Equipment Performance

High precision between the portable monitoring units used in the canyon campaigns was necessary for the calculation of accurate decay rates because of the relatively small differences in concentrations expected at higher floors. A robust quality assurance and quality control process was required because (a) interunit precision varied over time and

Table 4. Preferred 2D LUR Model Results

Preferred Model	Variables ^a	Estimate	Partitioned R^2	Parameters
NO ₂ (µg/m ³)	Intercept	7.84e+01		R^2 : 0.46
	ExpRL.1000(m)	1.61e-03	0.060	Adj. R^2 : 0.43
	MainRL.50(m)	9.67e-02	0.134	LOOCV R^2 : 0.39
	ElvRL.5000(m)	3.02e-04	0.221	HEV R^2 : 0.56
	OpArT.300(m)	-1.27e-04	0.047	RMSE: 27.7 µg/m ³ N: 75 Moran I: -0.256 Measured (µg/m ³): Mean = 107 (43, 213)
NO (µg/m ³)	Intercept	7.07e+01		R^2 : 0.50
	ElvRL.500(m)	1.06e-02	0.192	Adj. R^2 : 0.48
	BldVolD.25(m)	3.73e+00	0.148	LOOCV R^2 : 0.28
	IndT.25(m)	1.98e-01	0.078	RMSE: 62.1 µg/m ³
	WPopDen.100(m)	5.29e+02	0.082	N: 40 Moran I: -0.0068 Measured (µg/m ³): Mean = 147 (21, 376)
PM _{2.5} (µg/m ³)	Intercept	3.67e+01		R^2 : 0.59
	ExpRL.25(m)	8.91e-02	0.056	Adj. R^2 : 0.54
	Dist_ShenzhenP(m)	-3.09e-04	0.168	LOOCV R^2 : 0.43
	CarPD.1000(m)	4.17e+05	0.151	RMSE: 4.0 µg/m ³
	CarPD.25(m)	1.68e+04	0.057	N: 64
	GovT.100(m)	-3.81e-04	0.066	Moran I: -0.228
	IndT.25(m)	1.38e-02	0.089	Measured (µg/m ³): Mean = 35 (25, 51)
BC (µg/m ³)	Intercept	2.51e+03		R^2 : 0.50
	ExpRL.3000(m)	9.48e-05	0.091	Adj. R^2 : 0.44
	ExpRL.50(m)	1.76e-02	0.075	LOOCV R^2 : 0.31
	Long(decimal degree)	-2.19e+01	0.089	RMSE: 3.7 µg/m ³
	CarPD.50(m)	3.23e+04	0.044	N: 76
	ComT.500(m)	-2.74e-05	0.037	Moran I: -0.129
	ResT.50(m)	-8.74e-04	0.050	Measured (µg/m ³):
	MixT.500(m)	-2.32e-05	0.053	Mean = 11 (6, 28)
	Lands.500(m)	-1.50e-04	0.065	

^a BldVolD = building volume density, CarPD = car park density, ComT = commercial total, Dist_ShenzhenP = Shenzhen, ElvRL = Elevated road length, ExpRL = expressways length, GovT = government total, IndT = industrial total, Lands = undeveloped lands, Long = longitude, MainRL = main road length, MixT = mixed use total, OpArT = open area total, ResT = residential total, WPopDen = population density

(b) changes in particulate composition meant that SidePak-to-reference-instrument (tapered-element oscillating microbalance FDMS) conversion factors and microAeth filter loading attenuation correction factors varied over time. Full results of the precision and scaling procedures are shown in Appendix A (Tables A.5 to A.8, Figures A.6 to A.9).

The TSI AM510 SidePak is an optical instrument that is factory calibrated by the manufacturers to the respirable fraction of standard ISO 12103-1, A1 Test Dust. It is standard practice to determine the calibration factor for a specific aerosol by

colocation with a reference instrument. The SidePak units performed well against the reference instruments throughout each campaign, with R^2 values of 0.92 and 0.97 for the warm and cool seasons, respectively. Reference scaling factors were 0.37 and 0.43, respectively (Appendix Figures A.6 and A.7), which are in line with previous studies in urban environments (Zhu et al. 2007).

To additionally test variations in reference scaling factors, colocation tests alongside FDMS reference monitors were carried out in three different locations with contrasting

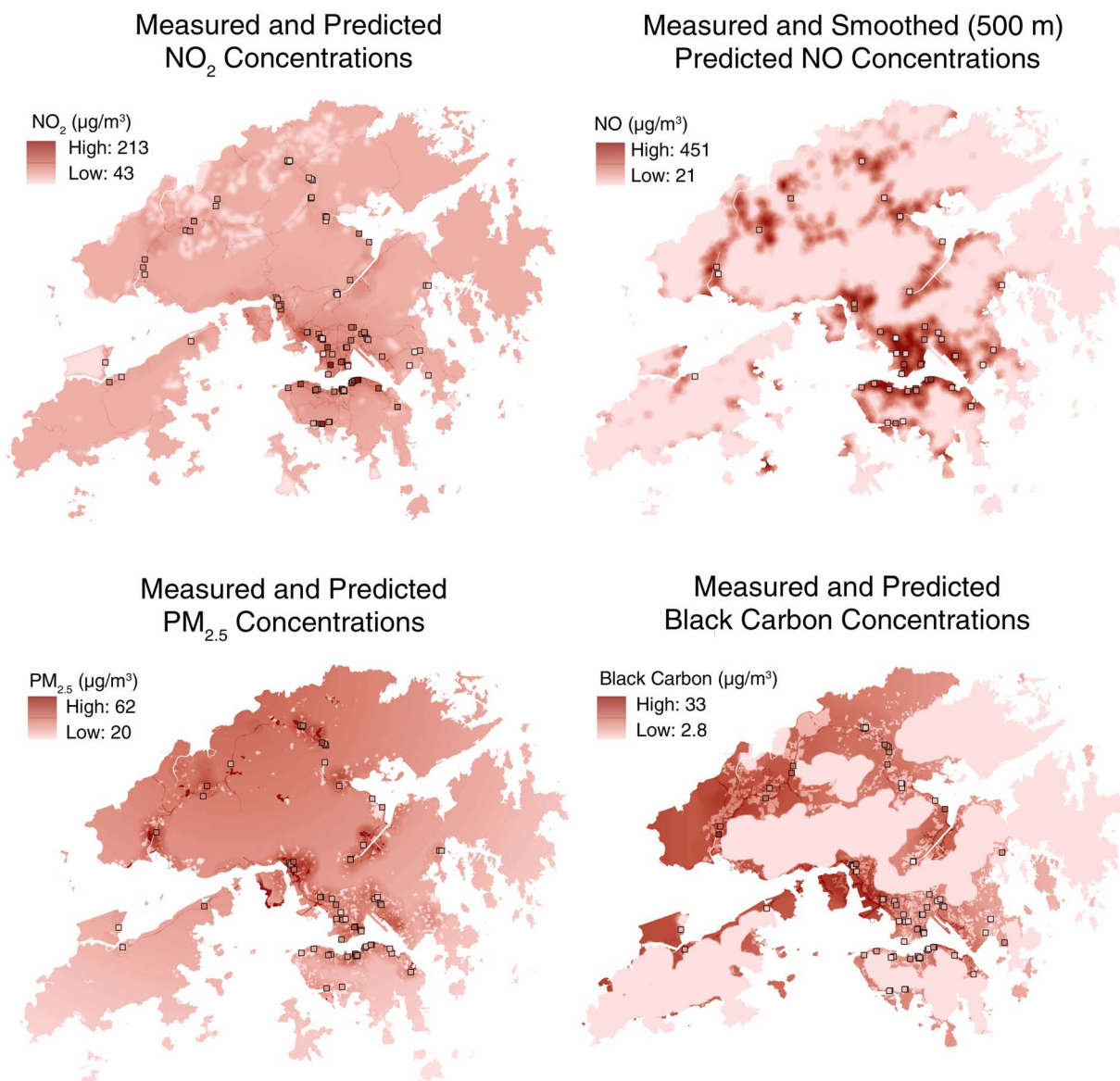


Figure 2. Prediction surfaces for the preferred (combined SC1 and SC2 road length) models described in Table 4. The squares represent measured concentrations at the monitor sites; predicted concentrations are displayed for all of Hong Kong.

local emissions (curbside, roadside, and rooftop). No significant difference in reference correction factors was identified within the precision of the instruments.

The Aethlabs AE51 microAethalometer measures the rate of change in absorption of transmitted light at 880 nm wavelength from deposited aerosol continuously collected onto a filter tab. Reference scaling of microAeth units was not possible as no reference BC monitors were operated in urban areas during the sampling campaigns.

Nine precision experiments were carried out during the fieldwork to test the stability of the units: at the start

and end of each campaign plus extra tests when units were returned from servicing or when borrowed units were used. In each test, linear regression analysis was used to derive correlation, offset, and gradient matrices between the reference unit (the unit colocated with the tapered-element oscillating microbalance FDMS reference monitor) and all other units. This testing revealed that the SidePak units had a high degree of correlation, but some had large offset and/or scaling factors relative to the reference unit. Scale factors tended to be stable over time, but certain units had highly variable offsets. A sample Sidepak correlation matrix from the winter

Table 5. Details of the Sampling Sites for the Canyon Campaigns, Including Floors on Which Sampling was Undertaken on Sides A and B^a

District & Site Code ^b	Road (District)	Aspect Ratio ^c	AADT	Description	Floor A	Height A (m)	Floor B	Height B (m)
Street Canyon								
Jordan (JDC1)	Man Ying Street (Kowloon)	7.4	Low	Old residential slab	1	6.3	2	9.2
					3	12.1	13	41.1
					6	20.8	—	—
					9	29.5	—	—
					15	46.9	—	—
Mong Kok (MKC1)	Hoi Wang Road (Kowloon)	3	Medium	Large residential towers	2	10.1	11	34.6
					5	18.3	14	42.8
					12	37.4	20	59.2
					20	59.2	—	—
Hung Hom (HHC1)	Hung Hom Road (Kowloon)	2.1	High	Large residential towers	2	17.2	2	17.2
					3	19.9	6	28.2
					5	25.5	13	47.5
					11	42	—	—
					14	50.3	—	—
North Point (NPC1)	Java Road (HK Island)	3.6	High	Mixed residential tower and slab	3	13.8	2	12
					5	21.6	17	53.3
					9	33.2	—	—
					10	37	—	—
					16	50.2	—	—
Open Street								
Sai Wan (SWO1)	Des Voeux Road West (HK Island)	—	High	Residential slab	2	11.4	—	—
					4	16.8	—	—
					11	35.7	—	—
					15	46.5	—	—
					21	62.7	—	—
Choi Hung (CHO1)	Lung Cheung Road (Kowloon)	—	High	Residential slab	1	2.6	—	—
					4	10.5	—	—
					6	15.7	—	—
					7	18.3	—	—
					19	49.8	—	—
AQMS Canyon								
Causeway Bay (CBAQMS)	Yee Wo Street (HK Island)	2.7	High	Mixed residential tower and slab	0	2	—	—
					12	36	—	—
Kwai Chung (KCAQMS)	Kwai Chung Road (Kowloon)	1.1	High	Mixed commercial tower and slab	0	2	—	—
					6	13	—	—
Kwun Tong (KTAQMS)	Kwun Tong Road (Kowloon)	1.5	High	Residential slab and commercial towers	0	2	—	—
					12	25	—	—
Mong Kok (MKAQMS)	Nathan Road (Kowloon)	3.9	High	Mixed residential tower and slab	0	2	—	—
Sham Shui Po (SSPAQMS)	Yen Chow Street (Kowloon)	0.9	High	Mixed residential and commercial towers	0	2	—	—
					8	17	—	—

^a See Figure 1 for descriptions of sides A and B. — = not applicable.

^b AQMS canyons were used only for validation purposes.

^c Vardoulakis et al. 2003 describes a regular canyon as having an aspect ratio of about 1.

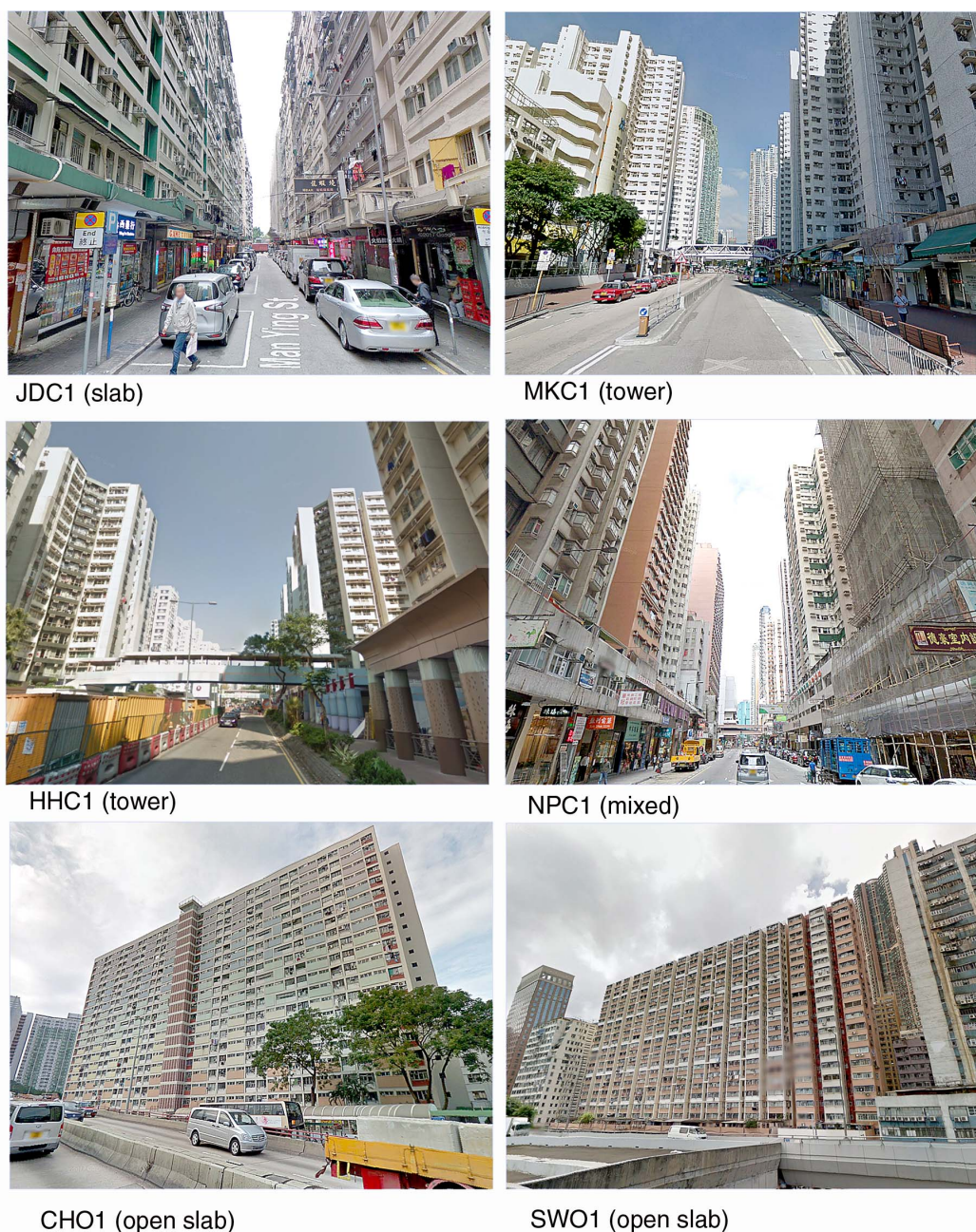


Figure 3. Photographs of the six canyon campaign monitoring locations illustrating prominent building type (tower or slab). Measurement sites: JDC1 = Jordan canyon; MKC1 = Mong Kok canyon; HHC1 = Hung Hom canyon; NPC1 = North Point canyon; CHO1 = Choi Hung open; SWO1 = Sai Wan open.

pre-campaign test is shown in Table 6, with precision scaling factors and offsets relative to the reference unit (S10) for each unit shown at the base of the table. This test identified that unit S03 had a fault and was taken out of service for the campaign. Note that faulty units had to be shipped back to the United Kingdom or the United States for repair, taking them out of service for several months.

The precision experiments showed that the microAeths were stable and consistent, with the majority of R^2 values in the correlation matrices at 98% or above and precision scale factors between 0.95 and 1.05. No units showed offsets. However, because of the high filter loading rates experienced in the polluted conditions typical during the campaigns, coupled with limited access to instruments in residences, an adapted version of the method used by

Virkkula and colleagues (2007) for attenuation correction had to be applied. Separate attenuation correction (β) factors were calculated for each canyon and each season to account for changing particulate atmospheric composition. Attenuation factors ranged from 0.004 to 0.019 and were typically higher during the warm season campaign than the cool season. A full set of attenuation correction factors is shown in Appendix Table A.7.

The AQMesh electrochemical units suffered several sensor failures, particularly associated with high rainfall conditions during the warm season. They also demonstrated irregular and unpredictable responses, which were evident during precision testing. A series of precision tests was carried out alongside the particle monitoring units. Unlike the particle monitoring units, the AQMesh units reported poor between-unit correlation, widely variable precision scaling factors, and large, inconsistent positive and negative offsets for each of the gas sensors. Between-unit precision of the temperature and relative humidity sensors was generally good, with high correlation and stable scaling. The results of these precision tests are shown in Appendix Table A.8.

It was also clear from time-series charts of the gaseous pollutant data that the sensors took between 6 and 24 hours to stabilize after deployment in the residences during the campaigns. After stabilization, between-unit offsets

appeared to be different from those measured before the unit's relocation. This combined evidence gave us insufficient confidence in the accuracy and, more important, precision of the electrochemical sensors to proceed with their use for calculating gaseous vertical decay rates.

These disappointing results were reported to the manufacturer, who has since updated data-processing algorithms and upgraded the NO₂ sensor to a new version. Tests in the United Kingdom indicate that the new algorithms produce greatly improved NO and CO precision, but without the sensor upgrade, the NO₂ precision remains poor. It is therefore possible that the NO and CO data may be salvageable in the future by the reapplication of processing algorithms on the historical data set by the manufacturers.

Vertical Decay Rates

As illustrated in Figure 4, PM_{2.5} showed strong seasonal differences in mean concentration throughout the day. Typically, during the warm season southwesterly winds bring monsoon rainfall to the region and relatively clean maritime air. A shift to northerly winds during the cool season leads to the import of continental air to Hong Kong. This air has traveled across Mainland China, including the heavily industrialized Pearl River Delta. This produced an increment of between 30 and 40 $\mu\text{g}/\text{m}^3$ over warm season concentrations. This effect was less marked in BC, which had a lower regional contribution. In addition to this

Table 6. PM_{2.5} SidePak Unit Correction Factors Correlation Matrix (R^2) Plus Offset and Scaling Factors for the Winter Canyon Pre-Campaign Precision Test^a

Unit	S01	S02	S03	S04	S07	S09	S10 ^b	S11	S12	CAN06
S01		1.00	0.21	0.97	0.98	0.99	1.00	0.96	1.00	1.00
S02	1.00		0.21	0.97	0.98	0.99	1.00	0.97	1.00	1.00
S03	0.21	0.21		0.12	0.27	0.24	0.25	0.28	0.25	0.19
S04	0.97	0.97	0.12		0.94	0.96	0.95	0.92	0.96	0.98
S07	0.98	0.98	0.27	0.94		0.96	0.98	0.99	0.99	0.98
S09	0.99	0.99	0.24	0.96	0.96		0.99	0.96	0.99	0.99
S10 ^b	1.00	1.00	0.25	0.95	0.98	0.99		0.98	1.00	0.99
S11	0.96	0.97	0.28	0.92	0.99	0.96	0.98		0.98	0.97
S12	1.00	1.00	0.25	0.96	0.99	0.99	1.00	0.98		0.99
CAN06	1.00	1.00	0.19	0.98	0.98	0.99	0.99	0.97	0.99	
Offset	1	5		41	29	2	0	3	1	5
Scale	1.01	1.02	—	0.95	0.91	1.14	1.00	1.89	0.96	1.28

^a Fill colors indicate degree of correlation, from dark green ($R^2 = 1.00$) through to dark red ($R^2 < 0.2$).

^b S10 was the reference unit during this test.

offset, lower dispersion conditions exaggerated diurnal variation in both pollutants during the cool season. Diurnal analyses from all six vertical monitoring locations are shown in Appendix Figures A.10 to A.15.

In all but one case (MKC1), the prevailing wind speed and direction during the monitoring campaigns were comparable with the 10-year mean. We are therefore confident that these results are representative of typical weather conditions in Hong Kong during each season. Supporting data are shown in Appendix Figure A.16.

Pollutant concentrations for each sampling site were plotted against height, with the addition of temporally corrected street-level model estimates. The general pattern was of a rapid decrease in concentrations over the first few meters, followed by a gradual decrease, no change, or gradual increase, dependent on canyon and season (Figure 5). There were exceptions, particularly during the cool season: JDC1, NPC1, and SWO1 all showed no decay in $PM_{2.5}$ with height during the cool season. Generally, decay of BC was greater than $PM_{2.5}$, perhaps reflecting the greater component of

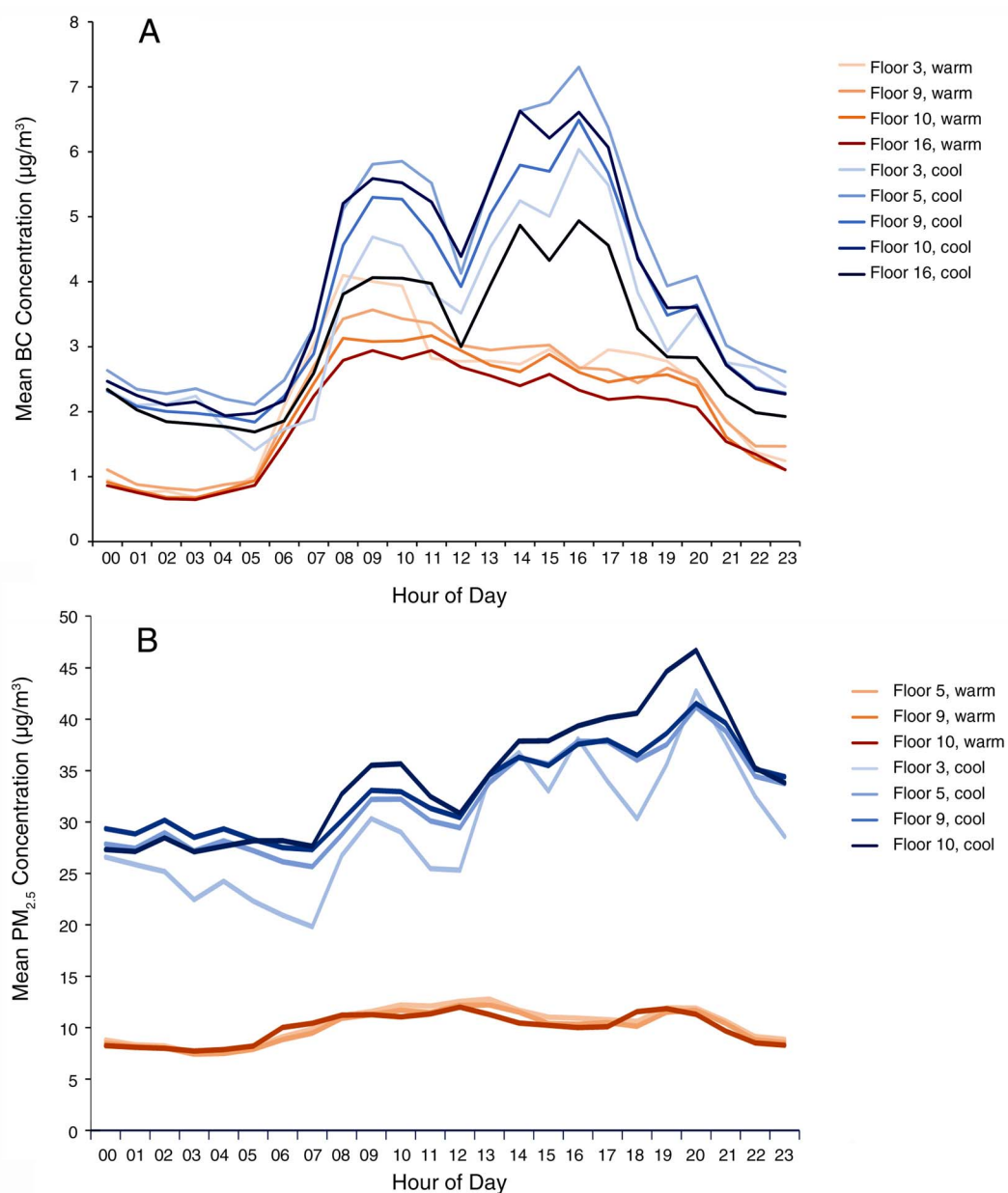


Figure 4. Mean diurnal variation in (A) BC and (B) $PM_{2.5}$ at the NPC1 site during the warm and cool seasons.

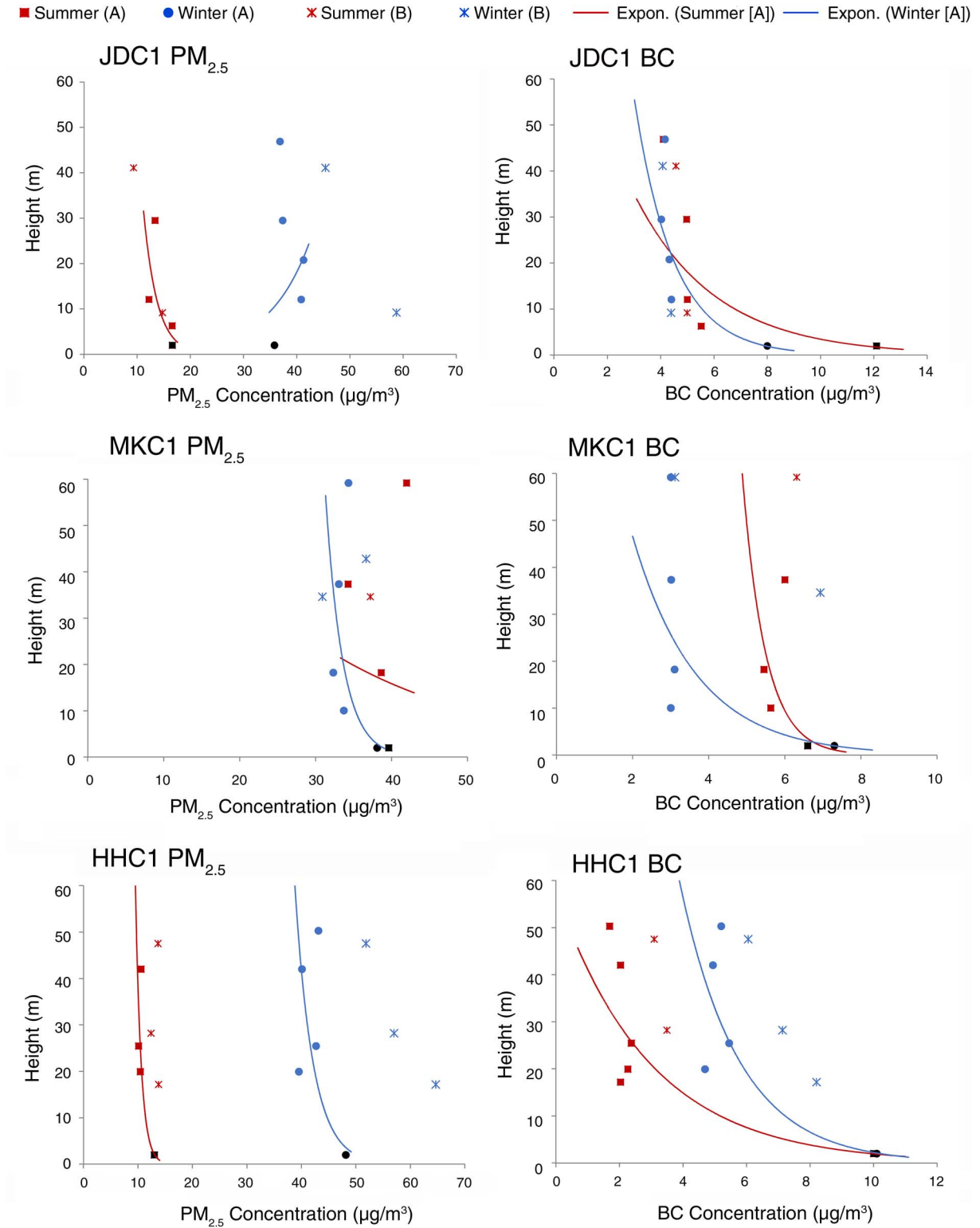


Figure 5. Vertical concentrations measured during the warm and cool season canyon campaigns. Values are matched means throughout the two-week sampling period (one week for side B). Exponential decay curves are only fitted for A-side sites. The 2-meter height concentrations are derived from temporally corrected 2D model estimates. *Figure continues next page.*

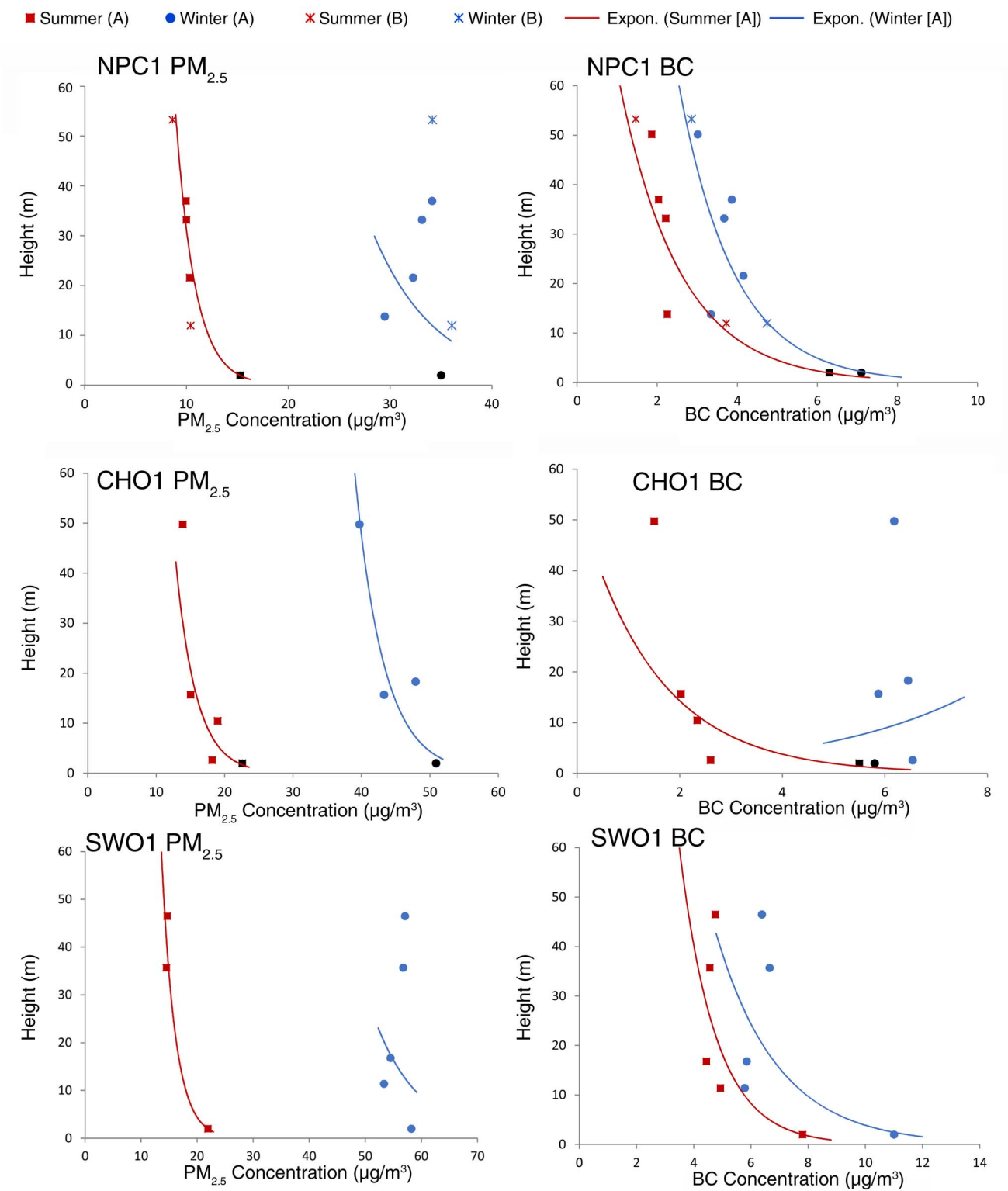


Figure 5 (Continued).

Table 7. Decay Rates (k) for Each Vertical Sampling Site Alongside Canyon Characteristics^a

Site Code ^b	Height/ Width Ratio	AADT	Canyon Type	Wind Direction ^c		Decay Rate (PM _{2.5})		Decay Rate (BC)	
				Warm	Cool	Warm	Cool	Warm	Cool
Street Canyons									
JDC1	High	Low	Slab	Para.	Para.	0.001	0	0.016	0.012
MKC1	Med	High	Tower	Perp.	Perp.	0.001	0.001	0.002	0.010
HHC1	Low	High	Tower	Perp.	Mixed	0.005	0.002	0.028	0.012
NPC1	Med	High	Mixed	Para.	Para.	0.012	0	0.021	0.013
SWO1	—	High	Slab (coast)	Perp.	Perp.	0.010	0	0.008	0.007
CHO1	—	High	Slab	Perp.	Perp.	0.008	0.005	0.018	0
Seasonal mean						0.009	0.001	0.016	0.009
Annual mean						0.004		0.012	
AQMS Canyons									
CBAQMS	Mid	High	Mixed	Para.	—	0.016	—	0.032	—
KCAQMS	Low	High	Mixed	Perp.	—	0.015	—	0.017	—
KTAQMS	Low	High	Mixed	Para.	—	0.003	—	n.a.	—
MKAQMS	Mid	High	Mixed	Perp.	—	0.002	—	0.016	—
SSPAQMS	Low	High	Tower	Perp.	—	-0.001	—	n.a.	—
Seasonal mean						0.007		0.022	

^a n.a. = not available; — = not applicable.

^b See Table 5 for site codes.

^c Wind direction (parallel, perpendicular, mixed) refers to the dominant wind direction recorded by the closest Hong Kong Observatory meteorological monitoring site relative to the canyon orientation.

local emissions for this pollutant. Only one site, CHO1, showed no decay with height. A sensitivity test was carried out to establish whether decay rates were dependent on the time of day, but results were similar throughout. An example plot of this diurnal analysis is shown in Appendix Figure A.17.

In most cases, concentrations on the B side of the canyon followed the same curve as the A side. However, both PM_{2.5} and BC concentrations measured on the B side of HHC1 were consistently higher than those on the A side.

Concentrations were then log-transformed to derive decay rates (k) for each canyon and season (Table 7). Decay rates calculated for AQMS locations were used for comparison, as they were derived from only two sampling heights. Nevertheless, seasonal means from the AQMS sites were similar to those from the canyon sites for both pollutants (0.007 vs. 0.009 for PM_{2.5} and 0.022 vs. 0.016 for BC).

While it was clear that decay rates were higher during the warm season than the cool, no robust patterns could be identified relating to the canyon physical parameters. This meant that differential decay rates could not be applied across the region according to canyon classification. It was therefore decided to use a single decay rate for each pollutant across the whole region for derivation of the 3D exposure layer ($k = 0.004$ and 0.012 for PM_{2.5} and BC, respectively).

Some degree of evaluation of the use of modeled street-level concentrations and application of a mean decay rate was possible at the five locations where paired rooftop and roadside monitoring was carried out alongside AQMS sites (see Table 5 for AQMS site details). First, temporally corrected PM_{2.5} and BC concentrations for these five locations were extracted from the 2D LUR. Then the warm season decay rates (0.009 and 0.016, respectively) were applied to

these modeled estimates to produce modeled rooftop-level concentration estimates. These were then compared with the monitored street and rooftop level concentrations (Table 8). Because of instrument faults, street-level BC concentrations at two sites were not available.

While the modeled $PM_{2.5}$ concentrations at street level compared well with the measured concentrations, the modeled magnitudes in decay were more variable, with a large underestimate evident at the CBAQMS site and a large overestimate at the MKAQMS site, relative to absolute concentrations. Conversely, the model produced relatively good estimates in BC decay, but uniformly overestimated street-level BC concentrations. The results shown in Table 8 are reproduced graphically in Appendix Figures A.18 and A.19.

While this evaluation was useful in illustrating model performance, a perfect match of modeled and measured concentrations was not expected. This is because the modeled concentrations and decay rates were selected to represent seasonal average conditions. Meteorological conditions during the monitoring period when measurements were taken would not be expected to match the sea-

sonal mean. Unusual meteorological conditions are likely to explain the lack of decay measured at the SSPAQMS site, which was not duplicated in the model, resulting in a decay overestimate.

Alternative Decay Exposure Profile

The exponential equation used to calculate the decay rates (Equation 2) assumes a continuous decay to infinity. However, it is clear from the mean vertical concentration profiles shown in Figure 5 that decay occurs to the point at which the local emissions are fully mixed. From that height upward, concentrations have reached the urban background, and little or no decay occurs. This is particularly evident in the cool season $PM_{2.5}$ profiles, due to the dominant regional component.

We made a conservative visual estimate that this fully mixed state was reached at a height of 20 meters above street level on average across all seasons and monitoring locations. A quantitative method could not be established with our data set because of the relatively small number of monitoring heights and variability in profiles. An alternative decay exposure profile was produced where concentration

Table 8. Comparison of Measured and Modeled $PM_{2.5}$ and BC Concentrations at the Five AQMS Monitoring Sites^a

Pollutant / Site Code ^b	Measured ($\mu\text{g}/\text{m}^3$)		Modeled ($\mu\text{g}/\text{m}^3$)		Over/Under Estimate ($\mu\text{g}/\text{m}^3$)	
	Street Level	Decay	Street Level	Decay	Street Level	Decay
$PM_{2.5}$						
CBAQMS	23.6	10.0	21.5	6.0	-2.1	-4.1
KCAQMS	15.7	4.0	18.2	3.1	2.5	-0.8
KTAQMS	17.5	1.9	18.2	5.0	0.7	3.1
MKAQMS	18.0	2.1	18.5	9.6	0.5	7.5
SSPAQMS	13.7	-0.2	14.5	2.8	0.8	3.0
BC						
CBAQMS	12.5	8.4	21.5	9.4	9.0	1.1
KCAQMS	7.1	1.9	13.4	3.8	6.3	1.9
KTAQMS	—	—	14.0	6.2	—	—
MKAQMS	9.8	6.9	11.6	8.4	1.8	1.5
SSPAQMS	—	—	13.2	4.2	—	—

^a — = missing data.

^b See Table 5 for site codes.

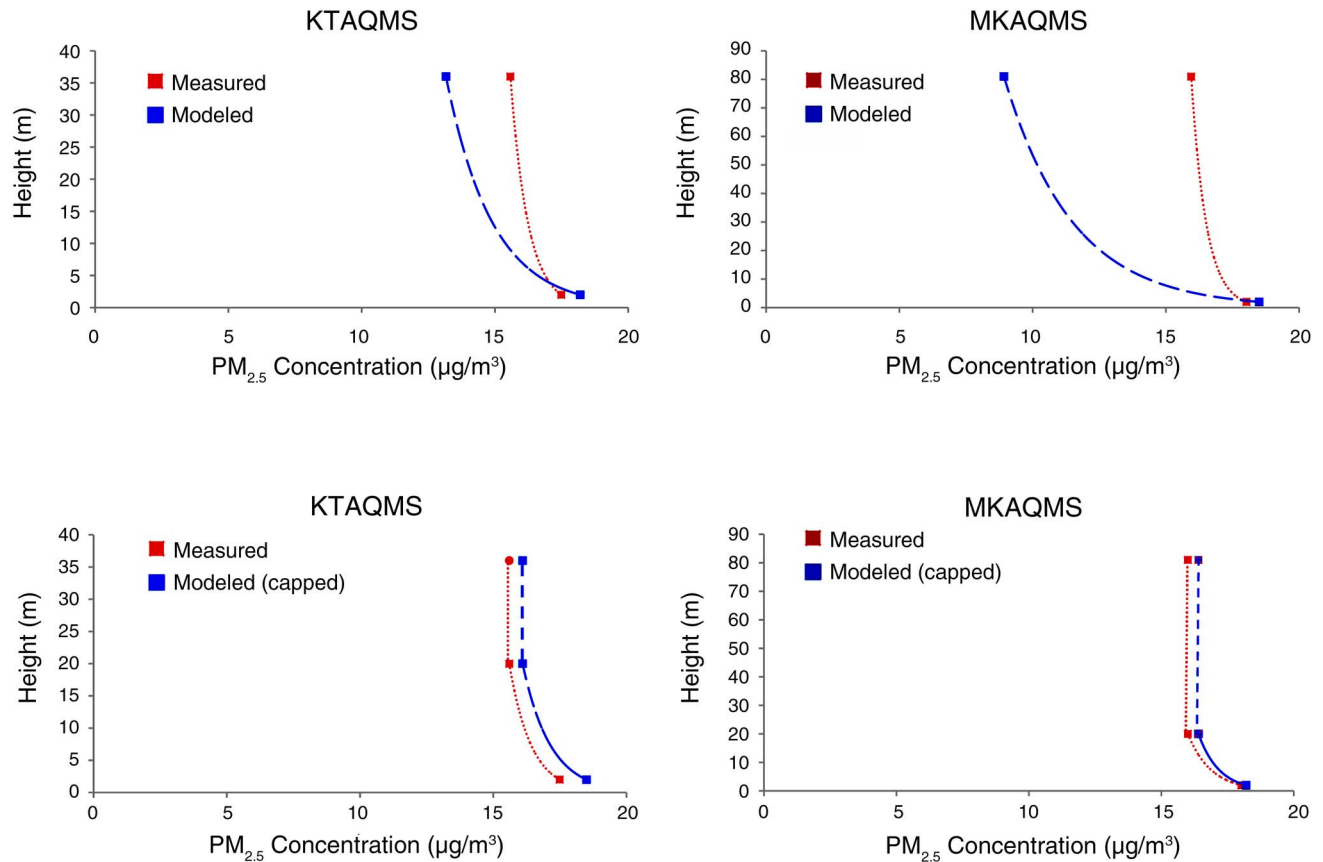


Figure 6. Vertical $PM_{2.5}$ profiles at two government network monitoring sites illustrating the impact of capping decay at 20 meters.

decay was capped at 20 meters (i.e., all exposure estimates at heights above 20 m were set at a value equal to the 20 m estimate). The impact of this capping is illustrated in Figure 6. A continuous decay profile produces a large underestimate in $PM_{2.5}$ concentration at rooftop level, particularly at the MKAQMS site, which is at 85 meters. This overestimate in decay is corrected when capped at 20 meters, and measured and modeled vertical profiles are in much closer agreement.

Infiltration Efficiencies

$PM_{2.5}$ and BC infiltration efficiencies were calculated for each home and season. The median F_{inf} for both $PM_{2.5}$ and BC during the cool season was 91% ($n = 23$ and 25, respectively). This dropped to 81% and 88% for $PM_{2.5}$ and BC, respectively ($n = 21$ and 22) during the warm season (Appendix Table A.9), reflecting the fact that residents were more likely to keep their windows closed and use their in-window air conditioning units during hot weather.

This was confirmed through analysis of the questionnaire data, which included frequency of air conditioning use during the sampling period. We found a significant negative correlation between air conditioning use and F_{inf} of $PM_{2.5}$ and BC during the warm season (analysis results are shown in Appendix Figure A.20). No resident reported air conditioner use during the cool season.

The F_{inf} for the mechanically ventilated office building was 45% and 40% during the cool and warm seasons, respectively.

WP3: INTEGRATION OF POPULATION MOVEMENTS TO CREATE A DYNAMIC 3D LUR MODEL

Exposure and Time Spent in Different Microenvironments

Maps showing mean concentrations in each TPU are shown in Appendix Figure A.22, with tabulated results shown in Appendix Table A.14 (available on the HEI website).

In line with published literature (de Nazelle et al. 2013) for a European location (Barcelona), we found that significantly higher pollutant exposure estimates in transport microenvironments and trips made on surface modes of transport contributed notably to the daily exposure of subjects, even though time spent in these microenvironments was considerably less (Table 9). Ambient exposure estimates were typically the second highest, although this varied spatially. For example, residents of the northwestern and Kowloon-area TPUs were exposed to ambient concentrations of $PM_{2.5}$ up to 75% higher than those living in northeastern TPUs. These spatial contrasts were amplified when accounting for diurnal variations, as most subjects traveled during morning and evening rush-hour periods. Lowest indoor exposure estimates were found in office buildings due to the low MVAC infiltration efficiency; however, this contrast was lessened slightly with the inclusion of diurnal factors, as these were somewhat higher than 1 during typical working hours (between 1.1 and 1.3 depending on the pollutant).

As expected, most of the subjects spent most of their time indoors, at their home residential address. On average across the whole population, time spent at home, in work, in school, and in transport (including traveling outdoors [walking, cycling]) was 62%, 23%, 10%, and 5%, respectively.

Model Stage 5 dynamic $PM_{2.5}$ exposure estimates for sample individuals within two population groups throughout a notional 24-hour period are shown in Figure 7 (mean across all TPUs). Each group has characteristic travel patterns, illustrated in the spikes in concentration around

afternoon–evening and during the day for ≥ 65 not working and 18–65 working age groups, respectively.

Time-Weighted Exposure by Model Stage

Time-weighted exposure estimates of all six modeling stages are shown in Table 10.

Examining the static models, overall exposures were 19%, 13%, and 27% higher outdoor (Stage 1) compared with the indoor estimates (Stage 2), for $PM_{2.5}$, BC, and NO_2 , respectively. The mean outdoor exposures were 32.0, 9.4, and 92.9 $\mu g/m^3$ for $PM_{2.5}$, BC, and NO_2 , respectively. It should be noted that these estimations are based on the 2D LUR results, and aggregated at the TPU level; floor of residence was not available in the travel survey database.

In addition to the static outdoor and indoor exposure estimates, time-weighted exposure estimates were calculated from the time participants spent at home and work and at other indoor locations (e.g., shopping centers) (Stage 3). Their destination was determined by the trip purpose in the travel survey questionnaire and their occupations. Comparing Stage 3 (dynamic indoor) with Stage 1 (static outdoor) results, 28%, 24%, and 27% decreases were seen for $PM_{2.5}$, BC, and NO_2 , respectively. When transport microenvironments were added (Stage 4), these differences decreased by 16%, 12%, and 24%, respectively, reflecting elevated exposures while in transit. The inclusion of diurnal factors decreased population mean exposure estimates slightly in comparison with the previous stage.

Model Stage 6 was added as a sensitivity test to examine movement effects as distinct from infiltration effects. The mean exposures for Stage 6 were 33.8, 9.6, and 90.9 $\mu g/m^3$

Table 9. Mean Concentrations in Microenvironments and Average Time Spent

Microenvironment	Mean Time Spent (hours)	Mean Concentration ($\mu g/m^3$)		
		$PM_{2.5}$	BC	NO_2
Home indoor	14.9	50.9	7.5	67.5
Commercial indoor	5.2	31.2	4.6	76.9
School indoor	2.5	50.3	7.4	65.2
Other indoor (natural)	0.1	56.4	8.3	68.1
Other indoor (MVAC)	0.2	30.6	4.5	65.9
Transport	1.1	61.8	9.1	98.8

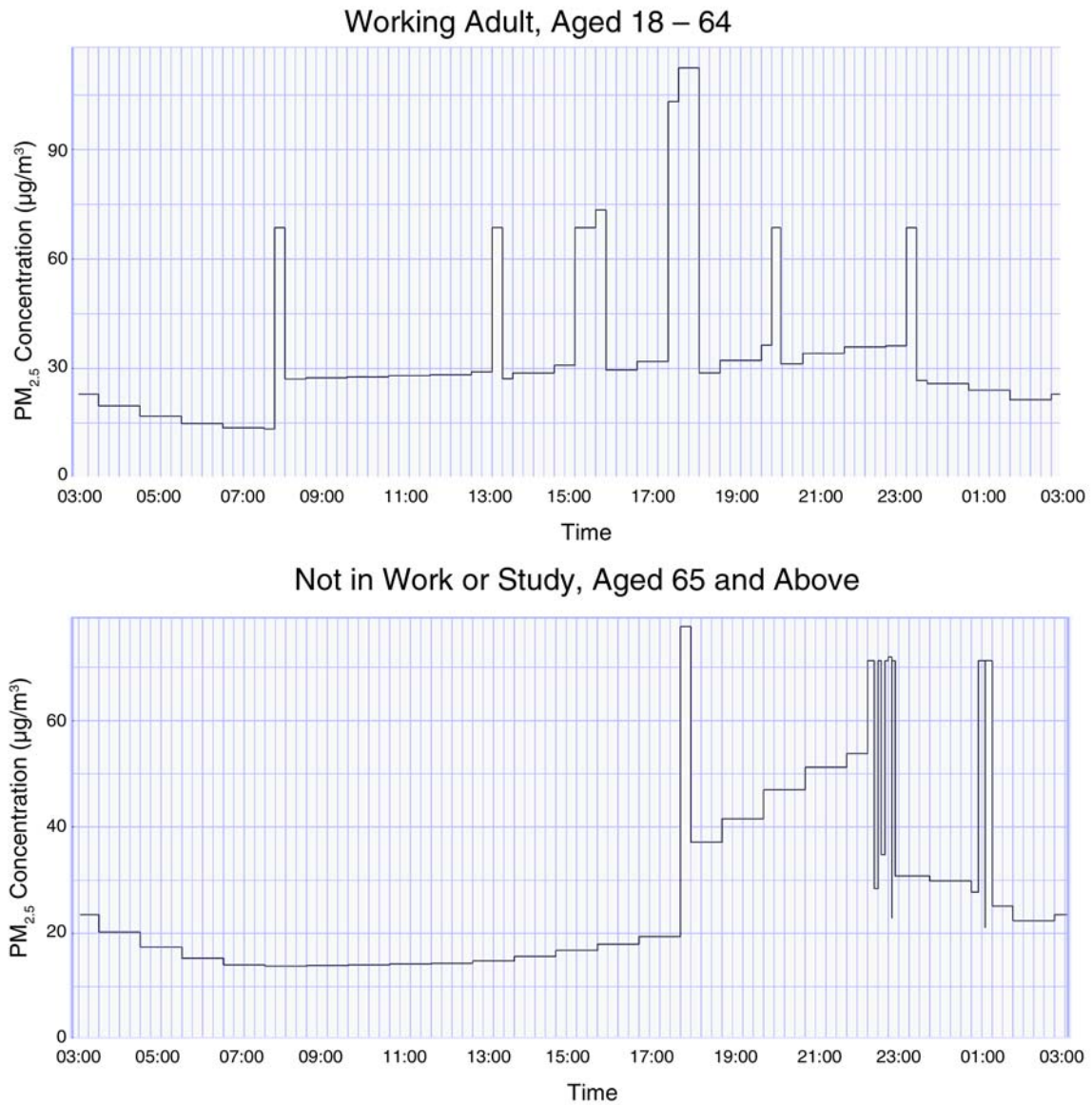


Figure 7. Modeled dynamic PM_{2.5} exposure (Stage 5) of two individuals over a 24-hour period.

for PM_{2.5}, BC, and NO₂, respectively, which were slightly higher than Stage 1 (static outdoor) exposures for PM_{2.5} and BC.

Overall, the inclusion of dynamic components decreased exposure estimates in comparison with standard static outdoor exposure estimates, principally driven by the indoor components, despite relatively high infiltration efficiencies. In the case of PM_{2.5}, exposure heterogeneity (represented by the standard deviation) increased, but it decreased in BC and NO₂ estimates.

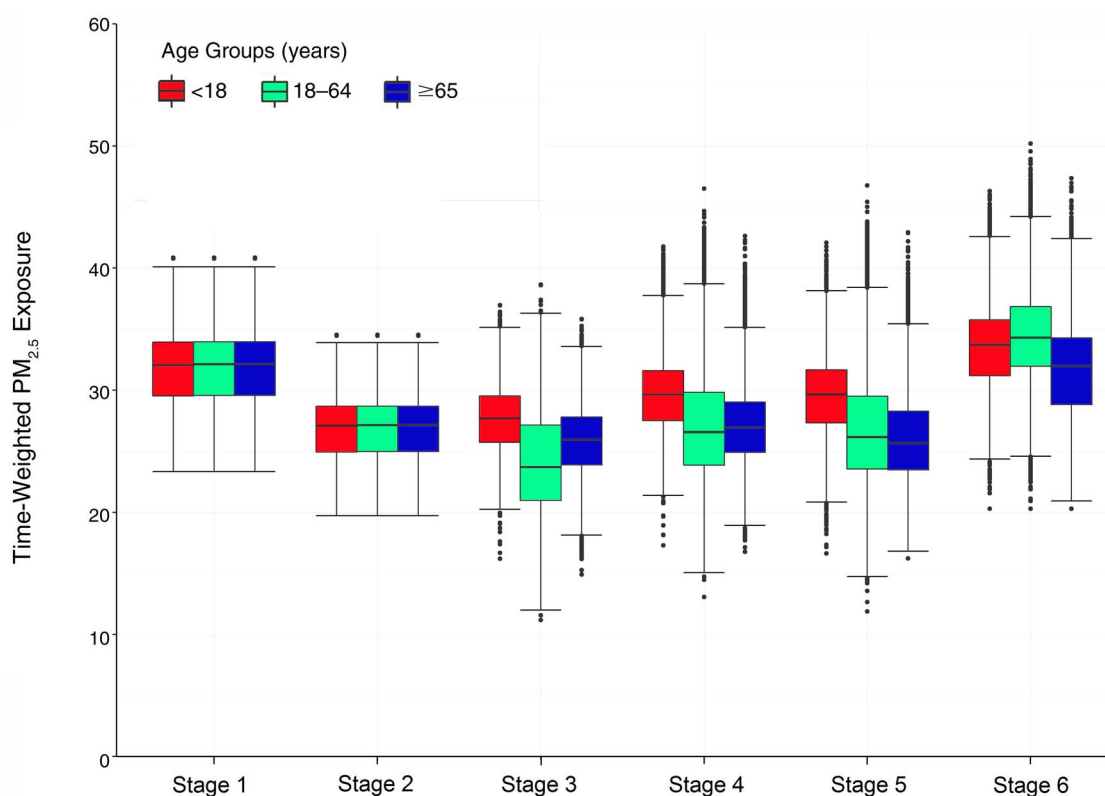
Stratified Analysis for Different Population Subgroups

Full numerical results and box plots for each model stage and each subgroup are presented in Appendix Figures A.23 to A.28 and Tables A.15 to A.18.

Time-weighted exposures for each model stage were split by age groups, population subgroup, and sex. Static outdoor and indoor exposure estimates (Stages 1 and 2) did not differ among groups as all behaviors were assumed to be equal; however, the addition of dynamic components (Stage 5) showed the lowest PM_{2.5} exposures with the ≥65 age group and the highest for the <18 age group (see Figure 8). Compared with the oldest age group, the youngest

Table 10. Time-Weighted Exposure Estimates for all Model Stages for the Survey Population

Stage / Microenvironment	Time-Weighted Exposure ($\mu\text{g}/\text{m}^3$) ($N = 89,358$)											
	PM _{2.5}				BC				NO ₂			
	Mean	Min	Max	SD	Mean	Min	Max	SD	Mean	Min	Max	SD
1 Static outdoor	32.0	23.3	40.8	3.4	9.4	2.8	18.5	3.5	92.9	56.2	141.1	15.1
2 Static indoor	27.0	19.7	34.5	2.8	8.3	2.5	16.4	3.1	73.4	44.4	111.4	12.0
3 Dynamic indoor	25.0	11.2	38.7	3.9	7.6	1.9	17.0	2.7	73.4	42.9	116.7	10.9
4 Dynamic indoor + transit	27.5	13.1	46.5	4.1	8.4	2.3	18.0	2.6	74.8	44.4	116.7	10.5
5 Dynamic indoor + transit + diurnal	27.1	11.9	46.8	4.2	7.8	1.2	21.5	2.8	71.3	24.9	122.7	14.3
6 Dynamic outdoor + transit + diurnal	33.8	20.3	50.2	3.9	9.6	1.3	22.0	3.4	90.9	31.5	147.7	18.1

**Figure 8.** Box plots of time-weighted PM_{2.5} exposures for each model stage split by age group.

showed an increase of 13%, 39%, and 14% for PM_{2.5}, BC, and NO₂, respectively.

Comparison of exposure estimates split by population subgroups revealed different patterns in static (Stages 1–2) and dynamic (Stage 5) models. The static model found that those who were neither in work nor study (i.e., “others”) had slightly higher exposures than other subgroups. However, the dynamic models found that students had higher PM_{2.5} and BC exposure than workers, and the lowest exposures were found with the “others” subgroup. Students had a 13% and 35% increase compared with that group for PM_{2.5} and BC, respectively. For students, the mean time-weighted exposures were 29.7 and 9.2 µg/m³ for PM_{2.5} and BC, respectively. For NO₂, working adults had the highest dynamic exposure with a mean time-weighted exposure of 75.5 µg/m³, which was 2% and 18% higher than those of the students and “others” subgroups.

Dynamic models found lower female exposures for all pollutants. Male exposures were 2%, 5%, and 4% higher than female in dynamic exposures when compared with static. For male subjects, the mean time-weighted exposures were 27.4, 8.1, and 72.8 µg/m³ for PM_{2.5}, BC, and NO₂, respectively.

WP4: MODEL EVALUATION AND TRANSLATION FOR APPLICATION IN OTHER MEGACITIES

Cohort Data

Out of the 66,820 subjects enrolled in the cohort, 63,218 (95%) were geocoded from their baseline residential addresses. Excluding subjects with missing individual-level covariates ($n = 589$; 0.88%), missing community-level covariates ($n = 22$; 0.03%), unavailable exposure estimates ($n = 838$; 1.25%), or unavailable or incorrect floor level information in addresses ($n = 838$, 1.25%), a total of 60,584 subjects were included in the analysis. The average residential height above street level was 38.7 meters (11th floor).

The spatial distribution of geocoded addresses of participants is shown in Appendix Figure A.29 (available on the HEI website). There were 8,553 subjects (13.3%) who had a change of address during the analysis period, in which case, address at baseline was used. Within the cohort, approximately 70% of the participants were 65–74 years of age. Around 67% of the participants were female, and about 26.4% of the total subjects had died by the end of the study period. Of the total number of deaths recorded ($n = 16,415$), 16,006 were from natural causes, and 409 were from external causes. The number of deaths from all cardiovascular and respiratory causes were 4,656 and 3,150, respectively. The number of deaths for each mortality outcome in the cohort is shown in Appendix Table A.20.

Exposure Data

Mean exposure estimates ranked in the order of highest to lowest were 2D, 3D, and D3D LUR (Appendix Table A.21). At baseline, D3D exposures were on average 20%, 50%, 50%, and 46% lower than the corresponding 2D exposure for PM_{2.5}, BC, NO, and NO₂, respectively. BC exhibited the largest range of values out of all pollutants, with a mean exposure of 6.6 ± 4.0 µg/m³ (D3D). Satellite-derived 2D and 3D PM_{2.5} exposures applied to the same study area and cohort (Wong et al. 2015, 2016) were included for comparison. LUR-estimated exposures were found to have higher means compared with satellite-derived exposures for PM_{2.5}. The 2D mean exposures were 42.4 µg/m³ (LUR) and 35.6 µg/m³ (satellite). The 3D mean exposures were 36.6 µg/m³ (LUR) and 33.7 µg/m³ (satellite). Satellite estimates generally had lower spatial heterogeneity as concentrations were averaged over a 1×1 km grid cell.

The correlations between different exposure estimates across pollutants and among 2D, 3D, and D3D exposures are shown in Table 11. High correlation between 3D and D3D exposures is expected as the analysis cohort was limited to age ≥ 65 by design; thus dynamic factors based on age and occupation groups would show less variation than if applied across an age-representative population.

We examined the trends in back-extrapolated annual concentrations for each pollutant, derived from government network monitoring data. While BC and NO concentrations decreased steadily over the 13-year study period (~50% and 35%, respectively), NO₂ and PM_{2.5} concentrations changed by <10% and remained well above the World Health Organization Air Quality Guidelines (World Health Organization 2016a).

Descriptive statistics of modeled and back-extrapolated exposure distributions from the 2D, 3D, and D3D LUR models, as well as the annual mean back-extrapolated 2D exposure trends, are shown in Appendix Tables A.21 and A.22 and Figure A.30 (available on the HEI website).

Associations Between Long-Term Air Pollution Exposure and Mortality

HRs were calculated per IQR increase in pollutant for each LUR model stage (Table 12). Generally, HRs for the 3D and D3D models were very similar, with more statistically significant associations found than in the 2D models. This indicates a homogenous distribution of changes in exposure estimates resulting from the addition of the dynamic model component.

A 3% increased risk of death from all natural causes was found with each IQR increase of PM_{2.5} (HR = 1.03; 95% CI = 1.01–1.06) and BC (HR = 1.03; 95% CI = 1.00–1.05) using 2D exposures. For PM_{2.5}, the HRs per IQR increase

Table 11. Correlation Coefficient (*r*) Matrix for 2D, 3D, and D3D Exposure Estimates for All Pollutants^a

		2D				3D				D3D			
		PM _{2.5}	BC	NO	NO ₂	PM _{2.5}	BC	NO	NO ₂	PM _{2.5}	BC	NO	NO ₂
2D	PM _{2.5}		0.32	0.15	0.00	0.65	0.24	0.07	-0.02	0.65	0.24	0.07	-0.02
	BC	0.32		0.05	0.12	0.24	0.83	0.05	0.09	0.24	0.83	0.05	0.09
	NO	0.15	0.05		0.47	0.16	0.07	0.68	0.31	0.16	0.07	0.68	0.31
	NO ₂	0.00	0.12	0.47		0.06	0.12	0.35	0.55	0.06	0.12	0.35	0.55
3D	PM _{2.5}	0.65	0.24	0.16	0.06		0.56	0.63	0.64	1.00	0.56	0.63	0.64
	BC	0.24	0.83	0.07	0.12	0.56		0.42	0.49	0.56	1.00	0.41	0.49
	NO	0.07	0.05	0.68	0.35	0.63	0.42		0.82	0.63	0.42	1.00	0.82
	NO ₂	-0.02	0.09	0.31	0.55	0.64	0.49	0.82		0.64	0.49	0.82	1.00
D3D	PM _{2.5}	0.65	0.24	0.16	0.06	1.00	0.56	0.63	0.64		0.56	0.63	0.64
	BC	0.24	0.83	0.07	0.12	0.56	1.00	0.42	0.49	0.56		0.42	0.49
	NO	0.07	0.05	0.68	0.35	0.63	0.41	1.00	0.82	0.63	0.42		0.82
	NO ₂	-0.02	0.09	0.31	0.55	0.64	0.49	0.82	1.00	0.64	0.49	0.82	

^a Correlations between 3D and D3D appear identical due to rounding.

in PM_{2.5} with all-natural-cause mortality were HR = 1.07 (95% CI = 1.04–1.09) for both 3D and D3D exposures. For BC, the HRs per IQR increase in BC with all-natural-cause mortality were HR = 1.05 (95% CI = 1.02–1.07) for both 3D and D3D exposures. Overall, results from 3D and D3D exposures were similar, but results differed significantly between 2D and both 3D and D3D. For NO, while a nonsignificant negative association was reported for all-natural-cause mortality for 2D exposure (HR = 0.99; 95% CI = 0.97–1.02), 3D and D3D exposures had significant positive associations (HR = 1.05; 95% CI = 1.02–1.07). Similar results were found for NO₂ and all-natural-cause mortality: HR for 2D exposure was 1.00 (CI = 0.97–1.03) compared with 1.06 (95% CI = 1.03–1.09) for 3D exposure and 1.06 (95% CI = 1.03–1.08) for D3D exposure.

The long-term air pollution exposure had strong effects on cardiovascular deaths. The HRs per IQR increase in PM_{2.5} for all cardiovascular causes of death were 1.06 (95% CI = 1.02–1.10) for 2D and 1.10 (95% CI = 1.05–1.14) for 3D and D3D. PM_{2.5} exposures were also significantly associated with subcategories of IHD and cerebrovascular deaths. Similarly, a 7%, 9%, and 10% increased risk of cardiovascular death was found with each IQR increase of BC for 2D, 3D, and D3D exposures, respectively. Positive associations were found only with 3D and D3D NO exposures and IHD

mortality (HR = 1.09; 95% CI = 1.01–1.17). For NO₂, significant associations with overall cardiovascular and the subcategory of IHD were reported with 3D and D3D exposures (HR = 1.09; 95% CI = 1.04–1.14 for overall cardiovascular, and HR = 1.15; 95% CI = 1.06–1.24 for IHD mortality). This association was the strongest of all pollutants. For respiratory mortality, the only significant associations found were between 3D and D3D PM_{2.5} and all respiratory deaths (HR = 1.06; 95% CI = 1.01–1.11).

PM_{2.5} exposure estimates and HRs were also available from a previously published study utilizing the same cohort (Wong et al. 2015), allowing a direct comparison of health outcomes. As IQR was not available for this study, comparisons were made based on calculated HRs per 10-µg/m³ increase in PM_{2.5}. Table 13 summarizes the calculated HRs per 10-µg/m³ increase using LUR models and satellite-based exposures for PM_{2.5}. A 10-µg/m³ increase in PM_{2.5} was associated with all-natural-cause mortality for both 2D estimates (HR = 1.06; 95% CI = 1.02–1.11 for LUR; and HR = 1.14; 95% CI = 1.07–1.22 for satellite estimates). In general, satellite exposure estimates had higher HRs than the other models, but their CIs were approximately twice as large as the CIs for the 3D and D3D models, indicating much greater uncertainty in associations. Only 3D and D3D LUR models found significant associations

Table 12. Adjusted Hazard Ratios (95%CI) per IQR Increase of Pollutants for Baseline Exposure^{a,b}

Pollutants / Cause of Death	2D	3D	D3D
PM _{2.5}	IQR: 5.5 µg/m ³	IQR: 7.5 µg/m ³	IQR: 7.0 µg/m ³
All natural causes	1.03 (1.01 to 1.06)	1.07 (1.04 to 1.09)	1.07 (1.04 to 1.09)
Cardiovascular	1.06 (1.02 to 1.10)	1.10 (1.05 to 1.14)	1.10 (1.05 to 1.14)
IHD	1.03 (0.97 to 1.10)	1.09 (1.03 to 1.17)	1.09 (1.03 to 1.17)
Cerebrovascular	1.06 (0.99 to 1.13)	1.08 (1.01 to 1.16)	1.08 (1.01 to 1.16)
Respiratory	1.02 (0.97 to 1.06)	1.06 (1.01 to 1.11)	1.06 (1.01 to 1.11)
Pneumonia	1.00 (0.94 to 1.06)	1.05 (0.99 to 1.12)	1.05 (0.99 to 1.12)
COPD	1.06 (0.97 to 1.15)	1.09 (1.00 to 1.19)	1.09 (1.00 to 1.19)
External causes	1.02 (0.90 to 1.16)	1.03 (0.90 to 1.19)	1.04 (0.90 to 1.19)
BC	IQR: 9.6 µg/m ³	IQR: 7.2 µg/m ³	IQR: 5.4 µg/m ³
All natural causes	1.03 (1.00 to 1.05)	1.05 (1.03 to 1.07)	1.05 (1.03 to 1.07)
Cardiovascular	1.07 (1.03 to 1.11)	1.09 (1.05 to 1.14)	1.10 (1.06 to 1.14)
IHD	1.08 (1.01 to 1.15)	1.10 (1.04 to 1.17)	1.11 (1.04 to 1.17)
Cerebrovascular	1.05 (0.98 to 1.13)	1.07 (1.01 to 1.14)	1.07 (1.01 to 1.15)
Respiratory	0.99 (0.94 to 1.04)	1.02 (0.97 to 1.06)	1.02 (0.97 to 1.06)
Pneumonia	0.99 (0.93 to 1.05)	1.01 (0.96 to 1.07)	1.01 (0.96 to 1.07)
COPD	0.98 (0.90 to 1.08)	1.01 (0.93 to 1.10)	1.01 (0.93 to 1.10)
External causes	1.18 (1.03 to 1.35)	1.15 (1.01 to 1.30)	1.15 (1.01 to 1.30)
NO	IQR: 167 µg/m ³	IQR: 203 µg/m ³	IQR: 151 µg/m ³
All natural causes	0.99 (0.97 to 1.02)	1.05 (1.02 to 1.07)	1.05 (1.02 to 1.07)
Cardiovascular	0.96 (0.91 to 1.00)	1.04 (0.99 to 1.09)	1.04 (0.99 to 1.09)
IHD	0.98 (0.91 to 1.05)	1.09 (1.01 to 1.17)	1.09 (1.01 to 1.17)
Cerebrovascular	0.96 (0.89 to 1.04)	1.01 (0.94 to 1.10)	1.01 (0.94 to 1.10)
Respiratory	1.00 (0.94 to 1.05)	1.06 (1.00 to 1.12)	1.06 (1.00 to 1.12)
Pneumonia	0.99 (0.93 to 1.06)	1.06 (0.99 to 1.13)	1.06 (0.99 to 1.13)
COPD	1.04 (0.94 to 1.15)	1.10 (0.99 to 1.22)	1.10 (0.99 to 1.22)
External causes	1.10 (0.94 to 1.28)	1.07 (0.92 to 1.25)	1.07 (0.92 to 1.26)
NO ₂	IQR: 26 µg/m ³	IQR: 38 µg/m ³	IQR: 31 µg/m ³
All natural causes	1.00 (0.97 to 1.03)	1.06 (1.03 to 1.09)	1.06 (1.03 to 1.08)
Cardiovascular	1.00 (0.95 to 1.05)	1.09 (1.04 to 1.14)	1.09 (1.04 to 1.14)
IHD	1.09 (1.00 to 1.18)	1.15 (1.06 to 1.24)	1.15 (1.06 to 1.24)
Cerebrovascular	1.00 (0.91 to 1.09)	1.06 (0.98 to 1.15)	1.06 (0.98 to 1.15)
Respiratory	0.99 (0.93 to 1.06)	1.06 (1.00 to 1.12)	1.06 (1.00 to 1.12)
Pneumonia	0.98 (0.90 to 1.06)	1.06 (0.99 to 1.14)	1.06 (0.99 to 1.14)
COPD	1.02 (0.90 to 1.15)	1.06 (0.96 to 1.18)	1.06 (0.96 to 1.18)
External causes	1.10 (0.92 to 1.31)	1.08 (0.93 to 1.27)	1.08 (0.93 to 1.27)

^a **Bolded** font = $P < 0.05$; 2D = street-level LUR; 3D = 2D + vertical decay; D3D = 3D + infiltration, mobility, and transport microenvironments.

^b Corrected for the following confounders: age, sex, body mass index, smoking status, physical exercise, education, monthly expenses, proportion of the population ≥ 65 years of age, proportion with $>$ secondary education, proportion that are smokers, average monthly income.

Table 13. Adjusted Hazard Ratios (95%CI) per 10- $\mu\text{g}/\text{m}^3$ Increase of $\text{PM}_{2.5}$ in Main Analysis^{a,b}

Cause of Death	2D	2D – Satellite ^c	3D	D3D
All natural causes	1.06 (1.02 to 1.11)	1.14 (1.07 to 1.22)	1.09 (1.06 to 1.12)	1.10 (1.06 to 1.13)
Cardiovascular	1.11 (1.03 to 1.19)	1.22 (1.08 to 1.39)	1.13 (1.07 to 1.19)	1.14 (1.08 to 1.21)
IHD	1.06 (0.95 to 1.19)	1.42 (1.16 to 1.73)	1.13 (1.03 to 1.23)	1.14 (1.04 to 1.25)
Cerebrovascular	1.11 (0.98 to 1.25)	1.24 (1.00 to 1.53)	1.11 (1.01 to 1.21)	1.12 (1.01 to 1.23)
Respiratory	1.03 (0.94 to 1.12)	1.05 (0.90 to 1.22)	1.08 (1.01 to 1.15)	1.09 (1.01 to 1.17)
Pneumonia	1.00 (0.90 to 1.11)	0.94 (0.77 to 1.14)	1.07 (0.98 to 1.16)	1.07 (0.98 to 1.17)
COPD	1.10 (0.95 to 1.29)	1.30 (0.98 to 1.74)	1.12 (1.00 to 1.26)	1.13 (0.99 to 1.28)
External causes	1.04 (0.82 to 1.32)	1.04 (0.69 to 1.58)	1.05 (0.87 to 1.26)	1.05 (0.86 to 1.28)

^a **Bolded** font = $P < 0.05$; 2D = street-level LUR; 3D = 2D + vertical decay; D3D = 3D + infiltration, mobility, and transport microenvironments.

^b Corrected for the following confounders: age, sex, body mass index, smoking status, physical exercise, education, monthly expenses, proportion of the population ≥ 65 years of age, proportion with > secondary education, proportion that are smokers, average monthly income.

^c From Wong et al. 2015. Note that satellite estimates had lower mean exposure concentrations due to lower spatial resolution.

with overall respiratory mortality (respectively, HR = 1.08; 95% CI = 1.01–1.15; and HR = 1.09; 95% CI = 1.01–1.17).

Sensitivity Analyses

We performed sensitivity analyses to observe changes to associations between exposure and mortality when (1) yearly exposure to pollutants was included as a time-dependent variable varying from year to year; (2) participants who died during the first year after enrollment were included; and (3) participants who died between years 1 and 3 were excluded. In addition, we performed two stratified analyses: (1) subject's age (as defined by two age groups: < 71 or ≥ 71 years old — based on the cohort's median age of 70) and (2) sex of the participants.

Significant associations found between BC, NO, and NO_2 exposures and mortality outcomes remained when yearly exposures were used, when deaths within the first year were included, or when deaths between years 1 and 3 were excluded. When 2D exposures were used, the associations between $\text{PM}_{2.5}$ and all-natural and overall cardiovascular mortality became nonsignificant when yearly exposures were used. For 3D and D3D $\text{PM}_{2.5}$ exposures, associations with IHD, cerebrovascular, and overall respiratory mortality were also nonsignificant when yearly concentrations were used. All other estimates and levels of significance were similar in the sensitivity analysis compared with main analysis results.

In the age-stratified analysis, the association between IQR increases in $\text{PM}_{2.5}$ and mortality was closer to the null

(or essentially null) in the ≥ 71 years age group compared with the < 71 years age group for all mortality outcomes. For 2D estimates, differences were pronounced for all natural causes (interaction P value=0.007), cardiovascular disease (interaction P value=0.001), and IHD (interaction P value=0.008). There was no evidence of consistent differences in any associations using between-D3D estimates, or in other pollutants for 2D estimates, and any mortality outcomes. There was no evidence of consistent differences according to the subjects' sex in D3D estimates, although more associations with outcomes were found in males than in females with the 2D exposures. The interaction of a potential effect modifier with $\text{PM}_{2.5}$ was formally evaluated. The P value for the interaction was obtained by inclusion of the interaction term of each potential effect modifier with the pollutant. The interaction was evaluated between air pollutants and the potential effect modifier by including the interaction term in the final model.

Results of the sensitivity analyses relating to yearly exposures, stratification by age, and stratification by sex are presented in Appendix Tables A.23 to A.32.

Application of Alternative Decay Profile

Epidemiological analysis was also applied to the cohort using the alternative decay profile illustrated in Figure 6 (i.e., applying a cap to decay at 20 m above street level, which is at floor six). The impact of this was to increase exposure estimates for those living above approximately floor six, leading to an overall increase in mean cohort exposure

(PM_{2.5} from 36.9 to 39.8 µg/m³, NO₂ from 71.5 to 87.8 µg/m³) and a decrease in exposure variability. Consequently, differences between street level (2D) and residential level (3D) exposure estimates also decreased. Recalculated HRs are shown in Appendix Table A.33 (available on the HEI website). The impact of application of this alternative profile on the 3D model was to decrease the magnitude of HRs across all mortality outcomes. Several previously significant associations became insignificant, including all-cause mortality for NO, cerebrovascular mortality for BC, and respiratory mortality for PM_{2.5}.

Visualization of 3D Dispersion Patterns

Screen captures from a sample 3D visualization animation are shown in Appendix Figure A.31. The full sample video can be seen at <http://geog.hku.hk/h-city/HKD3D.html>. Work is still ongoing to refine this visualization and extend it to cover the whole urban region.

DISCUSSION AND CONCLUSIONS

The Hong Kong D3D study had the overarching aim of creating and evaluating an advanced TRAP exposure model methodology that incorporated population mobility and residential height above street level, using Hong Kong, a densely populated Asian city, as a case study. Our principal hypothesis was that the inclusion of dynamic and vertical components in TRAP exposure models applied to Asian cities would lead to increased confidence in associated health outcomes.

The study had four main components: (1) the creation of a street-level LUR model for the Hong Kong region through an extensive seasonal sampling campaign; (2) the derivation of a canyon typology and associated vertical decay rate, through multiheight paired in–out sampling campaigns in several locations representative of population exposure; (3) creation of a series of dynamic model components incorporating infiltration efficiencies and population mobility utilizing an extensive travel behavior survey; and (4) application of a staged modeling approach to an existing cohort to compare mortality risk estimates.

In achieving this aim, several practical and methodological obstacles had to be overcome. On the whole, the original study plan was adhered to, but a few adjustments had to be made, most notably, the exclusion of gaseous pollutants from the vertical sampling campaign results because of sensor performance issues, and the simplification of canyon typology because there was no robust identifiable pattern in canyon TRAP dispersion patterns. Conversely, we achieved more than we anticipated in the creation of

dynamic modeling components and the application to the existing cohort.

IMPLICATIONS FOR FUTURE USE OF LOW-COST AIR QUALITY SENSORS

The development of a new generation of relatively low-cost air pollution sensors has generated a great deal of interest, both in the research community and in public interest groups (U.S. Environmental Protection Agency 2016). This study used relatively high-cost (~4,000 USD per unit) active samplers for PM_{2.5}, BC, and gaseous pollutants. While these samplers have advantages over passive samplers, we identified several major shortcomings that should be considered by others designing spatial sampling campaigns in Asian cities and elsewhere across the world. First, harsh sampling conditions — variously, high temperatures, intense rainfall, wind storms, high humidity, and high particulate levels, which are typical in tropical and subtropical climates — take their toll on sensitive electronics. Every active sampling unit we deployed required maintenance at least once during our campaigns, and several back-up units were required while repairs were carried out. Second, active samplers are more visible, heavier, and more expensive to replace than passive samplers. Safety and security are therefore major concerns, both to personnel and equipment. Our spatial sampling campaigns relied on collaboration with the Hong Kong EPD. Hong Kong is widely considered a very secure city, and our only losses were some passive samplers removed by concerned locals. No active samplers could be hung outside of buildings, necessitating the use of sampling tubing (for pumped PM samplers) and a manifold (for electrochemical samplers). Third, a high degree of interunit precision is necessary when deploying samplers in networks to detect spatial and vertical variations in TRAP. The development of refined methods of data scaling and ratification was required to achieve the necessary precision in each of the PM units. Such precision could not be achieved with the electrochemical gas sensors, which did not respond well to being regularly moved, and these data had to be excluded from further analysis.

In our experience, very careful experimental design is required if the low-cost electrochemical sensors currently available are to be used effectively in spatial exposure measurement campaigns where accurate representation of within-neighborhood variations is required. This is primarily due to issues with unstable baseline measurements creating bias of a magnitude greater than the spatial variation being investigated. While all instruments suffer from some degree of bias, this has been well characterized in more established monitors, and robust, demonstrably

consistent methods for correction can be developed. The strong influence of a range of factors (including temperature, humidity, cross-gas interference, and signal noise), which combine to produce a complex pattern of interference in real-world conditions, makes consistent correction methods challenging to develop. Until such correction methods can be documented and demonstrated, the use of such electrochemical sensors has to be questioned closely before being incorporated into future studies.

DEVELOPMENT OF A 2D LAND-USE REGRESSION MODEL FOR HONG KONG

The street-level (2D) LUR modeling captured important spatial parameters and represented spatial patterns of air quality in Hong Kong that were consistent with the literature (Chiu and Lok 2011; Kok et al. 1997; Shi et al. 2016; Yu et al. 2004). Higher concentrations of gaseous pollutants were centered in Kowloon and the northern region of Hong Kong Island, consistent with the importance of motor vehicle traffic as a dominant source of local NO and NO₂ (Tian et al. 2011). PM_{2.5} and BC predictions exhibited a north–south/west–east gradient, with higher concentrations in the northwest. This appears to be due to regional transport from Mainland China. A similar gradient in PM₁₀ concentrations, noted previously in an analysis of the rooftop AQMS, was attributed to transport from Mainland China (Chiu and Lok 2011). Further, Kok and colleagues (1997) reported elevated BC concentrations in the western regions of the territory and similarly attributed these higher levels to regional sources. A recent LUR model of PM_{2.5} restricted to downtown Hong Kong indicated spatial patterns similar to those of the HK 2D model (Shi et al. 2016). For BC, the port was also an area of elevated predicted values. Yu and colleagues (2004) had noted the port as an important emission source affecting spatial distribution of BC levels with increases in background BC concentrations around the port, depending on the seasonal direction of the prevailing wind. Shipping lane variables were not, however, present in any of the final exposure models in the current study.

While the degree of explained variance of the models was modest, they were within the range seen with other LUR modeling efforts (e.g., Hoek et al. 2008). Given the complex urban morphology of Hong Kong compared with most of the European and North American cities, a somewhat reduced explained variance was expected. Compared with LUR models developed in other Asian cities where urban morphology, vehicle use, and building design may be similar, LUR models that were developed with dedicated sampling campaigns reported similar R^2 values (shown in Appendix Table A.3, available on the HEI website).

VERTICAL DECAY OF TRAP AND DERIVATION OF A CANYON TYPOLOGY

Our canyon sampling campaign was designed to capture variations in TRAP within canyons by height, time of day, and wind conditions. We selected canyons that had a range of aspect ratios, building configurations, and alignment to the prevailing wind. In practice, measurements did not show sufficiently consistent patterns in vertical pollutant concentrations to isolate the impact of many of these variables. We found no evidence of strong TRAP stagnation in typical weather conditions, even in high AADT narrow canyons such as NPC1. TRAP either was fully mixed within the canyon (decay rate approximately zero) or decayed rapidly over the lower floors.

It is important to note that our objective was to characterize population-level vertical exposure, not to produce a detailed explanation of emission dispersion patterns, such as that created by fluid dynamics models. While complex modeled eddies of the type identifiable through computational fluid dynamics are important for urban design, our results suggest that they are of less importance in urban canyons of the type typical in Hong Kong when assessing population exposure levels. Indeed, it may be that we found no evidence of stagnation because of improvements in urban street canyon design over the past 50 years. In Hong Kong, continuous slab-type buildings have largely been replaced by individual residential towers, many laid out in gridded estates with little or no vehicle traffic allowed within. New slab constructions are built at an angle, and many are pierced with voids at higher levels; both designs are intended to increase air flow. While these construction methods have had the primary aim of reducing heat stress (Deng et al. 2016; Ng 2009), they have also had the beneficial effect of increasing the dispersion of TRAP and other air pollution sources, such as cooking.

Our original intention was to produce a coupled street canyon typology with specific TRAP vertical decay rates for each canyon type. By creating such a classification system, street-level exposure estimates within high-density urban landscapes could be scaled vertically according to basic canyon geometry. Our results led us to the conclusion that derivation of such a classified system was not possible, and we assumed a single mean decay rate across the region. Widespread vertical sampling campaigns are challenging to execute, requiring large resources to identify suitable locations, recruit building and flat owners, and deploy and manage samplers. In our view, the addition of sampling in additional canyons would not have produced a substantially different result. However, uncertainties remain, and improvements could be made to subsequent vertical sampling campaigns. The addition of

street-level sampling in all canyons would remove the necessity for temporally corrected model estimates, but would introduce additional practical considerations. Time-resolved measurements were not as informative as expected, and paired windward and leeward sampling was difficult to interpret.

An additional limitation in the vertical decay calculation was the separation of local and regional pollution components. Assuming that regional pollutant sources are well dispersed across the urban area, vertical decay occurs only in the local pollutant component. Thus, an improved version of Equation 2 would be:

$$C_h = C_r + C_{h=0} e^{-kh}, \quad (7)$$

where C_r is the regional component of concentration C . This approach would bring the k (decay rate) for BC and $PM_{2.5}$ much closer together; BC being a primary component of local $PM_{2.5}$. In this study, this improvement could have been achieved through a rooftop sampling campaign mirroring that of the street-level campaign. Emissions-based modeling methods would be able to make this separation more easily than the empirical LUR method that we employed. An attempt was made to incorporate this alternative decay pattern by capping decay to a height of 20 meters, but further measurements would be required to confirm this height estimate.

We found seasonal $PM_{2.5}$ decay rates (k factors) of 0.009 and 0.001 for the warm and cool seasons, respectively, highlighting the dominance of regional $PM_{2.5}$ sources during the cool season (see Table 7). For BC, the seasonal difference was 0.016 and 0.009. The single mean decay rates across the region for $PM_{2.5}$ and BC were 0.004 and 0.012, respectively. Direct comparisons with these decay rates are difficult because of varying methodology; however, Chan and Kwok (2000) reported a decay rate for PM_{10} in Hong Kong of 0.017 from a campaign in the cool season. In common with Wu and colleagues (2002), we found little diurnal variation in decay rates.

BUILDING INFILTRATION EFFICIENCIES

A major advantage of the vertical monitoring campaign design was that paired in-out monitoring could be added relatively simply, allowing the calculation of infiltration efficiencies for the Hong Kong housing stock. We found that median F_{inf} values for both BC and $PM_{2.5}$ were especially high during the cool season (91%), indicating that residents were breathing only slightly lower levels of these pollutants indoors than was measured in ambient air. Median infiltration efficiencies were somewhat lower during the warm season (81% and 88% for $PM_{2.5}$ and BC,

respectively), and we found a significant negative correlation between air conditioning use and infiltration efficiencies of $PM_{2.5}$ and BC. The MESA-Air study reported a median infiltration efficiency for $PM_{2.5}$ across seven urban communities in North America of 62%, although the median for New York was 82% and was therefore similar to what we found in Hong Kong (Allen et al. 2012).

During the cool season, when $PM_{2.5}$ concentrations are typically far higher in Hong Kong, residents were more likely to open their windows, leading to a greater infiltration of outdoor air. Therefore, higher ambient concentrations and higher infiltration efficiencies acted together to increase population exposure.

Infiltration efficiencies for the mechanically ventilated office building were 45% and 40% during the cool and warm seasons, respectively. While we only measured infiltration efficiencies in one such building, this is similar to those reported in other studies for occupied HVAC buildings (Chatoutsidou et al. 2015; Fisk et al. 2000). Only a very small proportion of high-value residences have mechanical ventilation, so few benefit from this protection. This finding has important socioeconomic implications for developing subtropical cities: those who can afford higher-specification homes are also more likely to have office jobs in similarly protected buildings. Conversely, these buildings have higher power requirements than naturally ventilated buildings and in many cases will contribute further to regional sources of $PM_{2.5}$ through fossil-fuel-based electricity generation.

DYNAMIC EXPOSURE MODELING

A population-representative travel behavior survey ($n = 89,358$) was used to further extend our exposure model to create a dynamic model comprising population mobility and derivation of time-weighted exposure estimates in different microenvironments. A staged approach was used to investigate the impact of each component on exposure estimates for the survey respondents. The vertical component of the model was not included as the survey did not record floor of residence.

Comparisons were made against the static outdoor exposure estimates. As expected, the addition of an indoor component decreased time-weighted exposure estimates, which were balanced out to some extent by the inclusion of transport microenvironments. Overall, mean time-weighted exposures for the full dynamic model were around 20% lower than the static outdoor estimates. The inclusion of diurnal factors had a greater impact on BC and NO_2 exposure estimates than on $PM_{2.5}$, because BC and NO_2 tend to vary more during the day than $PM_{2.5}$.

Smith and colleagues (2016) combined a nested dispersion modeling technique with building infiltration factors and travel behavior to create a dynamic exposure model for London. They found that the dynamic model produced estimated exposures 37% lower for $PM_{2.5}$ and 63% lower for NO_2 than the static ambient model. This difference is likely to be driven by the much lower mean infiltration efficiencies used for London (31% and 56% for NO_2 and $PM_{2.5}$, respectively).

If these differences were equally distributed across the population, then their inclusion would have little impact on health outcome analyses. A stratified analysis of population subgroups was carried out to test the hypothesis that the dynamic model increased variation in exposure estimates.

The stratified analysis confirmed this hypothesis. Higher levels of exposures were found with working adults and students than for those neither in work nor study. This was due to increased mobility, despite relatively low concentrations in office locations, particularly in BC estimates. The results consistently found higher exposures with persons under age 18, compared with other age groups. The exposures to $PM_{2.5}$, BC, and NO_2 were respectively 13%, 39%, and 14% higher for the under-age-18 population compared with the population of people who were age 65 or older. One explanation for this is that most students' schools were located within the same TPU, and many commuted to school by walking. This pattern of increased exposure with longer travel time has been described by others in exposure monitoring studies (Chau et al. 2002; de Nazelle et al. 2013), and has been suggested to partially offset the physical activity benefits of walking (Hankey et al. 2012). We also assumed natural ventilation in schools, with higher infiltration rates than in office buildings. Spatial contrasts were amplified when accounting for diurnal variation in pollutants, as most subjects traveled during morning and evening rush-hour periods, indicating that population mobility is an important consideration beyond that of transport microenvironment effects.

We found the addition of additional exposure model components increased the gap between male and female exposures, with the female population having lower exposures to air pollution by approximately 4%. A study in Vancouver (Setton et al. 2010), which examined only the working population, found no significant difference in exposure by sex. However, a higher than 50% proportion of women in our survey data were in the nonworking category, which is likely to account for the different finding.

Many of our model results reflect those of Chau and colleagues (2002), who used portable samplers to examine exposure to PM_{10} , NO_2 , and CO for different age groups in 20 different microenvironments in Hong Kong. They

found that the Hong Kong population spent around 86% of the time indoors and around 8% (two hours) commuting. However, higher pollutant exposures were experienced during commuting, so commuting contributed a disproportionately high amount to the 24-hour average, particularly for NO_2 . They found high concentrations at restaurants, bars, and transport microenvironments, but low concentrations in offices. For both PM_{10} and NO_2 , concentrations in offices were much lower than in residential buildings. Concentrations monitored at schools were around four times those in offices. Out of 400 subjects sampled, the under-18 age group was found to have the highest exposures.

A key uncertainty in our transport microenvironment component arose from a lack of contemporary factors from recent monitoring surveys for all pollutants and modes of transport. Such surveys could be considered as part of the sampling requirements for development of similar dynamic models if published factors are not available.

STAGED EPIDEMIOLOGICAL ANALYSIS OF MORTALITY RATES IN AN ELDERLY COHORT

The availability of an existing cohort data set of elderly Hong Kong residents ($n = 66,820$) facilitated the calculation and comparison of mortality risk estimates for the different exposure models. We further incorporated results from an earlier study on the same cohort but used satellite-derived exposure estimates.

Overall, the results indicated that the addition of a vertical component to the exposure model modified the associations between long-term exposure to air pollution and mortality. The application of exposure estimates that incorporated infiltration, vertical, and, to a lesser extent, dynamic components produced narrower confidence intervals and increased the number of significant associations with all-natural-cause, cardiovascular disease, and respiratory disease mortality outcomes.

When considering only 2D exposure, $PM_{2.5}$ was significantly associated with elevated risks of mortality only from all-natural and cardiovascular causes. When 3D and D3D exposure models were used, associations increased, and narrower CIs led to additional significant associations with cardiovascular subgroups and respiratory causes. Similarly, no significant associations were found for NO_2 using the 2D model, but mortality from all natural causes, cardiovascular disease, and IHD became significant in the 3D model. Very little difference in associations was detected between the 3D and D3D model. This is because the population mobility of the elderly cohort was relatively modest since the cohort included only persons age 65 and older, producing little variation in exposure estimates.

The one anomaly occurred between BC and external causes of death where an unexplained significant association was reported. This may be a result of left-truncated exposure distribution or it may be due to high variability of estimates around a low mean. As expected, particulate pollutants displayed more health effects than did gaseous pollutants.

While air pollution is known to vary vertically and in street canyons (Berkowicz et al. 1996; Meroney et al. 1996; Vardoulakis et al. 2003), as well as between outdoor, indoor (Allen et al. 2012; Hystad et al. 2009), and transport microenvironments (Adams et al. 2001; Kaur and Nieuwenhuijsen 2009), few studies have taken these factors into consideration when investigating the long-term health effects of air pollution. This issue becomes more important in high-rise urban areas where activities take place in high buildings. Studies have included variables representing the 3D landscape in LUR models to improve street-level exposure estimates (Eeftens et al. 2013; Su et al. 2008; Tang et al. 2013). Wong and colleagues (2016) applied horizontal-vertical $PM_{2.5}$ exposure estimates to assess cancer mortality by geocoding the vertical height of addresses, but they did not assess the epidemiological effects between the use of 2D and 3D exposures.

The range of associations was coherent with other cohort studies that looked at long-term exposure to air pollution and mortality. Associations were more pronounced with cardiovascular mortality, which is in common with findings in other study areas. The ESCAPE study (Beelen et al. 2014) found similar associations. HRs for $10\text{-}\mu\text{g}/\text{m}^3$ increases in $PM_{2.5}$ were 1.15 (95% CI: 1.13–1.16) for all-natural-cause mortality and 1.31 (95% CI: 1.27–1.35) for IHD, consistent with our finding.

The principal limitation of this evaluation phase of the study was the use of a cohort not representative of the whole population. This meant that the dynamic components could not be fully tested. This presents a challenge as most health outcome data sets are age-biased in some way. Conversely, most published studies on dynamic exposure to air pollutants have been based on personal monitoring studies (e.g., Özkaynak et al. 2013; Steinle et al. 2013), which cannot easily be applied to cohorts to represent mobility and exposure patterns for the general population. Effort is required to bring together population-representative dynamic exposure methods with epidemiological data sets that have heterogeneous mobility patterns in order to fully test the impact of this component of exposure. We found that contrasts in exposure between dynamic and static models were greatest in pollutants with relatively high spatial variability; BC, NO, and NO_2 are more influenced by traffic and other local emissions sources than is $PM_{2.5}$.

This conclusion was consistent with Setton and colleagues (2011), who compared mobility- and residential-based exposures of NO_2 in Canada.

We also used modeled exposures that were back-extrapolated, for a comparatively long period, to match cohort data. However, previous studies have found high correlations among annual air pollution concentrations, even over a period of more than 10 years (Beelen et al. 2008), as major roads that influence air pollution exposure are likely to have been in place for the entire period.

IMPACT OF MODEL ASSUMPTIONS

As with all modeling exercises, we had to make a number of assumptions and simplifications in the development of the advanced exposure model. We were able to carry out a limited evaluation of some of these assumptions by utilizing street-level and rooftop monitoring results at five independent locations. These evaluations showed that while the model produced good results in some conditions, it performed less well in others. This is not a surprise; our aim was to develop a mean exposure model that could be applied in epidemiological studies to estimate long-term health effects.

While the model could be improved in a number of areas, the advantage of the resulting simple methodology proposed is that it could be applied within any urban area with a significant proportion of the population living above street level. With regard to the vertical component of the model, a decay profile could be applied to any street-level model, whether it is produced by LUR, dispersion modeling, or hybrid methods. Indeed, it would be straightforward to add a vertical component to appropriate existing epidemiological studies in cities other than Hong Kong where floor of residence is known in order to explore whether our findings are repeated.

APPLICATION OF TRAP EXPOSURE METHODOLOGY IN OTHER HIGH-RISE ASIAN CITIES

We aimed to create an incremental exposure assessment methodology without onerous demands on input data that could therefore be applied to other megacities across Asia and the developing world. Such input data could be specific to the study, gathered through monitoring campaigns, or readily available from previous comparable studies or accessible government data sets.

The demonstration of reasonable LUR models to describe spatial variability in pollutant concentrations in Hong Kong suggests this to be a viable modeling method for high-density, high-rise cities, which are especially common in Asia. Further, these results suggest the utility

of model development using traditional sampling methods and relatively low-labor, low-data-intensive predictors. More complex urban development predictors, such as aspect ratio, that one might expect to be important in modeling a high-density, high-rise city, were not present in any of the final exposure models. This suggests that the added complexity in the spatial distribution of air pollutants in high-density, high-rise cities is reflected in the models' performance rather than in the selection of predictors.

Our vertical monitoring campaign was intensive and resource heavy, but the results suggest that such a comprehensive campaign is not necessary to derive broadly applicable results in other cities. However, as described earlier in this section, there are significant practical challenges in carrying out vertical campaigns, particularly in cities less secure and collaborative than Hong Kong. Where building configurations are similar to those in Hong Kong, such as in many Mainland Chinese cities, stock decay factors may be used, although care must be taken when considering pollutants with large regional components, such as $PM_{2.5}$. Our results suggest that severe stagnation, which would strongly affect decay rates, does not occur except in exceptional circumstances, either geographical or meteorological.

Our study benefited from a large travel behavior survey data set with population-representative sampling. Such large surveys are unlikely to be available in many Asian cities, but the importance of urban transport planning in densely populated cities is sufficiently high to make it likely that some form of survey exists in most. Several recent studies have demonstrated the use of mobile phone locational data in assessing population mobility for dynamic air pollution exposure assessments (de Nazelle et al. 2013; Dewulf et al. 2016; Nyhan et al. 2016). While these methods generate very large volumes of data, they have little context, requiring further assumptions about sex, age, and purpose of travel; therefore, they do not necessarily present a direct alternative to travel surveys. Where exposure estimates are applied to an epidemiological study, the cohort demographic may dictate the necessity of a dynamic component; we demonstrated that incorporation of the dynamic component did not improve associations in our elderly cohort.

There are distinct differences in terms of exposure to consider in Asian cities versus European and North American cities that can be capitalized upon to advance understanding of the health impacts of TRAP. These include relatively high infiltration efficiencies and population density, homogenous ethnicity, cohabiting extended families, greatly contrasting seasonal exposure levels, and the often unexplored potential for large-scale interventions. These opportunities make barriers such as data availability,

quality, and access, unregulated emissions, and sometimes extreme occupational exposures worth challenging.

IMPLICATIONS OF FINDINGS

To date this is the first comprehensive study to investigate the health effects of traffic-related air pollution using detailed vertical and dynamic air pollution exposure assessment techniques. The results from the study provided evidence that considering air pollution exposure in a dynamic 3D landscape would benefit epidemiological studies. Significant associations were found between mortality and air pollution that would not have been found had standard 2D LUR or satellite exposure models been used.

We also identified differential exposures between population subtypes that would not be present in static exposure models, including higher exposures for those under the age of 18 and marginally higher exposures for male subjects. As more studies incorporate population mobility, such contrasts will become better defined, leading to increased variation in estimates across a population and between pollutants (Smith et al. 2016).

Improved urban building design appears to be stimulating the dispersion of local TRAP emissions in street canyons, including broken canyons, tower estates, and angled building layout. Importantly, we found no clear evidence of stagnation reaching the upper floors of buildings. The practice of setting aside lower floors of residential towers for commercial and leisure use means that most of the Hong Kong population is not exposed to undispersed TRAP emissions in their homes, where they spend the majority of their time.

Conversely, infiltration factors found in homes were close to 1, and residences provided little protection from ambient air pollution. This is particularly critical when considering regional pollutants, such as $PM_{2.5}$, where height above street level makes little difference. There are also socioeconomic implications of this finding; those residents who can afford to live in mechanically ventilated buildings will have nearly half the exposure of those who cannot.

One of our stated aims was to create an incremental exposure assessment methodology that balanced exposure error with input data availability and that would be applicable to other megacities across Asia and the developing world. While there are several uncertainties associated with this study that could be improved in later iterations, we have demonstrated that the creation of effective advanced

exposure models is possible in Asian cities without undue burden on resources.

A number of assumptions and simplifications had to be made in developing our dynamic three-dimensional exposure model. Yet it is intuitive that street-level TRAP exposure estimates will overestimate exposure for residents living in adjacent high-rise buildings. Our results provide evidence that this misclassification leads to a lower association between mortality and air pollution exposure. However, for vertical exposure patterns to be taken into consideration for epidemiological studies, the floor of residence must be recorded in health record data. While this requirement is likely to be difficult for the total population in most countries, it should be feasible within cohort studies. We recommend that the floor of residence be routinely recorded as part of basic participant personal details at recruitment and follow up.

ACKNOWLEDGMENTS

We are extremely grateful to the Environmental Protection Department of HK SAR for assistance and collaborative work during the spatial field campaigns, access to air quality monitoring stations, and the supply of reference monitoring data. We acknowledge the assistance of the Lands Department of the HK SAR for granting access to digital topographic maps of Hong Kong. Wind velocity data at reference height were computed and provided courtesy of Professor Jimmy Fung at the Institute for the Environment, Hong Kong University of Science and Technology. M. Lee was supported in part by funding from a Natural Sciences and Engineering Research Council (Canada) CREATE-Atmospheric Aerosol Program fellowship at the University of British Columbia.

We would also like to thank the participating residents who provided regular access to their homes during the canyon monitoring campaigns.

REFERENCES

Abt E, Suh HH, Catalano P, Koutrakis P. 2000. Relative contribution of outdoor and indoor particle sources to indoor concentrations. *Environ Sci Technol* 34(17):3579–3587.

Adams HS, Nieuwenhuijsen MJ, Colvile RN, McMullen MAS, Khandelwal P. 2001. Fine particle (PM_{2.5}) personal exposure levels in transport microenvironments, London, UK. *Sci Total Environ* 279(1):29–44.

Aguilera I, Sunyer J, Fernández-Patier R, Hoek G, Aguirre-Alfaro A, Meliefste K, et al. 2008. Estimation of outdoor NO_x, NO₂, and BTEX exposure in a cohort of pregnant women using land use regression modeling. *Environ Sci Technol* 42(3):815–821; doi:10.1021/es0715492.

Allen RW, Adar SD, Avol E, Cohen M, Curl CL, Larson T, et al. 2012. Modeling the residential infiltration of outdoor PM(2.5) in the Multi-Ethnic Study of Atherosclerosis and Air Pollution (MESA Air). *Environ Health Perspect* 120(6):824–830.

Allen RW, Gombojav E, Barkhasragchaa B, Byambaa T, Lkhasuren O, Amram O, et al. 2013. An assessment of air pollution and its attributable mortality in Ulaanbaatar, Mongolia. *Air Qual Atmos Health* 6(1):137–150.

Amini H, Taghavi-Shahri SM, Henderson SB, Naddafi K, Nabizadeh R, Yunesian M. 2014. Land use regression models to estimate the annual and seasonal spatial variability of sulfur dioxide and particulate matter in Tehran, Iran. *Sci Total Environ* 488-489:343–353.

Beelen R, Hoek G, van Den Brandt PA, Goldbohm RA, Fischer P, Schouten LJ, et al. 2008. Long-term effects of traffic-related air pollution on mortality in a Dutch cohort (NLCS-AIR study). *Environ Health Perspect* 116(2):196.

Beelen R, Raaschou-Nielsen O, Stafoggia M, Andersen ZJ, Weinmayr G, Hoffmann B, et al. 2014. Effects of long-term exposure to air pollution on natural-cause mortality: an analysis of 22 European cohorts within the multicentre ESCAPE project. *Lancet* 383:785–795.

Berkowicz R, Palmgren F, Hertel O, Vignati E. 1996. Using measurements of air pollution in streets for evaluation of urban air quality — meteorological analysis and model calculations. *Sci Total Environ* 189:259–265.

Brauer M, Henderson S, Marshall J. 2006. A land use regression road map for the Burrard Inlet area local air quality study. Available: <https://open.library.ubc.ca/cIRcle/collections/facultyresearchandpublications/304/items/1.0048202> [accessed 18 August 2016].

Capannelli G, Gollo E, Munari S, Ratto G. 1977. Nitrogen oxides: analysis of urban pollution in the city of Genoa. *Atmos Environ* 11(8):719–727.

Census and Statistics Department. 2002. Hong Kong 2001 population census TAB on CD-ROM. www.censtatd.gov.hk.eproxy2.lib.hku.hk/major_projects/2001_population_census/ [accessed 10 May 2017].

Census and Statistics Department. 2011. Thematic Household Survey. Report No. 48. Gov Hong Kong Spec

- Adm Reg 2011. Available: http://smokefree.hk/UserFiles/resources/Statistics/Thematic_Household_Survey_No48.pdf [accessed 10 May 2017].
- Cerin E, Chan KW, Macfarlane DJ, Lee K, Lai PC. 2011. Objective assessment of walking environments in ultra-dense cities: development and reliability of the environment in Asia Scan Tool–Hong Kong version (EAST-HK). *Health Place* 17:937–945.
- Chan LY, Chan CY, Qin Y. 1999. The effect of commuting microenvironment on commuter exposures to vehicular emission in Hong Kong. *Atmos Environ* 33(11):1777–1787.
- Chan LY, Kwok WS. 2000. Vertical dispersion of suspended particulates in urban area of Hong Kong. *Atmos Environ* 34(26):4403–4412.
- Chatoutsidou SE, Ondracek J, Tesar O, Tørseth K, Zdímal V, Lazaridis M. 2015. Indoor/outdoor particulate matter number and mass concentration in modern offices. *Build Environ* 92:462–474.
- Chau CK, Tu EY, Chan DWT, Burnett J. 2002. Estimating the total exposure to air pollutants for different population age groups in Hong Kong. *Environ Int* 27(8):617–630.
- Chen L, Bai Z, Kong S, Han B, You Y, Ding X, et al. 2010. A land use regression for predicting NO₂ and PM₁₀ concentrations in different seasons in Tianjin region, China. *J Environ Sci* 22(9):1364–1373.
- Chiu SL, Lok R. 2011. Variations of respirable suspended particulates in Hong Kong: cross-boundary and local effects. *Annals of GIS* 17(2):113–124.
- Clougherty JE, Kheirbek I, Eisl HM, Ross Z, Pezeshki G, Gorczyński JE, et al. 2013. Intra-urban spatial variability in wintertime street-level concentrations of multiple combustion-related air pollutants: the New York City Community Air Survey (NYCCAS). *J Expo Sci Environ Epidemiol* 23(3):232–240.
- Cohen B. 2004. Urban growth in developing countries: a review of current trends and a caution regarding existing forecasts. *World Develop* 32(1):23–51.
- de Nazelle A, Seto E, Donaire-Gonzalez D, Mendez M, Matamala J, Nieuwenhuijsen MJ, et al. 2013. Improving estimates of air pollution exposure through ubiquitous sensing technologies. *Environ Pollut* 176:92–99.
- Deng Y, Chan EHW, Poon SW. 2016. Challenge-driven design for public housing: the case of Hong Kong. *Front Arch Res* 5(2):213–224.
- Dewulf B, Neutens T, Van Dyck D, de Bourdeaudhuij I, Panis L, Beckx C, et al. 2016. Dynamic assessment of inhaled air pollution using GPS and accelerometer data. *J Transp Health* 3(1):114–123.
- Dockery DW, Pope CA, Xu X, Spengler JD, Ware JH, Fay ME, et al. 1993. An association between air pollution and mortality in six U.S. cities. *N Engl J Med* 329:1753–1759.
- Eeftens M, Beekhuizen J, Beelen R, Wang M, Vermeulen R, Brunekreef B, et al. 2013. Quantifying urban street configuration for improvements in air pollution models. *Atmos Environ* 72:1–9.
- Eeftens M, Beelen R, Fischer P, Brunekreef B, Meliefste K, Hoek G. 2011. Stability of measured and modelled spatial contrasts in NO₂ over time. *Occup Environ Med* 68:765–770.
- Environmental Protection Department. 2016. Guidelines on the Estimation of PM_{2.5} for Air Quality Assessment in Hong Kong. Available: www.epd.gov.hk/epd/english/environmentinhk/air/guide_ref/guide_aqa_model_g5.html [accessed 1 Dec 2016].
- ESCAPE. 2012. Exposure assessment manual procedure for extrapolation back in time. Available: www.escapeproject.eu/manuals/Procedure_for_extrapolation_back_in_time.pdf [accessed 1 Dec 2016].
- Fisk WJ, Faulkner D, Sullivan D, Mendell MJ. 2000. Particle concentrations and sizes with normal and high efficiency air filtration in a sealed air-conditioned office building. *Aerosol Sci Technol* 32:527–544.
- Gordon J. 2012. Intermodal Passenger Flows on London's Public Transport Network [MSc Thesis]. Berkeley, CA:University of California, Berkeley. Available: <https://dspace.mit.edu/handle/1721.1/78242> [accessed 1 Sept 2017].
- Government of Hong Kong. 2015. Hong Kong — the Facts. Available: www.gov.hk/en/about/abouthk/facts.htm [accessed 1 Dec 2016].
- Government of Hong Kong Information Services Department. 2015. Population factsheet. Available: www.gov.hk/en/about/abouthk/factsheets/docs/population.pdf [accessed 1 Dec 2016].
- Gradko International. 2012. Technical Data Sheet: TDS 1. Available: www.gradko.com/environmental/products/no2-and-nitrogen-oxides-diffusion-tubes.shtml [accessed 1 Dec 2016].

- Gulliver J, de Hoogh K, Hansell A, Vienneau D. 2013. Development and back-extrapolation of NO₂ land use regression models for historic exposure assessment in Great Britain. *Environ Sci Technol* 47(14):7804–7811.
- Hankey S, Marshall JD, Brauer M. 2012. Health impacts of the built environment: within-urban variability in physical inactivity, air pollution, and ischemic heart disease mortality. *Environ Health Perspect* 120(2):247–253.
- Henderson SB, Beckerman B, Jerrett M, Brauer M. 2007. Application of land use regression to estimate long-term concentrations of traffic-related nitrogen oxides and fine particulate matter. *Environ Sci Technol* 41(7):2422–2428.
- Hoek G, Beelen R, de Hoogh K, Vienneau D, Gulliver J, Fischer P, et al. 2008. A review of land-use regression models to assess spatial variation of outdoor air pollution. *Atmos Environ* 42(33):7561–7578.
- Hystad PU, Setton EM, Allen RW, Keller PC, Brauer M. 2009. Modeling residential fine particulate matter infiltration for exposure assessment. *J Expo Sci Environ Epidemiol* 19(6):570–579.
- Jensen P, Rouquier JB, Ovtracht N, Robardet C. 2010. Characterizing the speed and paths of shared bicycle use in Lyon. *Trans Res Part D: Trans Environ* 15(8):522–524.
- Kaufman JD, Adar SD, Allen RW, Barr RG, Budoff MJ, Burke GL, et al. 2012. Prospective study of particulate air pollution exposures, subclinical atherosclerosis, and clinical cardiovascular disease: The Multi-Ethnic Study of Atherosclerosis and Air Pollution (MESA Air). *Am J Epidemiol* 176(9):825–837.
- Kaur S, Nieuwenhuijsen MJ. 2009. Determinants of personal exposure to PM_{2.5}, ultrafine particle counts, and CO in a transport microenvironment. *Environ Sci Technol* 43(13):4737–4743.
- Khreis H, Nieuwenhuijsen MJ. 2017. Traffic-related air pollution and childhood asthma: recent advances and remaining gaps in the exposure assessment methods. *Int J Environ Res Public Health* 7:14(3).
- Kirchstetter TW, Novakov T. 2007. Controlled generation of black carbon particles from a diffusion flame and applications in evaluating black carbon measurement methods. *Atmos Environ* 41(9):1874–1888.
- Kohavi R. 1995. A study of cross-validation and bootstrap for accuracy estimation and model selection. *Internat Joint Conf Artificial Intelligence* 14(2):1137–1145.
- Kok GL, Lind JA, Fang M. 1997. An airborne study of air quality around the Hong Kong territory. *J Geophys Res* 102(D15):19043–19057.
- Lam TH, Ho SY, Hedley AJ, Mak KH, Leung GM. 2004a. Leisure time physical activity and mortality in Hong Kong: case-control study of all adult deaths in 1998. *Ann Epidemiol* 14(6):391–398.
- Lam TH, Li ZB, Ho SY, Chan WM, Ho KS, Li MP, et al. 2004b. Smoking and depressive symptoms in Chinese elderly in Hong Kong. *Acta Psychiatr Scand* 110:195–200.
- Lee SC, Chang M. 1999. Indoor air quality investigations at five classrooms. *Indoor Air* 9(2):134–138.
- Lee SC, Chang M. 2000. Indoor and outdoor air quality investigation at schools in Hong Kong. *Chemosphere* 41(1):109–113.
- Lee SC, Guo H, Li WM, Chan LY. 2002. Inter-comparison of air pollutant concentrations in different indoor environments in Hong Kong. *Atmos Environ* 36(12):1929–1940.
- Li XL, Wang JS, Tu XD, Liu W, Huang Z. 2007. Vertical variations of particle number concentration and size distribution in a street canyon in Shanghai, China. *Sci Total Environ* 378(3):306–316.
- Lumley T. 2009. Leaps: regression subset selection. R package version 2.9. Available: <http://CRAN.R-project.org/package=leaps> [accessed 1 Dec 2016].
- Marshall JD, Granvold PW, Hoats AS, McKone TE, Deakin E, Nazaroff WW. 2006. Inhalation intake of ambient air pollution in California's South Coast Air Basin. *Atmos Environ* 40(23):4381–4392.
- Meroney RN, Pavageau M, Rafailidis S, Schatzmann M. 1996. Study of line source characteristics for 2-D physical modelling of pollutant dispersion in street canyons. *J Wind Eng Ind Aero* 62(1):37–56.
- Ng E. 2009. Policies and technical guidelines for urban planning of high density cities — air ventilation assessment (AVA) of Hong Kong. *Build Environ* 44(7):1478–1488.
- Nyhan M, Grauwil S, Britter R, Misstear B, McNabola A, Laden F, et al. 2016. “Exposure Track” — the impact of mobile-device-based mobility patterns on quantifying population exposure to air pollution. *Environ Sci Technol* 50(17):9671–9681.
- O'Brien RM. 2007. A caution regarding rules of thumb for variance inflation factors. *Qual Quant* 41(5):673–690.

- Özkaynak H, Baxter LK, Dionisio KL, Burke J. 2013. Air pollution exposure prediction approaches used in air pollution epidemiology studies. *J Expo Sci Environ Epidemiol* 23(6):566–572.
- Park SS, Hansen ADA, Cho SY. 2010. Measurement of real time black carbon for investigating spot loading effects of Aethalometer data. *Atmos Environ* 44(11):1449–1455.
- Pope CA III, Burnett RT, Thun MJ, Calle EE, Krewski D, Ito K, et al. 2002. Lung cancer, cardiopulmonary mortality, and long-term exposure to fine particulate air pollution. *JAMA* 287:1132–1141.
- Saraswat A, Apte JS, Kandlikar M, Brauer M, Henderson SB, Marshall JD. 2013. Spatiotemporal land use regression models of fine, ultrafine, and black carbon particulate matter in New Delhi, India. *Environ Sci Technol* 47(22):12903–12911.
- Schooling CM, Chan WM, Leung SL, Lam TH, Lee SY, Shen C, et al. 2016. Cohort Profile: Hong Kong Department of Health Elderly Health Service Cohort. *Int J Epidemiol* 45(1):64–72.
- Setton EM, Keller CP, Cloutier-Fisher D, Hystad PW. 2008. Spatial variations in estimated chronic exposure to traffic-related air pollution in working populations: a simulation. *Int J Health Geogr* 7:39.
- Setton E, Keller CP, Cloutier-Fisher D, Hystad PW. 2010. Gender differences in chronic exposure to traffic-related air pollution — a simulation study of working females and males. *Prof Geogr* 62(1):66–83.
- Setton E, Marshall JD, Brauer M, Lundquist KR, Hystad P, Keller P, et al. 2011. The impact of daily mobility on exposure to traffic-related air pollution and health effect estimates. *J Expo Sci Environ Epidemiol* 21(1):42–48.
- Shi Y, Lau KK, Ng E. 2016. Developing street-level PM_{2.5} and PM₁₀ land use regression models in high-density Hong Kong with urban morphological factors. *Environ Sci Technol* 50(15):8178–8187.
- Smith JD, Mitsakou C, Kitwiroon N, Barratt BM, Walton HA, Taylor JG, et al. 2016. London hybrid exposure model: improving human exposure estimates to NO₂ and PM_{2.5} in an urban setting. *Environ Sci Technol* 50(21):11760–11768.
- Spalt EW, Curl CL, Allen RW, Cohen M, Williams K, Hirsch JA, et al. 2016. Factors influencing time-location patterns and their impact on estimates of exposure: the Multi-Ethnic Study of Atherosclerosis and Air Pollution (MESA Air). *J Expo Sci Environ Epidemiol* 26(4):435.
- Steinle S, Reis S, Sabel CE. 2013. Quantifying human exposure to air pollution — moving from static monitoring to spatio-temporally resolved personal exposure assessment. *Sci Total Environ* 443:184–193.
- Su JG, Brauer M, Buzzelli M. 2008. Estimating urban morphometry at the neighborhood scale for improvement in modeling long-term average air pollution concentrations. *Atmos Environ* 42(34):7884–7893.
- Szipro AA, Sampson PD, Sheppard L, Lumley T, Adar SD, Kaufman JD. 2010. Predicting intra-urban variation in air pollution concentrations with complex spatio-temporal dependencies. *Environmetrics* 21(6):606–631.
- Tang R, Blangiardo M, Gulliver J. 2013. Using building heights and street configuration to enhance intraurban PM₁₀, NO_x, and NO₂ land use regression models. *Environ Sci Technol* 47(20):11643–11650.
- Therneau T. 2015. A Package for Survival Analysis in S. version 2.38. Available: <https://CRAN.R-project.org/package=survival> [accessed 23 Oct 2017].
- Tian LW, Hossain SR, Lin H, Ho KF, Lee SC, Yu ITS. 2011. Increasing trend of primary NO₂ exhaust emission fraction in Hong Kong. *Environ Geochem Health* 33:623–630.
- Transport Department. 2014. Travel Characteristics Survey 2011 — Final Report. Available: www.td.gov.hk/en/publications_and_press_releases/publications/free_publications/travel_characteristics_survey_2011_final_report/index.html [accessed 1 Dec 2016].
- United Nations, Department of Economic and Social Affairs, Population Division. 2015. World Population Prospects: The 2015 Revision, Key Findings and Advance Tables. ESA/P/WP.241. New York:United Nations.
- U.S. Environmental Protection Agency. 2016. Air Sensor Toolbox. Available: www.epa.gov/air-sensor-toolbox/air-sensor-toolbox-what-epa-doing#overview [accessed 1 Dec 2016].
- Vardoulakis S, Fisher BEA, Pericleous K, Gonzalez-Flesca N. 2003. Modelling air quality in street canyons: a review. *Atmos Environ* 37(2):155–182.
- Vardoulakis S, Gonzalez-Flesca N, Fisher BEA. 2002. Assessment of traffic-related air pollution in two street canyons in Paris: implications for exposure studies. *Atmos Environ* 36(6):1025–1039.
- Virkkula A, Makela T, Hillamo R, Yli-Tuomi T, Hirsikko A, Hameri K, et al. 2007. A simple procedure for correcting

loading effects of aethalometer data. *J Air Waste Manag Assoc* 57(10):1214–1222.

Wang M, Beelen R, Eeftens M, Meliefste K, Hoek G, Brunekreef B. 2012. Systematic evaluation of land use regression models for NO₂. *Environ Sci Technol* 46(8):4481–4489.

Wang R, Henderson S, Sbih H, Allen R, Brauer M. 2013. Temporal stability of land use regression models for traffic-related air pollution. *Atmos Environ* 64:312–319.

Wong CM, Lai HK, Tsang H, Thach TQ, Thomas GN, Lam K, et al. 2015. Satellite-based estimates of long-term exposure to fine particles and association with mortality in elderly Hong Kong residents. *Environ Health Perspect* 123(11):1167–1172.

Wong CM, Tsang H, Lai HK, Thomas GN, Lam KB, Chan KP, et al. 2016. Cancer mortality risks from long-term exposure to ambient fine particle. *Cancer Epidemiol Biomarkers Prev* 25(5):839–845.

World Health Organization. 2016a. Ambient (outdoor) air pollution database, by country and city [Data file]. Available: www.who.int/phe/health_topics/outdoorair/databases/cities/en/ [accessed 1 Dec 2016].

World Health Organization. 2016b. International Statistical Classification of Diseases and Related Health Problems 10th Revision. Available: <http://apps.who.int/classifications/icd10/browse/2016/en> [accessed 1 Dec 2016].

Wu CD, MacNaughton P, Melly S, Lane K, Adamkiewicz G, Durant JL, et al. 2014. Mapping the vertical distribution of population and particulate air pollution in a near-highway urban neighborhood: Implications for exposure assessment. *J Expo Sci Environ Epidemiol* 24(3):297–304.

Wu Y, Hao J, Fu L, Wang Z, Tang U. 2002. Vertical and horizontal profiles of airborne particulate matter near major roads in Macao, China. *Atmos Environ* 36(31):4907–4918.

Yang F, Kaul D, Chun Wong K, Westerdahl D, Sun L, Ho K. 2015. Heterogeneity of passenger exposure to air pollutants in public transport microenvironments. *Atmos Environ* 109:42–51.

Yu JZ, Tung JWT, Wu AWM, Lau AKH, Louie PKK, Fung JCH. 2004. Abundance and seasonal characteristics of elemental and organic carbon in Hong Kong PM₁₀. *Atmos Environ* 38(10):1511–1521.

Zhu K, Zhang J, Liou PJ. 2007. Evaluation and comparison of continuous fine particulate matter monitors for measurement of ambient aerosols. *J Air Waste Manag Assoc* 57:1499–1506.

MATERIALS AVAILABLE ON THE HEI WEBSITE

Appendix A and Additional Materials 1 contain supplemental material not included in the printed report. They are available on the HEI Web site, www.healtheffects.org/publications.

Appendix A. WP1–WP4 Tables and Figures

Additional Materials 1. Additional Information Regarding the Sampling Sites, Measurements, and Modeling

ABOUT THE AUTHORS

Benjamin Barratt has a Ph.D. from King's College London and an M.Sc. from the University of Portsmouth. He is a senior lecturer in the Division of Analytical and Environmental Sciences & Lau China Institute, King's College London, U.K., and an honorary assistant professor, University of Hong Kong, HK SAR. Barratt has 15 years of experience conducting multidisciplinary research contracts within both academia and the public sector. He has specialized in characterizing pollutant sources and behavior using dedicated monitoring networks for the evaluation of air quality interventions, including the London Congestion Charging Scheme, Low Emission Zone. He has co-authored three HEI Research Reports, each examining population exposure in relation to TRAP. His current research focuses on the use of personal exposure monitoring to establish direct links between environmental stress and health outcomes. He leads the Exposure Science team within the Environmental Research Group and is an investigator within the MRC-PHE Centre for Environment and Health (www.environment-health.ac.uk). Barratt was principal investigator on the study and lead investigator for WP2.

Martha Lee has an M.Sc. from the University of British Columbia, Canada, where she is a research assistant. Her research interests are in outdoor air quality exposure and its associated adverse health effects. Lee was responsible for the fieldwork and development of LUR in WP1, which was her thesis project.

Paulina Wong has a Ph.D. from the University of Hong Kong and an M.Sc. from the University of Auckland. She is an assistant professor in the Science Unit at Lingnan University,

Hong Kong, and was formerly senior research assistant in the Department of Geography, University of Hong Kong, HK SAR. Wong specializes in urban climate research with a focus on urban heat island effects and ecological modeling. She is proficient in geographic data processing, statistical analysis, and microclimate field monitoring and surveys. She has been a Fulbright scholar and is a certified geographical information system (GIS) professional. Her recent research addresses environmental impacts and their effects on health-related problems in Hong Kong. She has made use of mobile geospatial technologies and cloud computing strategies to assist the process of georeferencing. Wong provided GIS expertise, supervised the canyon fieldwork campaigns, and carried out analysis of vertical decay rates in WP2.

Robert Tang has a Ph.D. and an M.Sc. from Imperial College London. He is a postdoctoral fellow at the School of Public Health, University of Hong Kong, HK SAR. While completing his Ph.D. at the MRC-PHE Centre for Environment and Health, Tang developed spatiotemporal air pollution models for exposure assessment using LUR, dispersion, hybrid techniques in GIS and Bayesian statistical framework. He was a research assistant for the EU FP7 EXPOsOMICS project, investigating the health effects of fine particulate matter. His current research is focused on air and noise pollution modeling; exposure assessments for epidemiological studies; and spatial analysis and long-term effects of air pollutants. Tang was lead investigator for WP3 and WP4.

Tsz Him Tsui has an M.P.H. from the Chinese University of Hong Kong and was formerly a research assistant at the School of Public Health, University of Hong Kong, HK SAR. Tsui specialized in population and global health during his M.P.H. studies. He led the canyon campaign fieldwork and contributed to the development of the dynamic model in WP3.

Wei Cheng has an M.Sc. from East China Normal University and is a Ph.D. candidate in the Department of Geography, University of Hong Kong, HK SAR. She is a geographer by training and specializes in cartography and geographic information science. She has done research on spatial analysis of crime in Shanghai and using remote sensing techniques to map vegetation and investigate evolution of urban river systems. She is pursuing a Ph.D. degree to investigate patterns of air pollutant dispersion in urban street canyons and visualization methods that can effectively display spatiotemporal movement of air pollutants within a 3D cityscape. Cheng developed the 3D visualizations in WP4.

Yang Yang holds a Master's degree in biostatistics and epidemiology from Peking Union Medical College, which focused on the associations between air pollution in Beijing and related health effects. She also carried out data analysis for the project "Traffic related air pollution and the health impacts in Three Typical Chinese Cities." Yang is an M.Phil. student at the School of Public Health, University of Hong Kong, HK SAR. She ran analyses relating to WP4.

Poh-Chin Lai has a Ph.D. and M.A. from the University of Waterloo. She is a professor in the Department of Geography and Honorary Deputy Director of the Geographical/Land Information System Research Centre, University of Hong Kong, HK SAR. Lai is an expert in the use of GIS information to identify associations between physical urban geography and environmental health risks. She has collaborated with international and local medical and public health professionals to develop and apply geospatial methodologies to understand spatial variation of health outcomes and health inequality. She has recently completed a study investigating relationships between incidences of tuberculosis and high-density urban residential characteristics, such as type of housing development, floor level of residence, and sky view factor. Previous studies have included the novel use of GIS systems to associate environmental factors with falls of older people and analyzing microclimate variation along a marathon course. These studies aim to examine effects of urban morphology on public health and the wellbeing of the people of Hong Kong. Lai provided local oversight and guidance for WP2.

Linwei Tian has a Ph.D. from the University of California–Berkeley, an M.Sc. from China CDC, and a M.B.B.S. from Shanxi Medical University, China. He is an associate professor at the School of Public Health, University of Hong Kong, HK SAR. Tian is an environmental epidemiologist with a focus on air pollution and health. He has been conducting field epidemiology and laboratory work on indoor air pollution and lung cancer in Xuan Wei County, which has the highest lung cancer rates among women in China. Using spatial analysis of coal use patterns and lung cancer rates in hundreds of villages, he has raised the hypothesis that crystalline silica (quartz) in coal smoke is an important risk factor in the lung cancer epidemic in rural Xuan Wei. Currently, he is working to quantify quartz and other carcinogens in coal smoke and to determine whether an exposure–response relationship can be found. Tian provided local oversight and guidance for WP3 and WP4.

Thuan-Quoc Thach has a Ph.D. from the University of Alberta and an M.Sc. from the University of Western Ontario. He is a scientific officer for the Department of

Community Medicine, University of Hong Kong, HK SAR. Thach is a biostatistician with wide experience in development and application of epidemiological and statistical methods for assessing environment and health issues. He was a coinvestigator in three previous HEI-funded projects (HEI Research Report 154, Public Health and Air Pollution in Asia [PAPA]; Research Report 169, Effects of Short-Term Exposure to Air Pollution on Hospital Admissions of Young Children for Acute Lower Respiratory Infections in Ho Chi Minh City, Vietnam; and Research Report 170, Impact of the 1990 Hong Kong Legislation for Restriction on Sulfur Content in Fuel). Thach provided local oversight and guidance for the fieldwork campaigns in WP1 and WP2.

Ryan Allen has a Ph.D. and an M.Sc. from the University of Washington. He is an associate professor on the Faculty of Health Sciences at Simon Fraser University, Canada. Allen's research interests are in the area of air pollution exposure assessment and epidemiology, with particular interests in the cardiovascular effects of air pollution and air quality in Asia. Allen led the infiltration efficiency analysis contained within WP2.

Michael Brauer has a Sc.D. from Harvard University. He is a professor in the School of Population and Public Health, University of British Columbia, Canada. Brauer has been a leader in the development of LUR models for TRAP and their application to epidemiological analyses. He developed the first LUR models for TRAP PM and developed the application of mobile monitoring, 3D urban morphometry, and meteorology to LUR models. He has a long history of research in the development of improved estimates of exposure to air pollution and in the assessment of exposure misclassification on epidemiological effect estimates. He has conducted an evaluation of LUR models and the incorporation of mobility on personal exposures, and an assessment of the impact of mobility on epidemiological effect estimates. He is also recognized as an expert on air quality in Asia and recently participated in the development of an LUR model for Delhi. Brauer was lead investigator on WP1 and provided scientific oversight of all work packages.

OTHER PUBLICATIONS RESULTING FROM THIS RESEARCH

Tang R, Tian L, Thach T-Q, Tsui TH, Brauer M, Lee M, et al. 2018. Integrating travel behavior with land use regression to estimate dynamic air pollution exposure in Hong Kong. *Environ Int* 113:100–108; <https://doi.org/10.1016/j.envint.2018.01.009>.

Lee M, Brauer M, Wong P, Tang R, Tsui TH, Choi C, et al. 2017. Land use regression modelling of air pollution in high density high rise cities: A case study in Hong Kong. *Sci Total Environ* 592:306–315.

Research Report 194, *A Dynamic Three-Dimensional Air Pollution Exposure Model for Hong Kong*, B. Barratt et al.

INTRODUCTION

Traffic emissions are an important source of urban air pollution. Exposure to traffic-related air pollution has been associated with various adverse health effects (HEI 2010; World Health Organization 2013). In 2010, HEI published Special Report 17, *Traffic-Related Air Pollution: A Critical Review of the Literature on Emissions, Exposure, and Health Effects*. This report, developed by the HEI Panel on the Health Effects of Traffic-Related Air Pollution, summarized and synthesized research related to the health effects from exposure to traffic emissions. The Panel concluded that exposure to traffic-related air pollution was causally linked to worsening asthma symptoms. It also found suggestive evidence of a causal relationship with onset of childhood asthma, nonasthma respiratory symptoms, impaired lung function, total and cardiovascular mortality, and cardiovascular morbidity (HEI 2010).

Because traffic-related air pollution is of public health interest, it is important to understand where and how people are exposed to traffic emissions. However, exposure assessment is challenging because traffic-related air pollution is a complex mixture of many particulate and gaseous pollutants and is characterized by high spatial and temporal variability (HEI 2010). The highest levels of traffic-related air pollution occur within a few hundred meters of major roads with the impact zone depending on the pollutant, geographic and land-use characteristics, and meteorologic conditions (Karner et al. 2010; Zhou and Levy 2007). Identifying an appropriate exposure metric that uniquely indicates traffic-related air pollution has been difficult, because many of the pollutants are also emitted from other combustion sources. A range of models, such as dispersion, land-use regression, and hybrid models, have been

developed to estimate exposure and some attempts to account for infiltration and time-activity patterns have been considered for more accurate estimates of personal exposure. Each of these exposure estimation approaches, however, has limitations, which have been discussed previously (HEI 2010). To improve exposure assessment of traffic-related air pollution for use in health studies, HEI issued RFA 13-1, *Improving Assessment of Near-Road Exposure to Traffic Related Pollution*, in 2013. HEI funded five studies under RFA 13-1 (see Preface).

In response to RFA 13-1, Dr. Benjamin Barratt from King's College London and his team submitted an application for a 2.5-year study, "The Hong Kong D3D Study: A Dynamic Three-Dimensional Exposure Model for Hong Kong." They proposed to estimate exposure to traffic-related air pollution using a dynamic three-dimensional (D3D*) land-use regression (LUR) model for Hong Kong. The HEI Research Committee recommended Dr. Barratt's application for funding because they liked the overall design of the study and the addition of a vertical component to the LUR model, which was a novel feature since previous air pollution exposure models have been largely two-dimensional. They thought such a model would have potential wide application given that high-density high-rise megacities have become more prominent globally. For example, the United Nations reported that there were 28 megacities in 2014, home to 453 million people; 16 of those megacities were located in Asia. Moreover, they have estimated that by 2030, the world is projected to have 41 megacities, each with 10 million inhabitants or more (United Nations 2015). High-rise buildings, which can house hundreds or even a few thousand people, are therefore of great interest and have risen rapidly in most megacities; such buildings can also create urban street canyons, which are the focus of the current study.

This Critique provides the HEI Review Committee's evaluation of the study. It is intended to aid the sponsors of HEI and the public by highlighting both the strengths and the limitations of the study and by placing the Investigators' Report into scientific and regulatory perspective.

Dr. Benjamin Barratt's 2.5-year study, "The Hong Kong D3D Study: A Dynamic Three-Dimensional Exposure Model for Hong Kong," began in March 2014. Total expenditures were \$642,977. The draft Investigators' Report from Barratt and colleagues was received for review in December 2016. A revised report, received in May 2017, was accepted for publication in June 2017. During the review process, the HEI Review Committee and the investigators had the opportunity to exchange comments and to clarify issues in both the Investigators' Report and the Review Committee's Critique.

This document has not been reviewed by public or private party institutions, including those that support the Health Effects Institute; therefore, it may not reflect the views of these parties, and no endorsements by them should be inferred.

* A list of abbreviations and other terms appears at the end of this volume.

APPROACH

AIMS

The overarching aim of the study was to create a D3D LUR model for Hong Kong that could be applied to other Asian megacities. The study had three main objectives:

1. to investigate the dispersion and distribution of air pollution in a three-dimensional urban landscape with high residential and traffic density;
2. to develop, evaluate, and demonstrate a dynamic three-dimensional traffic-related air pollution exposure model; and
3. to create an incremental exposure assessment methodology that can be applied in megacities across Asia.

METHODS

To address those aims, the study was divided into 4 work packages. Work packages 1 to 3 were the development of three models with increasing complexity: a two-dimensional LUR model, a three-dimensional model, and a dynamic three-dimensional model, respectively. Work package 4 was the application of those models to a cohort.

Two-Dimensional LUR Models (Work Package 1)

Barratt and colleagues conducted street-level outdoor monitoring campaigns to measure particulate matter $\leq 2.5 \mu\text{m}$ in aerodynamic diameter ($\text{PM}_{2.5}$), black carbon (BC), nitrogen monoxide (NO), and nitrogen dioxide (NO_2) concentrations at about 100 locations during two weeks in the warm season and two weeks in the cold season of 2014. The study leveraged data from a NO_2 sampling campaign conducted by the Hong Kong Environmental Protection Department during the same periods at many of the same locations. The Critique Table provides more information about the monitoring campaigns. Data were corrected for temporal variation and for systematic differences across instruments and sampling methods, using colocated instruments and regulatory monitor locations. These corrected data were used to develop two-dimensional LUR models to estimate long-term exposure in the whole of Hong Kong. In total, 373 spatial predictor variables were available for model building; these included multiple buffer areas, ranging from 25 to 5,000 meters for about 50 different predictor variables being considered. Among the predictor variables were *conventional* variables, such as traffic intensity and road length, land-use variables, and distance to sources (e.g., ports or airports), as well as some more complex urban development predictors, such as

aspect ratio (the ratio of building height to street width) to capture street canyons. Model development was based on a supervised semi-automatic selection process, with predictors removed if their sign was inconsistent with a priori hypotheses and if not statistically significant ($P \geq 0.10$). The maximum number of predictor variables allowed in the model was set to one for every ten observations. In total, 36 models were developed: 4 pollutants \times 3 data sets (warm season, cold season, and average of both seasons) \times 3 different traffic predictors (traffic intensity, road length, and both variables combined). The investigators preferred the models that combined measurements from both seasons and used road-length predictor variables, and they used those in all subsequent analyses. Model performance was evaluated using a leave-one-out cross validation as well as a hold-out evaluation for NO_2 where they held 20 random sites for evaluation only instead of using all sites for model building. The number of observations for the preferred models was 64 ($\text{PM}_{2.5}$), 76 (BC), 75 (NO_2), and 40 (NO).

Three-Dimensional LUR Models (Work Package 2)

In addition to the two-dimensional outdoor street-level spatial monitoring campaigns described earlier, the investigators carried out vertical outdoor and indoor air pollution monitoring of $\text{PM}_{2.5}$ and BC at four heights on both sides of six streets for two weeks in the warm season and two weeks in the cold season (Critique Table). Four street canyons (i.e., roads with adjoining high-rise buildings on both sides) and two open streets (with high-rise buildings on one side only) were selected for monitoring, representing a range of different traffic and street characteristics. Residents living on different floors along those streets were approached and asked to participate in the sampling campaign. If they agreed, sampling equipment was placed inside (and outside the windows or balcony) of their apartments. The mean sampling height of the lowest sampling point across the streets was 10 meters above street level (1st residential floor). The maximum sampling height was 60 meters (21st residential floor). The ground floors were occupied by mainly shops and businesses, and no street-level measurements were obtained. NO and NO_2 measurements were not reported because of the poor quality of the electrochemical sensors used. For example, precision tests showed widely variable and unexplained differences within a sensor and poor agreement between sensors. Outdoor $\text{PM}_{2.5}$ and BC data were used to develop three-dimensional LUR models. Vertical decay functions were derived assuming an exponential function; in sensitivity analyses the investigators capped the concentration decay at 20 meters (approximately the 6th floor); in other words, all exposure estimates at heights above 20 meters were set at a value equal

Critique Table. Details of the Spatial and Canyon Monitoring Campaigns in Hong Kong

Equipment and Sampling Period	Site Selection	Sampling Regime
Spatial Monitoring to Develop Two-Dimensional LUR Model		
<ul style="list-style-type: none"> SidePak AM510 (PM_{2.5}); MicroAeth AE51 (BC); Ogawa badges and Gradko diffusion tubes (NO, NO₂) April 2014–May 2014 (summer campaign); November 2014–January 2015 (winter campaign) 	<ul style="list-style-type: none"> Sampling at street level using lampposts at about 2.5 m off the ground. Site selection was based on geographical location, traffic intensity, land use, and population density, and was aimed to maximize variation in those factors. Number of sites differed per pollutant and season: ranging between 43 and 97 sites. Number of observations for the preferred models was 64 (PM_{2.5}), 76 (BC), 75 (NO₂) and 40 (NO). 	<ul style="list-style-type: none"> Sampling duration of 24 hours (PM_{2.5} and BC) and 2 or 3 weeks (NO/NO₂) per season. For logistical and budgetary reasons, not all sites were simultaneously sampled. Data were corrected for temporal variation using regulatory monitoring sites. In addition, data were corrected for systematic differences across instruments and sampling methods.
Canyon Monitoring to Develop Three-Dimensional LUR Model		
<ul style="list-style-type: none"> SidePak AM510 (PM_{2.5}); MicroAeth AE51 (BC); AQMesh electro-chemical sensors (NO, NO₂)* August 2014–September 2014 and May 2015–June 2015 (summer campaign); October 2014–March 2015 (winter campaign). 	<ul style="list-style-type: none"> Sampling at 6 streets (4 canyon streets, 2 open streets) with different traffic and street characteristics. At each street, monitoring was conducted at four heights on both sides of the street (ranging between 10 and 50 m above street level). Streets were selected based on population density, traffic intensity, canyon aspect ratio, canyon length, and prevailing winds. 	<ul style="list-style-type: none"> Sampling duration was 2 weeks (1 week for paired indoor measurements) per season for all pollutants. Streets were sampled sequentially.

*Data not reported because of poor quality.

to the 20-meter estimate. To estimate the missing concentrations at lower floors (i.e., from street level to 10 m), the investigators used the modeled two-dimensional LUR street-level estimate. Indoor sampling was included to assess infiltration rates; this information was integrated into the dynamic LUR model described below. Infiltration rates were assessed following methods similar to those in the Multi-Ethnic Study of Atherosclerosis and Air Pollution (MESA-AIR) cohort (Allen et al. 2012). An approach was developed to identify periods affected by indoor sources (e.g., cooking), and those periods were not used in the calculations. Note that participants were not allowed to smoke inside.

Dynamic Three-Dimensional LUR Models (Work Package 3)

To incorporate time–activity patterns into the LUR exposure models, the investigators developed what they

termed *dynamic* models. A population-representative travel behavior survey was available from the Transport Department of Hong Kong to develop dynamic LUR models for PM_{2.5}, BC, and NO₂. Survey data were available from ~89,000 Hong Kong residents for one representative weekday in 2011. Information on travel mode, travel time, location, and purpose of the trips was used to construct time–activity patterns for each survey subject. This information was combined with results from previous monitoring studies in different modes of transport in Hong Kong to predict exposure in different transport microenvironments. This information was integrated with outdoor air pollution estimates from the two-dimensional LUR model and indoor infiltration estimates to arrive at dynamic time-weighted air pollution exposure estimates. Next, dynamic exposure factors were derived for different age (below 18, 18–64, 65 and above), sex (male, female),

and population subgroups (working adults, students, neither in work nor study). Limitations of the survey were that it did not include the residential address or the floor. As a result, the dynamic modeling was based on the smallest spatial administrative unit in Hong Kong (tertiary planning unit [TPU, $N = 289$], which is comparable to zip codes in the United States) and did not include a three-dimensional component.

Application to the Cohort (Work Package 4)

Finally, Barratt and colleagues applied the exposure models with increasing complexity in an epidemiological study using an existing elderly cohort of 66,000 Hong Kong residents to evaluate the potential impact of exposure measurement error in mortality estimates. The cohort was recruited in 1998–2001, and mortality data were collected until the end of 2011. The average residential height above street level was 39 meters (~11th floor). More details about the cohort can be found in Schooling and colleagues (2016). The investigators ran standard Cox proportional hazard models that were adjusted for important individual-level confounder variables such as age, sex, body mass index, physical activity, smoking, and socioeconomic status (the last variable also at the TPU level). Exposure was estimated at the recruitment residential address using the two-dimensional LUR estimate for 2014, and back-extrapolated to the recruitment period using regulatory monitoring sites. Subsequently, investigators matched the participants' floor of residence with the derived pollutant's vertical decay rate to estimate three-dimensional exposure. Next, they applied dynamic exposure factors accounting for exposure in various indoor, outdoor, and transport micro-environments. They assumed that no participants in the cohort worked or studied because they were elderly, and information on occupation was not collected. Health estimation for the cohort was performed for all four pollutants using single-pollutant models. Because of the lack of data for NO and NO₂, the investigators used vertical gradients and dynamic exposure factors of BC instead.

SUMMARY OF RESULTS

EXPOSURE MODELS WITH INCREASING COMPLEXITY

- The investigators reported a rather modest prediction accuracy of the two-dimensional LUR models, with explained variances of 0.50–0.60, though they indicated this was consistent with LUR estimates from other Asian cities. The number of predictor variables

ranged from four to eight, and all models included only conventional variables such as traffic, land use, coordinates, and distance to large regional emission sources.

- Generally, the investigators reported only modest vertical decay of PM_{2.5} and BC, with most of the decay happening over the first few meters. As a result, it appeared that the vast majority of the population lives within the well-mixed zone. In addition, vertical decay across the canyons and seasons did not vary by much. Therefore, for the three-dimensional LUR model, a single exponential decay rate was calculated for PM_{2.5} and BC (0.004 and 0.012, respectively). Results were sensitive to the choice of the model: sensitivity analyses revealed influences of substituting modeled two-dimensional LUR estimates for missing measurements at lower floors and assuming that the air was well mixed at heights above 20 meters.
- When the investigators compared the results of the dynamic LUR model with results from the static outdoor and indoor estimates in the survey population, they found that estimates from the dynamic model were about 20% lower on average, mostly due to the addition of an indoor component. As expected, addition of an in-transit component increased exposure estimates. In subgroup analyses, dynamic exposure estimates were higher for working adults and students than for less mobile populations; higher for populations under age 18 than for populations over age 65; and slightly higher for males than for females.
- PM_{2.5} and BC home infiltration rates were reported to be relatively high (81%–91% depending on pollutant and season). Home infiltration rates were somewhat lower in the warm season due to the increased use of air conditioning and closed windows.

APPLICATION OF THE EXPOSURE MODELS TO THE COHORT

- Associations were fairly similar when comparing results from the complex models with the two-dimensional models for PM_{2.5}, BC, NO, and NO₂. Neither the incorporation of vertical gradients nor that of dynamic components, including indoor pollutant infiltration, into the exposure estimates resulted in meaningful or consistent changes in the associations with all-natural-cause, cardiovascular, and respiratory mortality in the Hong Kong elderly cohort. Only the association between NO₂ and cardiovascular mortality changed substantially — from a null finding to a positive finding — when a vertical gradient was added, and this result was consistent in sensitivity analyses where the

investigators assumed that the air was well mixed at heights above 20 meters (Critique Figure).

- The dynamic part of the model could not be fully tested in the cohort application given the use of an elderly cohort instead of a population-representative sample. Thus only a limited number of dynamic exposure factors could be applied: namely, those from age category 65 and above, sex, and the population subgroup “neither in work nor study.” Partly because of this, correlations between estimates from the dynamic exposure model and the vertical gradient exposure model were very high, hampering the application to the cohort.

REVIEW COMMITTEE EVALUATION

In its independent review of the study, the HEI Review Committee concluded that Barratt and colleagues conducted a novel study — one of the first to integrate vertical gradients and time–activity patterns into an air pollution exposure model. The Committee noted several strengths and limitations of the study, as described below.

STRENGTHS OF THE STUDY

The extensive air quality measurements, the development of exposure models using state-of-the-art modeling practices, and the application of those models to estimate exposure for epidemiological analyses of an existing Hong Kong cohort were considered strengths of the study. The extensive spatial monitoring campaigns provided a wealth of air quality measurements to support the development of exposure models. For example, multiple pollutants were sampled and measurements were conducted in both the warm and cold seasons. The collaboration with the Hong Kong Environmental Protection Department was helpful in this regard. In addition, the investigators included many quality assurance/quality control tests to make sure the data were of good quality. They conducted many colocated tests, including validation with reference monitors, and used them to correct the measurements for systematic differences across devices, if needed.

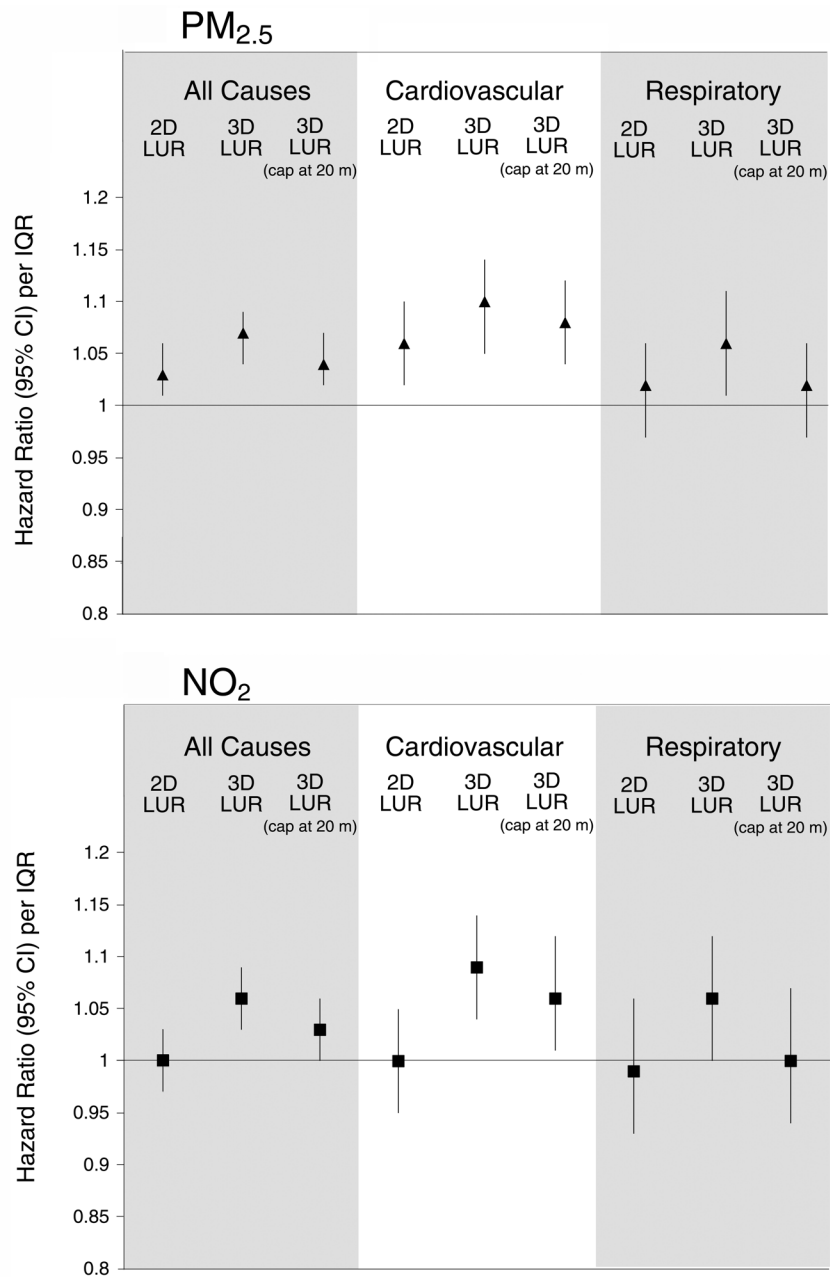
Regarding LUR modeling, the Committee commended the authors for using many of the recommended best practices (Hoek et al. 2008). For example, all two-dimensional models in this study had at least 40 monitoring sites, as has been recommended. In addition, sampling sites were selected that maximized the range of values in pollution concentrations and spatial variables. Moreover, many spatial predictors were considered in the models to ensure that available variables likely to be related to air pollution were evaluated. In addition, to decrease potential for overfitting,

the investigators limited the number of predictors allowed to no more than 10% of the total number of observations. Moreover, the models were appropriately evaluated using a leave-one-out cross validation and, for NO₂ models where more sampling sites were available, a hold-out validation.

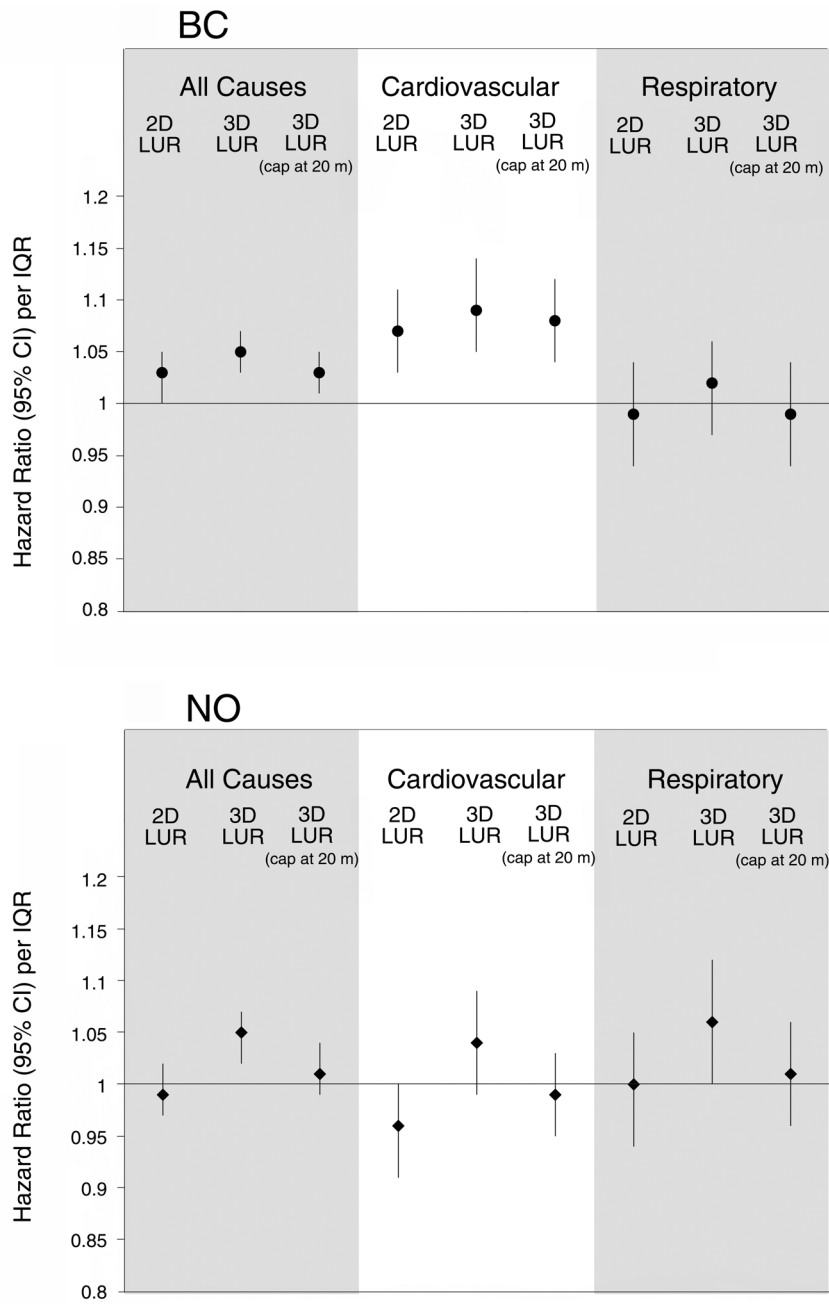
The Committee also thought the application of the different exposure models in an epidemiological study was another strength. The investigators used a well-characterized, existing elderly cohort to evaluate the potential impact of exposure measurement error in mortality estimates. It was also useful that the investigators compared their results with those from a previous epidemiological analysis in the same cohort that used satellite data for the exposure assessment (Wong et al. 2015). The Committee concluded that Barratt and colleagues have found fairly similar associations when comparing results from the complex models to the two-dimensional models for PM_{2.5}, BC, NO, and NO₂. Neither the incorporation of vertical gradients nor that of dynamic components, including indoor pollutant infiltration, into the exposure estimates resulted in meaningful or consistent changes in the associations with all-natural-cause, cardiovascular, and respiratory mortality in the Hong Kong elderly cohort. This conclusion differs slightly from the investigators’ interpretation of the epidemiological results for reasons summarized below.

DATA CHALLENGES

The investigators encountered a number of challenges in the study, many of which were outside their control, and they developed approaches to compensate for those challenges in a variety of ways. The Committee found it difficult to ascertain the impacts of the various workarounds on the findings because the consequences of many of those workarounds on the results were not fully investigated. For example, there were harsh sampling conditions (e.g., intense rainfall, high humidity, and high temperature) that resulted in some missing data and data quality issues. In addition, recruitment and access to apartments was challenging in the vertical air pollution monitoring campaign, especially at lower floors; this resulted in a lack of measurements from street level to the first sampling point (10 m above street level). For the derivation of vertical decay rates, therefore, the investigators used modeled two-dimensional LUR estimates to fill in the missing measurements at lower floors. Moreover, there were issues with the quality of the NO and NO₂ data from low-cost electrochemical sensors, so those data were not reported. Therefore, the investigators applied the decay function of BC to the vertical NO₂ and NO models. There were other issues that were not explored in depth, such as the effect of averaging across different types of canyons to



Critique Figure. Association between air pollutants (PM_{2.5}, NO₂, BC, and NO) and mortality using different exposure models (two-dimensional versus three-dimensional models; dynamic model not shown). See the Investigators' Report Table 12 and Appendix Table A.33 for interquartile ranges (available on the HEI website). (Figure continues next page.)



Critique Figure (Continued).

derive a single decay rate, as well as many other modeling decisions, on the modeled estimates. The Committee realized that this study was exploratory in many respects but thought that it would have been useful to further explore the impacts of the various workarounds on the findings.

ADDING A VERTICAL COMPONENT TO THE EXPOSURE MODEL

During the review of the report, the Committee was particularly interested in the vertical gradient component of the model because this is the most novel aspect of this study. They requested that the investigators further explore this aspect. In response, Barratt and colleagues evaluated the impact of the various modeling choices on the vertical gradient component of the exposure model (see Investigators' Report Table 8 and Figure 6), and also on the health estimations in the cohort (Appendix Table A.33). The added analyses were revealing, because they showed that results were sensitive to the choice of the model; sensitivity analyses revealed the influence of substituting the modeled two-dimensional LUR estimates for missing measurements at lower floors and assuming that the air was well mixed at heights above 20 meters. As a result, when the vertical concentration decay was capped at 20 meters, exposure estimates were increased for those living above 20 meters (approximately above floor 6), and associations in the cohort were somewhat reduced. Only the association between NO_2 and cardiovascular mortality changed substantially — from a null finding to a positive finding — when a vertical gradient was added, and the result was consistent in sensitivity analyses where the investigators capped the vertical decay at 20 meters. However, it should be noted that in the NO_2 (and NO) model, the BC decay rate was used to fill the gap in vertical measurements — a workaround that was unfortunately not further explored. While this imputation may be appropriate with the data at hand, it should be noted that BC, NO_2 , and NO have quite distinct spatial and temporal patterns, and different background levels (HEI 2010; Karner et al. 2010). This substantially reduced the Committee's confidence in the vertical NO_2 and NO models and led the Committee to conclude that the incorporation of vertical gradients into the exposure estimates did not meaningfully change the associations with all-natural-cause, cardiovascular, and respiratory mortality in the Hong Kong elderly cohort. This conclusion differs slightly from the investigators' interpretation of the epidemiological results; they put more emphasis on statistical significance and concluded that higher associations and a greater number of significant associations were found for the more complex models that would not have been found had two-dimensional exposure models

been used solely. Being cautious about over-reliance on statistical significance (e.g., Lash 2017), the Committee focused more on the magnitude of the observed associations across the different exposure models and whether the associations were consistent in sensitivity analyses. Overall, the Committee thought the study provided important insights because it shows that adding complexity to an exposure model does not necessarily improve the estimation of health effects, likely because new sources of uncertainty are introduced at the same time. This has been shown in some other applications as well (e.g., Baxter et al. 2013; Szpiro et al. 2011, 2013).

Several previous studies have evaluated whether the incorporation of a vertical gradient, or more generally street configuration and building height to capture exposure in canyon streets, improves LUR exposure predictions (Brauer et al. 2003; Eeftens et al. 2013; Shi et al. 2016; Su et al. 2008; Tang et al. 2013; Wu et al. 2014). Some earlier studies used data collected from field observations (Brauer et al. 2003) or estimations from satellite imagery (Su et al. 2008), whereas more recent studies were based on geographical data available in geographical information system (GIS) environments, allowing for potential wide-scale application (Eeftens et al. 2013; Shi et al. 2016; Tang et al. 2013). More important, all but one (Wu et al. 2014) of the previous LUR studies were based only on air pollution measurements from street-level monitoring, which limits the comparison to the current study. On the whole, the addition of a vertical gradient, street configuration, and building height appears to improve exposure model performance, although the added value may be modest — ranging from essentially no improvement to an approximately 15% point increase in explained variance, depending on pollutant and study area. One study in another Asian city (Kaohsiung, Taiwan) that did include vertical measurements (Wu et al. 2014) reported a much higher explained variance (~50% point increase) when the investigators included sampling height as a predictor in the $\text{PM}_{2.5}$ model. The explained variance of the $\text{PM}_{2.5}$ model was, however, low without sampling height (0.12), and notably the variable sampling height did not add much in most $\text{PM}_{2.5}$ composition models.

The one previous study in Hong Kong (Shi et al. 2016) showed approximately a 10% point increase in explained variance in PM_{10} and $\text{PM}_{2.5}$ models when adding building height and other street configuration factors to the exposure model (although readers should note that that study did not include vertical measurements). Notably, the current study did not show an effect of including aspect ratio and other more complex urban development predictors in the model; those variables were therefore not included in the preferred two-dimensional LUR models. In addition, the

difference in results between the two Hong Kong studies may be due to the difference in study area: the study by Shi and colleagues (2016) modeled only the downtown Hong Kong area with the highest density of high-rise buildings and street canyons, whereas the current study developed LUR models for the entire city, including the less-developed areas.

ADDING A DYNAMIC COMPONENT TO THE EXPOSURE MODEL

The Committee thought more insights were gained from the vertical gradient model than from the dynamic component of the model. To develop the dynamic part of the model, survey data were used from ~89,000 Hong Kong residents for one weekday in 2011, which is a very large sample and one that was representative of the general Hong Kong population. However, it remains a snapshot, and data were available only at an aggregated level (TPU, comparable to zip codes in the United States) instead of an individual level, because no residential addresses were available in the survey. Therefore, interpretation of dynamic and time-weighted exposures remains difficult.

Other recent studies have attempted to integrate time-activity patterns into long-term exposure models at a fine spatial resolution using a variety of approaches (e.g., Beckx et al. 2009; Dons et al. 2014; Lane et al. 2015; Smith et al. 2016). Though challenging, the Committee thought the inclusion of time-activity patterns into exposure models for health studies remains an important area for future research because it is known that exposure during transit may contribute substantially to a person's average exposure, in spite of the fact that time spent in transit makes up only a relatively small proportion of a person's day. Activity-based or hybrid exposure models, which include space-time activity data, were also recommended by the HEI Traffic Panel in 2010 (HEI 2010). The investigators' original plan to explore individual-level smart payment card data for public transportation, whose use is widespread in Hong Kong, was unfortunately not possible because of privacy and data-protection issues. Smart card data may be a useful resource in the future if privacy issues can be satisfactorily resolved.

DEVELOPMENT OF THE TWO-DIMENSIONAL EXPOSURE MODELS

The Committee commended the investigators for using many of the recommended best practices for LUR modeling (Hoek et al. 2008). However, the Committee noted that the prediction accuracy of the two-dimensional LUR models was rather modest, with explained variances of 0.50–0.60, despite offering a very large number of potential

predictors to the model. The investigators argued that the two-dimensional LUR prediction accuracy was comparable to that in other studies in Asian cities (see Appendix Table A.3), and that prediction accuracy tends to be lower in Asia than in European and American cities because of the complex urban morphology and other features.

However, the Committee thought that the modest prediction accuracy may also suggest that alternative modeling strategies would be necessary for further improvements and that certain decisions by the Barratt team may have influenced the modest prediction accuracy. First, the investigators made the decision to disregard a large amount of valuable data by selecting only sites that had valid measurements during both the summer and winter campaigns. Second, influential observations could have contributed to the modest predictions, considering the large drop between the explained variance (R^2) of the model and the leave-one-out cross-validated variance (LOOCV R^2); the Committee thought it would have been useful to investigate this further. Third, to limit overfitting, the investigators applied a rule of thumb — allowing no more than 1 predictor per 10 observations — but they seem to have selected the maximum permissible number of predictors for each of the preferred models, suggesting there would be room for further improvements if other strategies and decisions were made. Fourth, considering the limited number of potential variables that the investigators' semi-automatic variable selection process permitted (they used the *leaps* package in R, which permits a maximum of $N-1$ variables), the preselection from the 373 predictors was quite extensive but not described. The Committee wondered about the influence of these decisions in this study and recommends taking such issues into account in future analyses.

OVERARCHING FINAL CONSIDERATIONS

The Review Committee concluded that the investigators took appropriate steps throughout the study to increase generalizability of results. However, it remains unclear whether the vertical gradient model is applicable to the entire city of Hong Kong and other Asian megacities with large populations living in high-rise buildings. For example, the investigators carefully selected six streets for vertical monitoring, representing a range of different traffic and street characteristics, but this remains a very small sample for a large city. Similarly, as is true for many other cohorts, the Hong Kong cohort was a convenience sample that is not representative of the general population. In addition, because it was an elderly cohort, the dynamic part of the exposure model could not be fully tested.

The relative benefits and risks of high-rise living and its impact on health due to factors unrelated to air pollution

research continue to be debated (e.g., Gifford 2007). For example, a study in Switzerland (Panzcak et al. 2013) documented that mortality from all causes was higher in people living on the ground floor compared with those living on higher floors, with level of floor serving as an indicator of socioeconomic status, given that residents on higher floors usually have higher socioeconomic status. However, other studies have found the opposite. For example, a study in Toronto that investigated cases of out-of-hospital cardiac arrest concluded that survival was greater on lower floors than higher floors because emergency response times were longer for residents living on higher floors, leading to lower survival rates (Drennan et al. 2016). It is clear that relationships between floor of residence in high-rise buildings and health are complex and highly contextual; they are influenced by cultural and socioeconomic characteristics of neighborhoods, levels of crime, physical characteristics of buildings, and air pollution and noise, among many other factors. Floor of residence may thus also act as a confounding factor in studies of the health effects of air pollution.

Finally, the Committee noted that the possibility of using any vertical gradient component in an exposure model is currently hampered by the fact that administrative data do not typically contain residential floor information. Therefore, the use of a vertical gradient component in exposure models for future epidemiological studies employing administrative data is likely to be limited.

SUMMARY AND CONCLUSIONS

Barratt and colleagues conducted a novel study — one of the first to integrate vertical gradients and time–activity patterns into an air pollution exposure model. The extensive air quality measurements, the development of exposure models using state-of-the-art modeling practices, and the application of those models to an existing Hong Kong cohort for epidemiological analyses were strengths of the study. The Review Committee concluded that Barratt and colleagues have found fairly similar associations when comparing results from the complex models to the two-dimensional models for $PM_{2.5}$, BC, NO, and NO_2 . Neither the incorporation of vertical gradients nor that of dynamic components, including indoor pollutant infiltration, into the exposure estimates resulted in meaningful or consistent changes in the associations with all-natural-cause, cardiovascular, and respiratory mortality in the Hong Kong elderly cohort.

The Committee noted that the investigators encountered many challenges in the study and developed approaches

to compensate for those challenges in a variety of ways, but the impacts of the various workarounds were not fully explored. Additionally, the Committee thought that the prediction accuracy of the two-dimensional LUR models was rather modest, which may suggest that alternative modeling strategies and decisions may be necessary for further improvements. The investigators' further exploration of the vertical gradient component of the model at the Committee's request was revealing because it showed that results were sensitive to the choice of the model. Sensitivity analyses revealed influences of substituting the modeled two-dimensional LUR estimates for missing measurements at lower floors and assuming that the air was well mixed at heights above 20 meters. The Committee thought more insights were gained from the vertical gradient model than from the dynamic component of the model because the latter was based on aggregated survey data, which makes interpretation difficult.

Based on the current study as well as findings from earlier studies, the addition of a vertical gradient — or, more generally, street configuration and building height to capture exposure in canyon streets — appears to improve exposure model performance, although the added value may be modest, depending on pollutant and study area. It should be realized that relationships between floor of residence in high-rise buildings and health are complex and highly contextual, and that floor of residence may act also as a confounding factor in studies of the health effects of air pollution. Although appropriate steps were taken throughout the study to increase generalizability of results, it remains unclear to what extent the vertical gradient model is applicable to the entire city of Hong Kong and to other Asian megacities with large populations living in high-rise buildings. Finally, the use of a vertical gradient component in exposure models for future epidemiological studies employing administrative databases is likely to be limited, partly because administrative data do not typically contain residential floor information.

ACKNOWLEDGMENTS

The Review Committee thanks the ad hoc reviewers for their help in evaluating the scientific merit of the Investigators' Report. The Committee is also grateful to Hanna Boogaard and Maria Costantini for oversight of the study, to Hanna Boogaard and Allison Patton for assistance in preparing its Critique, to Carol Moyer for science editing of this Report and its Critique, and to Fred Howe, Hilary Selby Polk, and Ruth Shaw for their roles in preparing this Research Report for publication.

REFERENCES

- Allen RW, Adar SD, Avol E, Cohen M, Curl CL, Larson T, et al. 2012. Modeling the residential infiltration of outdoor PM_{2.5} in the Multi-Ethnic Study of Atherosclerosis and Air Pollution (MESA Air). *Environ Health Perspect* 120: 824–830.
- Baxter LK, Dionisio KL, Burke J, Ebel Sarnat S, Sarnat JA, Hodas N, et al. 2013. Exposure prediction approaches used in air pollution epidemiology studies: Key findings and future recommendations. *J Expo Sci Environ Epidemiol* 23:654–659.
- Beckx C, Panis L, Arentze T, Janssens D, Torfs R, Broekx S, et al. 2009. A dynamic activity based population modeling approach to evaluate exposure to air pollution: Methods and application to a Dutch urban area. *Environ Impact Assess Rev* 29:179–185.
- Brauer M, Hoek G, van Vliet P, Meliefste K, Fischer P, Gehring U, et al. 2003. Estimating long-term average particulate air pollution concentrations: Application of traffic indicators and geographic information systems. *Epidemiology* 14:228–239.
- Dons E, Van Poppel M, Kochan B, Wets G, Int Panis L. 2014. Implementation and validation of a modeling framework to assess personal exposure to black carbon. *Environ Int* 62:64–71.
- Drennan IR, Strum RP, Byers A, Buick JE, Lin S, Cheskes S, et al. 2016. Out-of-hospital cardiac arrest in high-rise buildings: Delays to patient care and effect on survival. *CMAJ* 188:413–419.
- Eeftens M, Beekhuizen J, Beelen R, Wang, M, Vermeulen R, Brunekreef B, et al. 2013. Quantifying urban street configuration for improvements in air pollution models. *Atmos Environ* 72:1–9.
- Gifford R. 2007. The consequences of living in high-rise buildings. *Archit Sci Rev* 50:2–17.
- HEI Panel on the Health Effects of Traffic-Related Air Pollution. 2010. *Traffic-Related Air Pollution: A Critical Review of the Literature on Emissions, Exposure, and Health Effects*. HEI Special Report 17. Boston, MA:Health Effects Institute.
- Hoek G, Beelen R, de Hoogh K, Vienneau D, Gulliver J, Fischer P, et al. 2008. A review of land-use regression models to assess spatial variation of outdoor air pollution. *Atmos Environ* 42:7561–7578.
- Karner A, Eisinger DS, Niemeier DA. 2010. Near-roadway air quality: Synthesizing the findings from real-world data. *Environ Sci Technol* 44:5334–5344.
- Lane KJ, Levy JI, Scammell MK, Patton AP, Durant JL, Mwamburi M, et al. 2015. Effect of time-activity adjustment on exposure assessment for traffic-related ultrafine particles. *J Expo Sci Environ Epidemiol* 25(5):506–516.
- Lash TL. 2017. The harm done to reproducibility by the culture of null hypothesis significance testing. *Am J Epidemiol* 186:627–635.
- Panczak R, Galobardes B, Spoerri A, Zwahlen M, Egger M. 2013. High life in the sky? Mortality by floor of residence in Switzerland. *Eur J Epidemiol* 28:453–462.
- Schooling CM, Chan WM, Leung SL, Lam TH, Lee SY, Shen C, et al. 2016. Cohort Profile: Hong Kong Department of Health Elderly Health Service Cohort. *Int J Epidemiology* 45:64–72.
- Shi Y, Lau KK, Ng E. 2016. Developing street-level PM_{2.5} and PM₁₀ land use regression models in high-density Hong Kong with urban morphological factors. *Environ Sci Technol* 50:8178–8187.
- Smith JD, Mitsakou C, Kitwiroon N, Barratt BM, Walton HA, Taylor JG, et al. 2016. London hybrid exposure model: Improving human exposure estimates to NO₂ and PM_{2.5} in an Urban Setting. *Environ Sci Technol* 50:11760–11768.
- Su JG, Brauer M, Buzzelli M. 2008. Estimating urban morphology at the neighborhood scale for improvement in modeling long-term average air pollution concentrations. *Atmos Environ* 42:7884–7893.
- Szpiro AA, Paciorek CJ. 2013. Measurement error in two-stage analyses, with application to air pollution epidemiology (with invited discussion). *Environmetrics* 24:501–517.
- Szpiro AA, Paciorek CJ, Sheppard L. 2011. Does more accurate exposure prediction necessarily improve health effect estimates? *Epidemiology* 22:680–685.
- Tang R, Blangiardo M, Gulliver J. 2013. Using building heights and street configuration to enhance intraurban PM₁₀, NO_x, and NO₂ land use regression models. *Environ Sci Technol* 47:11643–11650.
- United Nations, Department of Economic and Social Affairs, Population Division. 2015. *World Urbanization Prospects: The 2014 Revision, (ST/ESA/SER.A/366)*. Available: <https://esa.un.org/unpd/wup/Publications/Files/WUP2014-Report.pdf> [accessed July 18, 2017].

Wong CM, Lai HK, Tsang H, Thach TQ, Thomas GN, Lam K, et al. 2015. Satellite-based estimates of long-term exposure to fine particles and association with mortality in elderly Hong Kong residents. *Environ Health Perspect* 123: 1167–1172.

World Health Organization. 2013. Review of evidence on health aspects of air pollution — REVIHAAP Project Technical Report. www.euro.who.int/__data/assets/pdf_file/0004/193108/REVIHAAP-Final-technical-report-final-version.pdf?ua=1 [accessed July 20, 2017].

Wu CF, Lin HI, Ho CC, Yang TH, Chen CC, Chan CC. 2014. Modeling horizontal and vertical variation in intraurban exposure to PM_{2.5} concentrations and compositions. *Environ Res* 133:96–102.

Zhou Y, Levy JI. 2007. Factors influencing the spatial extent of mobile source air pollution impacts: A meta-analysis. *BMC Public Health* 7:89.

ABBREVIATIONS AND OTHER TERMS

2D	two-dimensional	KCAQMS	Kwai Chung AQMS
3D	three-dimensional	KTAQMS	Kwun Tong Road AQMS
AADT	annual average daily traffic	LOOCV	leave-one-out cross validation
AQMS	air quality monitoring station	LUR	land-use regression
BC	black carbon	MESA-Air	Multi-Ethnic Study of Atherosclerosis and Air Pollution
CBAQMS	Causeway Bay AQMS	MKAQMS	Mong Kok AQMS
CHO1	Choi Hung open measurement site	MKC1	Mong Kok canyon measurement site
CI	confidence interval	MRC-PHE	Medical Research Council – Public Health England
CO	carbon monoxide	MVAC	mechanical ventilation and air conditioning
COPD	chronic obstructive pulmonary disease	NIHR	National Institute for Health Research
D3D	dynamic three-dimensional	NO	nitric oxide
EHSC	Hong Kong Department of Health's Elderly Health Service	NO ₂	nitrogen dioxide
EPD	Environmental Protection Department	NO _x	oxides of nitrogen
ESCAPE	European Study of Cohorts for Air Pollution Effects	NPC1	North Point canyon measurement site
FDMS	filter dynamic measurement system	RMSE	root mean square error
F_{inf}	infiltration efficiency	PM _{2.5}	particulate matter $\leq 2.5 \mu\text{m}$ in aerodynamic diameter
GIS	geographical information system	PM ₁₀	particulate matter $\leq 10 \mu\text{m}$ in aerodynamic diameter
HEPA	high efficiency particulate air	SC	sampling campaign
HEV	hold-out evaluation	SD	standard deviation
HHC1	Hung Hom canyon measurement site	SSPAQMS	Sham Shui Po AQMS
HK	Hong Kong	SWO1	Sai Wan open measurement site
HK 2D	Hong Kong 2-dimensional sampling	TPU	tertiary planning unit
HK SAR	Hong Kong Semi-Autonomous Region	TRAP	traffic-related air pollution
HR	hazard ratio	UK	United Kingdom
ICD-10	International Classification of Diseases, 10th Revision	VIF	variance inflation factor
IHD	ischemic heart disease	WP	work package
IQR	interquartile range		
JDC1	Jordan canyon measurement site		

RELATED HEI PUBLICATIONS: TRAFFIC, METHODS, AND MULTIPOLLUTANTS

Number	Title	Principal Investigator	Date
Research Reports			
183	Development of Statistical Methods for Multipollutant Research <i>Part 3. Modeling of Multipollutant Profiles and Spatially Varying Health Effects with Applications to Indicators of Adverse Birth Outcomes</i>	J. Molitor	2016
179	Development and Application of an Aerosol Screening Model for Size-Resolved Urban Aerosols	C.O. Stanier	2014
178	National Particle Component Toxicity (NPACT) Initiative Report on Cardiovascular Effects	S. Vedal	2013
177	National Particle Component Toxicity (NPACT) Initiative: Integrated Epidemiologic and Toxicologic Studies of the Health Effects of Particulate Matter Components	M. Lippmann	2013
175	New Statistical Approaches to Semiparametric Regression with Application to Air Pollution Research	J.M. Robins	2013
152	Evaluating Heterogeneity in Indoor and Outdoor Air Pollution Using Land-Use Regression and Constrained Factor Analysis	J.I. Levy	2010
140	Extended Follow-Up and Spatial Analysis of the American Cancer Society Study Linking Particulate Air Pollution and Mortality	D. Krewski	2009
139	Effects of Long-Term Exposure to Traffic-Related Air Pollution on Respiratory and Cardiovascular Mortality in the Netherlands: The NLCS-AIR Study	B. Brunekreef	2009
138	Health Effects of Real-World Exposure to Diesel Exhaust in Persons with Asthma	J. Zhang	2009
133	Characterization of Metals Emitted from Motor Vehicles	J.J. Schauer	2006
131	Characterization of Particulate and Gas Exposures of Sensitive Subpopulations Living in Baltimore and Boston	P. Koutrakis	2005
130	Relationships of Indoor, Outdoor, and Personal Air (RIOPA) <i>Part I. Collection Methods and Descriptive Analyses</i>	C.P. Weisel	2005
	<i>Part II. Analyses of Concentrations of Particulate Matter Species</i>	B.J. Turpin	2007
127	Personal, Indoor, and Outdoor Exposures to PM _{2.5} and Its Components for Groups of Cardiovascular Patients in Amsterdam and Helsinki	B. Brunekreef	2005

(Continued)

Copies of these reports can be obtained from HEI; PDFs are available for free downloading at www.healtheffects.org/publications.

RELATED HEI PUBLICATIONS: TRAFFIC, METHODS, AND MULTIPOLLUTANTS

Number	Title	Principal Investigator	Date
Special Reports			
19	Diesel Emissions and Lung Cancer: An Evaluation of Recent Epidemiological Evidence for Quantitative Risk Assessment	HEI Diesel Epidemiology Panel	2015
17	Traffic-Related Air Pollution: A Critical Review of the Literature on Emissions, Exposure, and Health Effects		2010
16	Mobile-Source Air Toxics: A Critical Review of the Literature of Exposure and Health Effects		2007
HEI Perspectives			
3	Understanding the Health Effects of Ambient Ultrafine Particles	HEI Review Panel on Ultrafine Particles	2013

Copies of these reports can be obtained from HEI; PDFs are available for free downloading at www.healtheffects.org/publications.

HEI BOARD, COMMITTEES, and STAFF

Board of Directors

Richard F. Celeste, Chair *President Emeritus, Colorado College*

Sherwood Boehlert *Of Counsel, Accord Group; Former Chair, U.S. House of Representatives Science Committee*

Enriqueta Bond *President Emerita, Burroughs Wellcome Fund*

Jo Ivey Boufford *President, New York Academy of Medicine*

Michael T. Clegg *Professor of Biological Sciences, University of California–Irvine*

Jared L. Cohon *President Emeritus and Professor, Civil and Environmental Engineering and Engineering and Public Policy, Carnegie Mellon University*

Stephen Corman *President, Corman Enterprises*

Linda Rosenstock *Dean Emeritus and Professor of Health Policy and Management, Environmental Health Sciences and Medicine, University of California–Los Angeles*

Henry Schacht *Managing Director, Warburg Pincus; Former Chairman and Chief Executive Officer, Lucent Technologies*

Research Committee

David L. Eaton, Chair *Dean and Vice Provost of the Graduate School, University of Washington–Seattle*

Jeffrey R. Brook *Senior Research Scientist, Air Quality Research Division, Environment Canada, and Assistant Professor, University of Toronto, Canada*

Francesca Dominici *Professor of Biostatistics and Senior Associate Dean for Research, Harvard T.H. Chan School of Public Health*

David E. Foster *Phil and Jean Myers Professor Emeritus, Department of Mechanical Engineering, Engine Research Center, University of Wisconsin–Madison*

Amy H. Herring *Professor of Statistical Science and Global Health, Duke University, Durham, North Carolina*

Barbara Hoffmann *Professor of Environmental Epidemiology, Institute of Occupational, Social, and Environmental Medicine, University of Düsseldorf, Germany*

Allen L. Robinson *Raymond J. Lane Distinguished Professor and Head, Department of Mechanical Engineering, and Professor, Department of Engineering and Public Policy, Carnegie Mellon University*

Ivan Rusyn *Professor, Department of Veterinary Integrative Biosciences, Texas A&M University*

Review Committee

James A. Merchant, Chair *Professor and Founding Dean Emeritus, College of Public Health, University of Iowa*

Kiros Berhane *Professor of Biostatistics and Director of Graduate Programs in Biostatistics and Epidemiology, Department of Preventive Medicine, Keck School of Medicine, University of Southern California*

Mark W. Frampton *Professor Emeritus of Medicine and Environmental Medicine, University of Rochester Medical Center*

Frank Kelly *Professor of Environmental Health and Director of the Environmental Research Group, King's College London*

Jana B. Milford *Professor, Department of Mechanical Engineering and Environmental Engineering Program, University of Colorado–Boulder*

Jennifer L. Peel *Professor of Epidemiology, Colorado School of Public Health and Department of Environmental and Radiological Health Sciences, Colorado State University*

Roger D. Peng *Professor of Biostatistics, Johns Hopkins Bloomberg School of Public Health*

Lianne Sheppard *Professor of Biostatistics, School of Public Health, University of Washington–Seattle*

HEI BOARD, COMMITTEES, and STAFF

Officers and Staff

Daniel S. Greenbaum *President*

Robert M. O'Keefe *Vice President*

Rashid Shaikh *Director of Science*

Jacqueline C. Rutledge *Director of Finance and Administration*

April Rieger *Corporate Secretary*

Hanna Boogaard *Consulting Senior Scientist*

Aaron J. Cohen *Consulting Principal Scientist*

Maria G. Costantini *Principal Scientist*

Philip J. DeMarco *Compliance Manager*

Hope Green *Editorial Project Manager*

Kathryn Liziewski *Research Assistant*

Allison P. Patton *Staff Scientist*

Hilary Selby Polk *Managing Editor*

Lindy Raso *Executive Assistant*

Anna S. Rosofsky *Staff Scientist*

Robert A. Shavers *Operations Manager*

Annemoon M.M. van Erp *Managing Scientist*

Donna J. Vorhees *Director of Energy Research*

Katherine Walker *Principal Scientist*



HEALTH
EFFECTS
INSTITUTE

75 Federal Street, Suite 1400
Boston, MA 02110, USA
+1-617-488-2300
www.healtheffects.org

RESEARCH
REPORT

Number 194
February 2018